To the Graduate Council:

I am submitting herewith a dissertation written by Michael John Franklin entitled "EFFECTS OF MICROBIAL BIOFILMS AND MICROBIAL METABOLIC ACTIVITY ON THE LOCALIZED CORROSION OF STEEL." I have examined the final copy of this dissertation for form and content and recommend that it be accepted in partial fulfillment of the requirements for the degree of Doctor of Philosophy, with a major in Microbiology.

David C. White, Major Professor

We have read this dissertation and recommend its acceptance:

Accepted for the Council:

Associate Vice Chancellor and
Dean of The Graduate School

EFFECTS OF MICROBIAL BIOFILMS AND MICROBIAL METABOLIC ACTIVITY ON THE LOCALIZED CORROSION OF STEEL

A Dissertation

Presented for the

Doctor of Philosophy

Degree

The University of Tennessee, Knoxville

Michael John Franklin

May 1991

This work is dedicated to my wife, Becky, who has endured many years of graduate school, and has always been loving and supportive.

ACKNOWLEDGEMENTS

I wish to thank my family for their support. In particular, I am greatful to Becky Franklin and Laura Franklin for making my life enjoyable. I also thank my parents Dr. Rudolph Franklin and Dr. and Mrs. William Baxter for their emotional as well as their financial support. I thank my grandparents Dr. and Mrs. Paul Eaton for their encouragement. I also wish to thank Dr. and Mrs. Reuben Smith and Mrs. Martha Smith for their assistance.

My major professor, Dr. David C. White, has provided me with the educational opportunity and the excellent environment to learn and to do research. For this, I am truely greatful. I wish to thank Dr. Hugh S. Isaacs, for allowing me to visit his laboratory, and for teaching me the scanning vibrating electrode technique. I also wish to thank the members of my committee Dr. Howard Adler, Dr. James Chambers, Dr. Thomas Montie, and Dr. Gary Sayler, for their valuble contributions.

Many people at the Institute for Applied Microbiology have contributed directly or indirectly to this research. I wish to thank all of these people. In particular, I wish to thank David Nivens for his help and for his insight. Other members of the lab to whom I am greatful are; Nick Dowling, Jim Guckert, Richard Jack, Chris Johnson, Melody Kirby, David Hedrick, Robert Mackowski, Marc Mittelman, Tom Phelps, Sydney Post, David Ringelberg, Anders Tunlid, and Arpad Vass.

ABSTRACT

Microbial biofilms, formed on metal surfaces exposed to aqueous environments, and the metabolic activity of the attached bacteria, can cause corrosion and premature failure of metal structures. Most of the corrosion attributed to microbial activity is localized, and in the form of pitting corrosion. Studies on the mechanisms of microbiologically influenced corrosion (MIC) have lagged behind other corrosion studies. However, studies on mechanisms of MIC are essential in mitigation of MIC problems. MIC studies have been difficult due in part to the difficulties in analyzing local activities of bacteria, spatially and temporally. In addition, most electrochemical techniques for analyzing corrosion are destructive to biofilms, and provide only indirect information on localized corrosion.

In this research, bacteria were isolated from corrosion tubercles. The isolates were characterized, and reexposed to steel samples in a laboratory test system to determine if corrosion observed in the field could be simulated in the laboratory. In this way, a test system was developed which could be used to study MIC under controlled laboratory conditions.

Recently developed electrochemical techniques were evaluated to determine the usefulness of these techniques in MIC studies. Electrochemical impedance spectroscopy (EIS) was shown to be a useful technique for evaluating corrosion

rates of individual metal samples over time. EIS was found to be nondestructive to bacterial biofilms. Potential applied during EIS analysis did not significantly alter the numbers of sessile bacteria, the numbers of sessile viable bacteria, or the activity of sessile bacteria. EIS was used to compare corrosion rates over time of steel exposed to bacteria and exposed to sterile medium. EIS was also used to study the corrosion rates of steel exposed to biofilms treated with oxidizing biocides. Results indicated that the bacterial isolates accelerated the rates of corrosion with respect to sterile controls. Oxidizing biocides increased the corrosion rates, even when most of the biofilm was removed.

Although EIS provided a useful means for evaluating corrosion rates over time, in these studies, the technique did not provide a direct means to evaluate mechanisms of localized corrosion influenced by microbial biofilms and bacterial activity. The scanning vibrating electrode technique (SVET) was used to study nonuniform current densities over corroding steel samples. The SVET technique was used to determine corrosion rates at localized sites, under variable applied polarization. In addition, the SVET was used at open circuit potential to study localized corrosion without destruction to the biofilms. The results of the SVET studies demonstrated that although steel coupons appeared passive in sterile medium, small pits formed on the

samples and subsequently became inactive (repassivated). In the presence of microbial biofilms, pits would initiate and repassivate for a certain amount of time, then would propagate rather than repassivate. Biofilms were necessary for pit propagation, since spent medium did not cause pit propagation. The time required for pit propagation was dependent on the viability of the bacteria as well as on the numbers of bacteria.

SVET studies in sterile media demonstrated that phosphate and buffer promoted repassivation of pits. The bacterial biofilms interfered with this repassivation, either by maintaining an aggressive environment within pits, or by preventing inhibiting ions from reaching anodic sites.

Incorporation of ^{14}C-acetate into insoluble cell material, and exposure of the labelled bacteria to X-ray film was used to localize microbial biosynthetic activity. Microautoradiography was used to detect the individually labelled bacteria. These studies were combined with studies of localized corrosion using the SVET. Most of the label observed with the X-ray film was associated with the anodic sites of the steel. The ^{14}C-acetate may have become chemically bound to the corrosion products. However, killed controls showed little label on the electrode surface. Alternatively, bacteria either caused initiation of pits by localized colonization, or bacteria preferentially attached

to corrosion products, enabling pits, initiated by chemical corrosion, to propagate.

TABLE OF CONTENTS

LIST OF TABLES

LIST OF FIGURES

FIGURE PAGE

CHAPTER VIII

CHAPTER IX

CHAPTER X

CHAPTER I

INTRODUCTION

In the plenary lecture delivered at the 5th International Congress on Metallic Corrosion, in 1972 Marcel Pourbaix described corrosion prior to the 1930's as "a calamity, a necessary evil, an unavoidable pestilence to which we had to submit without being able to control or even understand it." However, with advances in the science of corrosion, "it is now possible to predetermine with full certainty, excellent - and even perfect - protection techniques, which may suppress corrosion almost fully, or even fully" (102). The major advances in corrosion science 1) the development of the mixed potential theory of corrosion (129), which describe the potential of corroding metals as a mixed potential imparted by the anodic loss of metal and the cathodic utilization of electrons; 2) the use of the potentiostat and the understanding of polarization curves to determine corrosion kinetics (119); 3) the development of corrosion thermodynamics, which describes the chemical and electrochemical reactions which can occur on metal, and can be used to define cathodic protection schemes (99); and 4) the better understanding of acid base reactions in the development and breakdown of passive films (112,113). Advancements in corrosion science have led to practical applications with economic importance. For example, Pourbaix states, in describing the development of a criterion for the cathodic protection of steel, that "the technical and economic importance of this criterion of

protection is very considerable, and out of all proportion to the cost entailed in its discovery and application"(102).

The philosophy that a better understanding of corrosion mechanisms is useful in mitigating corrosion problems can be applied to the relatively new discipline within corrosion termed microbiologically influenced corrosion (MIC). In recent years MIC has received considerable attention. (This year over 90 papers dealing with MIC were submitted to an international congress on MIC). The attention to MIC has been primarily due to the observation of premature unexpected failures of metal structures, including corrosion resistant alloys, exposed to untreated water. Understanding mechanisms by which bacteria facilitate corrosion has lagged behind other corrosion studies.

Understanding mechanisms of MIC will require studies of microbial biofilms and studies of the activities of microbes within biofilms. These studies must then be incorporated into known corrosion mechanisms. In this introduction a review on biofilm formation, activities, and methods of biofilm detection is given. Also concepts of corrosion science are briefly reviewed, with emphasis on the electrochemical techniques used in the research presented here. The reviewed corrosion concepts include corrosion thermodynamics, including the ideas of passivity and breakdown of passivity (localized corrosion), and corrosion kinetics. The techniques for measuring corrosion rates

including Tafel plots, linear polarization technique, electrochemical impedance spectroscopy (EIS), and the scanning vibrating electrode technique (SVET) are reviewed. Proposed mechanisms of MIC are reviewed, and finally the approach used in this research to better understand MIC mechanisms is discussed.

CHAPTER II

LITERATURE REVIEW

BIOFILMS AND EFFECTS OF SURFACES ON ATTACHED BACTERIA

When structures are exposed to untreated water, bacteria can attach to surfaces and form films, termed biofilms. Geesey et al. (38) have estimated that as many as 500 to 10^4 times as many bacteria are found on one square centimeter of a surface as compared to a cubic centimeter of overlying water. The biofilms formed can have many economically beneficial and detrimental effects. Beneficial effect of biofilms include the removal of organic carbon from wastewater. The waste water is exposed to biofilms contained on structures such as gravel, where the biofilms convert much of the organic carbon to gaseous products such as methane and carbon dioxide. Biofilms can be used in the degradation of toxic compounds and in the sorption and concentration of heavy metals from water. The detrimental effects of biofilms are best exemplified when untreated water is used in cooling systems. In these cases biofilms can form on the walls of the pipes and create several problems, including increased pressure drop of the cooling water, lessening of the heat transfer properties, and increased corrosion rates of the pipes (18).

Many investigators have suggested that bacteria gain certain survival advantages by adhering to surfaces. Zobell (131) suggested that the adsorption of nutrients to surfaces creates a nutrient rich environment in an otherwise nutrient limited environment. A number of studies have compared the

activities of surface bound bacteria with the bulk phase organisms (30,32,62,63). In many of those studies the activity of the surface associated bacteria was greater than the activity of the bacteria in solution. For example, Fletcher showed that the uptake of ^{14}C-glucose was greater for attached bacteria than for free living cells (31). Jeffery and Paul (62,63) obtained similar results for the uptake of ^{3}H-thymidine. However other studies have shown decreased activity of surface bound bacteria (126). van Loosdrecht et al. (126) have reviewed over seventy papers pertaining to the effects of surfaces on bacteria. They claimed that no study has shown a direct influence on microbial activity due to the presence of a surface, such as "changes in the structure and permeability of the membranes as an immediate consequence of the presence of a nearby surface" (126). They claimed that any observed effects are indirect and caused by, for example, adsorption and desorption of molecules to the surface or changes in the geometry of the space around the adhering cell. They also demonstrate that the conditioning film formed by adsorption of molecules to surfaces is so thin that less than 0.1% of the cell surface would be directly exposed to the conditioning film.

In spite of these claims that surfaces do not directly influence the metabolic activity of bacteria, some metabolic activities of certain bacteria do appear to respond directly

to surfaces. The marine bacterium Vibrio parahaemolyticus changes from a short rod-shaped organism with a single polar flagellum when in solution, to an elongated rod with multiple lateral flagella when attached to a surface. Belas et al. (7) using gene fusions of a bioluminescence gene, lux, to the genes controlling lateral flagella production, laf, have demonstrated that the change is due to the restriction of movement of the polar flagellum. The movement of the polar flagellum can be restricted by increased viscosity, antibody agglutination, or perhaps attachment to a surface (7). Change from the swimming to the swarming phenotype has also been observed for the bacterium Serratia marcesans (2). Bartlett and Silverman (6) have shown that an insertion sequence causes the reversible expression of extracellular polysaccharide in Pseudomonas atlantica. Since extracellular polysaccharide from this organism is expressed in greater quantities when the organism is attached to a surface (89), surfaces may somehow trigger the exchange of this insertion sequence and hence the production of extracellular polysaccharide. Thus surfaces may directly affect certain activities in bacteria.

Bacteria appear to gain certain survival advantages by being associated with a surface or a biofilm, such as increased protection from toxic compounds (71). By being in close contact with other cells in a biofilm, biofilms may facilitate this exchange of DNA (114,115).

BIOFILM FORMATION

Several reviews and a book have been written characterizing biofilms and biofilm formation (17,18,19,42,69). Charackalis and Cooksey (18) described the steps in the formation of biofilms as 1) transport of bacteria and molecules from the bulk phase to the surface exposed to an aqueous environment; 2) formation of an organic conditioning film on the surface of a structure exposed to an aqueous environment; 3) reversible attachment of bacteria on the surface, followed by irreversible adhesion of the bacteria; 4) growth of the attached organisms forming microcolonies and thick biofilms; 5) detachment of the bacteria from the surface. Detachment can occur any time after the cells are reversibly or irreversibly adhered to the surface. In addition to the processes described by Charackalis and Cooksey (18), growth of biofilms can lead to changes within the biofilm. These changes can lead to succession of species within the biofilms and species-species interactions. For example, strictly anaerobic bacteria have been found to multiply in biofilms when the bulk solutions is aerobic (60), suggesting that environments within the biofilm were anaerobic. The following is a brief review of the formation of biofilms and of some of the techniques used to detect biofilm formation and activity.

The transport of molecules and bacteria to surfaces depends on whether the solution is stagnant, or whether the flow over the surface is turbulent or laminar (18). In stagnant systems, diffusion, gravity, and bacterial motility play the primary role in the transport of bacteria to surfaces. Under flow conditions, fluid dynamics are important. The bacteria are first transported to the viscous layer of water adjacent to the surface. Faster flow in laminar systems decreases the thickness of this viscous layer. Once the bacteria are within this viscous layer, diffusion and motility play roles in transport of the bacteria to the surface (18). Similar principles apply to the transport of bacteria in turbulent systems. The bacteria can be brought to the viscous layer by eddies in the solution. However, once the bacteria are in the viscous layer, diffusion and motility play roles in transport (18).

There is debate on whether or not an organic conditioning film is necessary for the attachment of bacteria to surfaces (18). An organic film forms rapidly upon exposure of a surface to aqueous environments. Baier (4) using attenuated total reflectance Fourier transform infrared spectroscopy has shown increases in the amide regions and the C-O stretch region in the infrared spectrum of germanium exposed to sterile water. Those results suggest that protein and carbohydrate material rapidly form on surfaces exposed to aqueous environments. It may be

difficult or impossible to place surfaces in water and not obtain a conditioning film. Thus, it is difficult to determine whether this film is required for bacterial adhesion or not.

The reversible and irreversible adhesion of bacteria was first described by Zobell (131) and later by Marshall et al (83). Marshall et al. (83) defined reversible adhesion as an association of the bacteria with the surface where the bacteria still exhibit Brownian motion and can be easily removed by rinsing. When bacteria are irreversible adhered to surfaces, rinsing will not dislodge the bacteria. Irreversible adhesion is time dependent and usually accompanied by the production of extracellular polymer (83).

The DLVO theory was used by van Loosdrecht (125) to characterize the forces involved in the initial stages of bacterial adhesion. The forces taken into account for the DLVO theory include van der Waals forces, which are usually attractive, and electrostatic interactions, which are usually repulsive. These authors (125) have diagramed these forces as a function of the separation distance of a bacterium to a solid surfaces. They have demonstrated that two minima occur where attraction to the surface is favored, and have suggested that the secondary minimum may favor reversible adhesion to the surface whereas the primary minimum may favor irreversible adhesion. The attractive forces are dependent on the ionic strength of the medium.

Evidence in favor of this theory is the interference reflection microscopy work by Fletcher (33) which showed a decreased separation distance of the bacteria with the surface upon increase of the ionic strength, consistent with the proposed theory. In addition, the DLVO theory provides for immediate irreversible adhesion to surfaces, without the formation of extracellular polymers. Immediate irreversible adhesion has been observed (31).

An alternative theory which has been used to explain bacterial attachment to surfaces is based on a thermodynamic model. Absolom et al. (1) proposed that the adhesion of bacteria to surfaces is dependent on the surface tension of the surface, of the medium, and of the bacteria. Using surfaces with various surface tensions, and media with different surface tensions, they have shown that bacteria with various surface tensions adhere to surfaces in similar fashion to the predicted model. They concluded that greater adhesion (cell/area) occurs on hydrophilic substrata when the surface tension of the bacteria is greater than that of the medium. Greater adhesion occurs to hydrophobic substrata when the opposite is true. This model provided a role for the effect of bacterial hydrophobicity on the adhesion to surfaces often described (108).

Once attached to a surface, bacteria can become irreversibly bound either by forces such as van der Waals forces or electrostatic interactions (125), or by polymer

bridging (83), through the production of extracellular substances such as extracellular polymer or organelles such as fimbriae. Irreversible adhesion is followed by an accumulation of biomass, including cellular and extracellular materials. Bryers and Charackalis (14) have used turbulent flow reactors to describe biomass accumulation within biofilms, and Rittman and McCarty (106,107) have used flow through reactors to define nutrient uptake by attached bacteria. Bryers and Charackalis (14) demonstrated that the biofilm production rate decreases with increasing thickness of the biofilm, probably due to mass transport limitations. Rittman and McCarty (106) used models to describe the mass of biofilms based on the substrate flux into the biofilm. The mass of the biofilm was dependent on the kinetics of substrate utilization by the biofilm, maintenance energy coefficient, and flux of nutrient to the biofilm. They observed a good correlation between the thickness of biofilms and nutrient uptake described by the model and actual biofilm thickness and nutrient uptake in reactors containing biofilms on glass beads (107).

TECHNIQUES TO STUDY BIOFILMS AND BIOFILM ACTIVITIES

Recent developments in analytical techniques used to characterize bacterial adhesion, biofilm accumulation, and metabolic activities of microbes within biofilms should make studies on the structure and on the activity of biofilms possible. The recent advances have included off-line and on-line techniques for studying biofilms. Off-line techniques used to characterize biofilms have included microscopic techniques (114), including light and electron microscopy, as well as traditional microbiological techniques such as acridine orange direct counts, and colony forming units. Diffuse reflectance FT-IR has also been used to study the relationship between cellular and extracellular material production in biofilms under differential fluid shear (85). Analysis of phospholipid fatty acid (PLFA) profiles of bacterial membranes can be useful in characterizing the community structure of biofilms (8,60,130). For example, Jack (60) used analysis of PLFA's to compare laboratory generated biofilms with different community structures to biofilms found associated with failed steel pipes. Another technique which may prove useful in characterizing biofilm community structure is ribosomal RNA probe analysis (3).

A recent advance on the microscopic techniques include the use of environmental scanning electron microscopy (B. Little, personal communication). This technique can be used

to view biofilms without dehydration. Bacteria in the complex matrix of extracellular polysaccharide can be studied with little sample preparation. Another technique which may be useful in detecting the three dimensional structure of biofilms in the scanning confocal laser microscopy technique (70).

On-line techniques for biofilm studies, currently being developed in Dr. David White's laboratory, include the quartz crystal microbalance (90), which can be used to detect changes in mass of a biofilm. In addition, the attenuated total reflectance fourier transform infrared spectroscopy technique (ATR-FTIR) is being used to detect not only changes in mass of biofilms but also changes in the physiological properties of bacteria in biofilms when exposed to varying conditions (90). For example, the technique has been used to detect increases in poly beta hydroxybutyrate and extracellular polymer production in response to nutrient stress (90).

Techniques for studying the activity of bacteria in their natural environments as well as attached bacteria have primarily focused on the rate of uptake or conversion of certain radiolabelled metabolic precursors (29,35,84,97,98,110). Phelps et al. (97,98) utilized incorporation of ^{14}C-acetate into lipids as a measure of microbial biosynthetic activity in natural gas transmission pipe-lines. They also analyzed the catabolic activity of

the bacteria with the production of ^{14}C-CO_2 and ^{14}C-acetate from ^{14}C-glucose and ^{14}C-palmitate. Mittelman et al. (85) used similar techniques to analyze the biosynthetic activities of biofilm bacteria in differential fluid shears. Autoradiography after incubation of bacteria with radiolabelled precursors has been used to evaluate the activity of individual bacteria as well as to localize bacterial activity in biofilms (27,80,118). Another technique which may provide in situ characterization of bacterial activity in biofilms is the reporter gene technique. This technique uses lux gene fusions to the promoters of certain genes. In this way, gene expression can be determined by light production by the bacteria. This technique has been used in in situ studies of naphthalene degradation (15,67) as well as in biofilm studies (86).

In the present research, primarily off-line techniques were used to characterize biofilms, including scanning electron microscopy, diffuse reflectance FT-IR, PLFA analyses, and standard microbiological techniques. Studies on activities of biofilm bacteria used incorporation of radiolabelled precursors into bacterial lipids.

CORROSION THERMODYNAMICS

Corrosion attributed to MIC is often localized corrosion, such as pitting or crevice corrosion. Corrosion thermodynamics can be useful in understanding passivation and localized corrosion (100,101,103). Therefore, a brief review of corrosion thermodynamics is described below.

Corrosion thermodynamics describe whether a reaction has a negative change in free energy at a given pH and potential, and therefore whether the reaction can proceed. Whether a reaction actually does proceed is dependent on other factors including the presence or absence of a protective passive film. Thermodynamics can not be used to describe the rate of a corrosion reaction.

Corrosion in its simplest form can be thought of as two half-cell reactions, an anodic reaction, where metal dissolves to form a cation

$$M \rightarrow M^{n+} + ne^- \qquad (1)$$

and a cathodic reaction, where electrons from the anodic reaction are consumed, for example by protons in deaerated water

$$2nH^+ + 2ne^- \rightarrow H_2 \qquad (2)$$

Under idealized conditions, where no metal oxidation is occurring, and under standard conditions, 1M ion concentration for ions and 1 atmosphere pressure for the gases, each half-reaction has a standard value for potential, E^o. The reactions of iron as described by Pourbaix (99) are used here as an example. The half-cell

potential for the reduction of iron is:

$$Fe^{2+} + 2e^- \rightarrow Fe \quad (E^\circ = -440 \text{ mV vs SHE}) \qquad (3)$$

and for hydrogen is $E^\circ = 0$ by definition. If the species are not at standard conditions, the potential of a half-reaction varies according to the Nernst equation.

$$E' = E^\circ + 2.303 \frac{RT}{nF} \log \frac{ox}{red} \qquad (4)$$

where R is the gas constant, T is the temperature (degrees Kelvin), F is the Faraday constant, ox is the activity of the oxidized species, and red is the activity of the reduced species. If the two half-cell reactions are placed in solution separated by an ion permeable membrane, and connected with a wire (the hydrogen ion reduction reaction taking place on an inert electrode) current will flow on the wire, due to the differences in electrode potential of the two half-reactions. The potential of the cell E_{cell} is the difference between the half-cell potentials. Thus, in the case of iron in a pH 1 solution with 10^{-3} M Fe^{2+} and hydrogen at atmospheric pressure the half cell potentials are:

$$E'_{Fe} = -0.44 + 0.059/2 \log 10^{-3} = -0.53 \qquad (5)$$

$$E'_{H} = 0 + 0.059 \log 10^{-1} = -0.059 \qquad (6)$$

the relationship between the potential and the change in free energy, ΔG, is

$$\Delta G = -nFE_{cell} \qquad (7)$$

therefore, $\Delta G = -2(96.5)(-0.059 - (-0.53)) = -90.9$ kJ/mole. Since the change in free energy is negative, the reaction can proceed as described.

Of course, iron oxidation to ferrous ions is not the only reaction that can occur. Iron can react electrochemically with water and oxygen to form a number of iron oxide species (99). In addition the iron ions can react chemically with water or oxygen to form iron oxides. The electrochemical reactions are dependent upon the pH of the solution and upon the potential of the sample. The chemical reactions are primarily dependent upon the pH of the solution. Therefore, a convenient way to summarize the many chemical and electrochemical reactions is to plot the thermodynamic equilibrium reactions on diagrams of pH versus potential. These diagrams are now termed Pourbaix diagrams after the originator (99). An example of the Pourbaix diagram for iron is given in Figure 1 (99). Line (a) represents the reduction of hydrogen ions to hydrogen, and line (b) represent the reduction of oxygen. It can be seen that if the electrochemical reaction of interest is below line (a) then the reaction is thermodynamically favorable under anaerobic and aerobic conditions. If the electrochemical reaction of interest is below line (b) then the reaction is thermodynamically favorable aerobically.

The Pourbaix diagram for iron shows that a "corrosion triangle" occurs where iron is directly oxidized to ferrous ions. However, at different pH's and potentials, iron is oxidized to insoluble precipitates such as Fe_3O_4 (magnetite) and Fe_2O_3 (hematite). These insoluble oxides can form a passive film, which is a protective layer that inhibits the

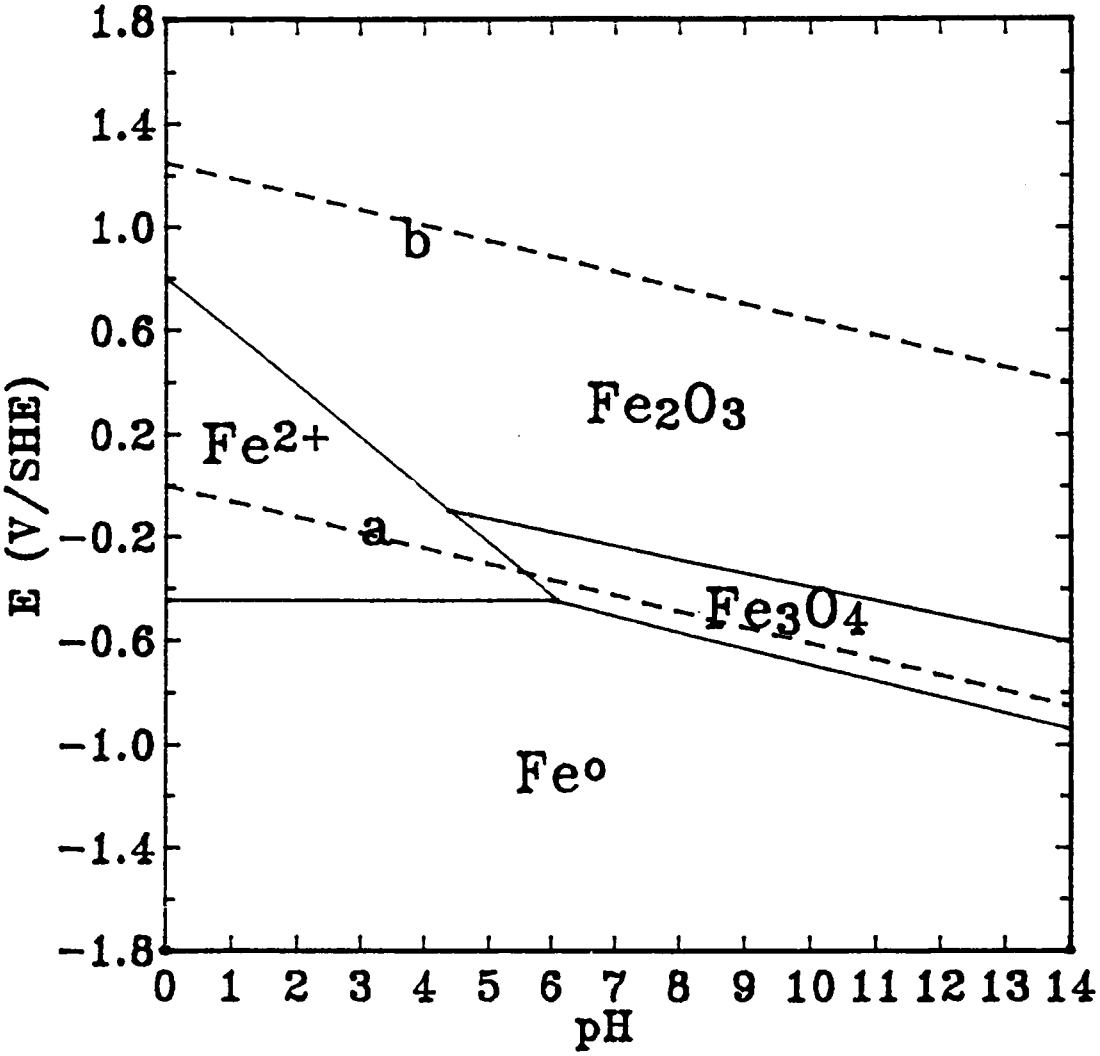

Figure 1. Pourbaix diagram for iron in water.

further oxidation of the metal. If one were to anodically polarize iron in a nonaggressive medium at pH 5, the potential versus current curve would appear as shown in Figure 2. Initially, as the potential was raised from approximately -600 mV/SHE to -200 mV/SHE the current would increase. This current increase would be due to the increased oxidation of the Fe° to Fe^{2+}. When the potential was raised above -200 mV/SHE the current would decrease and then would remain at a constant level up to 1 V/SHE independent of the applied potential. This decrease and leveling of the current would be due to the build up of a passive film which inhibits the further oxidation of iron. Following the passive region on the polarization curve, the current would increase rapidly. In this case, the increase in current would be due to the oxidation of water to hydrogen and hydroxide ions, as shown in line (b) of the Pourbaix diagram. The increase in current at high potentials can also be due to the localized breakdown of the passive film, resulting in localized corrosion.

The Pourbaix diagram shown in Figure 1 shows the thermodynamic equilibria for iron under idealized conditions where no aggressive ions or inhibiting ions are in solution. However, most anions are either aggressive or inhibitory, and therefore can change the equilibria seen in Figure 1. One of the most aggressive anions is chloride which has been studied with respect to its influences on corrosion. Hoar

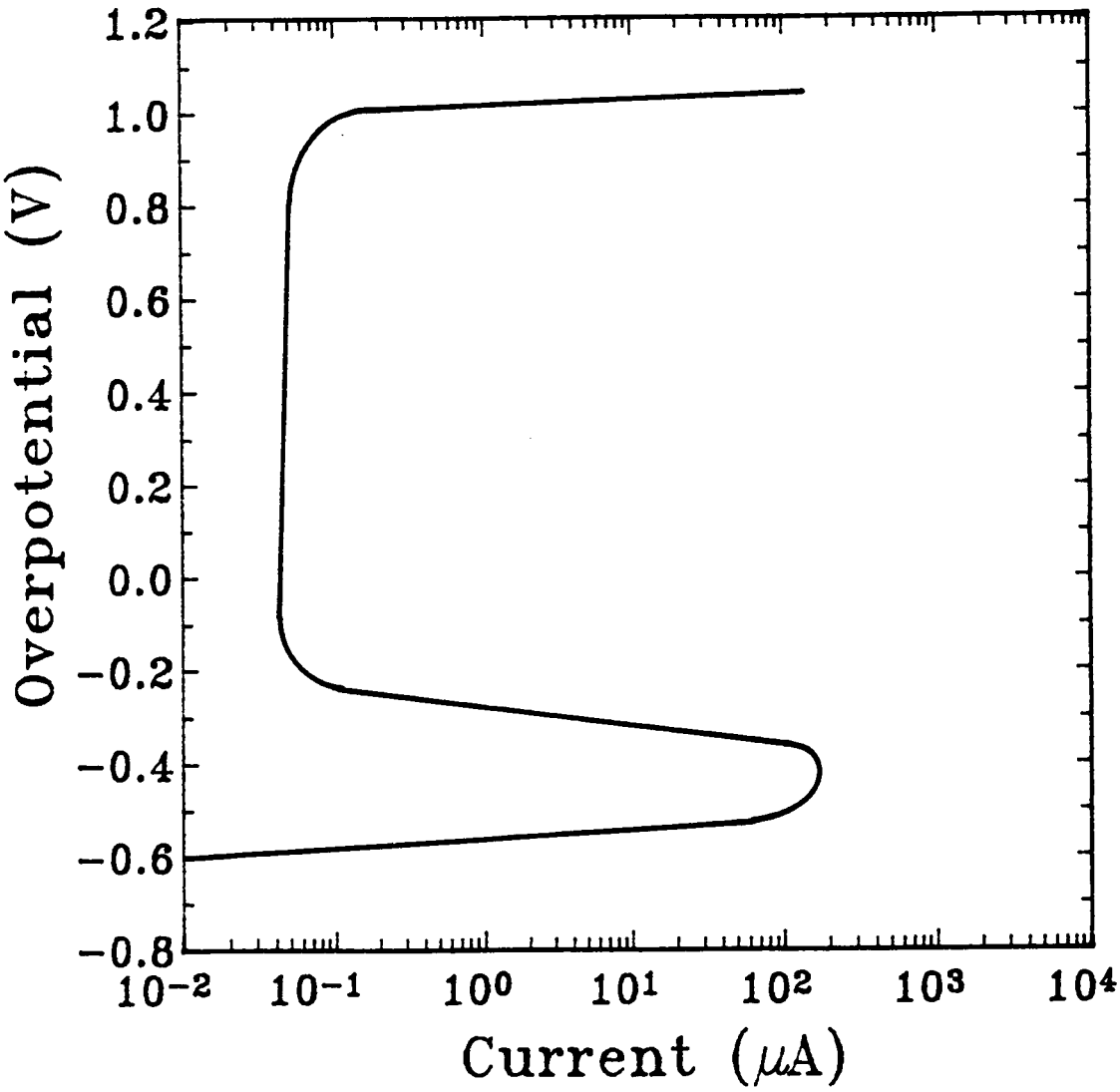

Figure 2. Idealized anodic polarization curve for iron in water at pH 5.

and Jacob (44) have described how chloride reacts with and causes the breakdown of passive films on stainless steel. Pourbaix has diagrammed schematically using pH vs potential diagrams the reactions of iron in a medium containing chloride ions (100). A schematic potential vs current diagram for iron in chloride at pH 9 is shown in Figure 3. The initial regions of active corrosion and passivation were the same as in nonaggressive medium. However, the rapid increase in current observed after the breakdown of the passive film was at a much lower potential than in nonaggressive medium. In addition, upon the lowering of the potential following the breakdown of the passive film, a hysteresis loop was observed. The pits therefore remained active following the lowering of the potential. If the increase in current at high potential was due to the oxidation of water, no hysteresis would have been observed.

Pitting corrosion results when the anodic reaction occurs at a much faster rate at localized sites than on the remaining metal surface. Thus, pitting corrosion results in spatial separation of the majority of the metal oxidation from a majority of the electron consumption. This spatial separation can cause very different conditions to occur in the electrolyte within the pits and over the cathodic areas. As describe above, iron oxidation results in the production of ferrous ions. These ferrous ions can react with oxygen

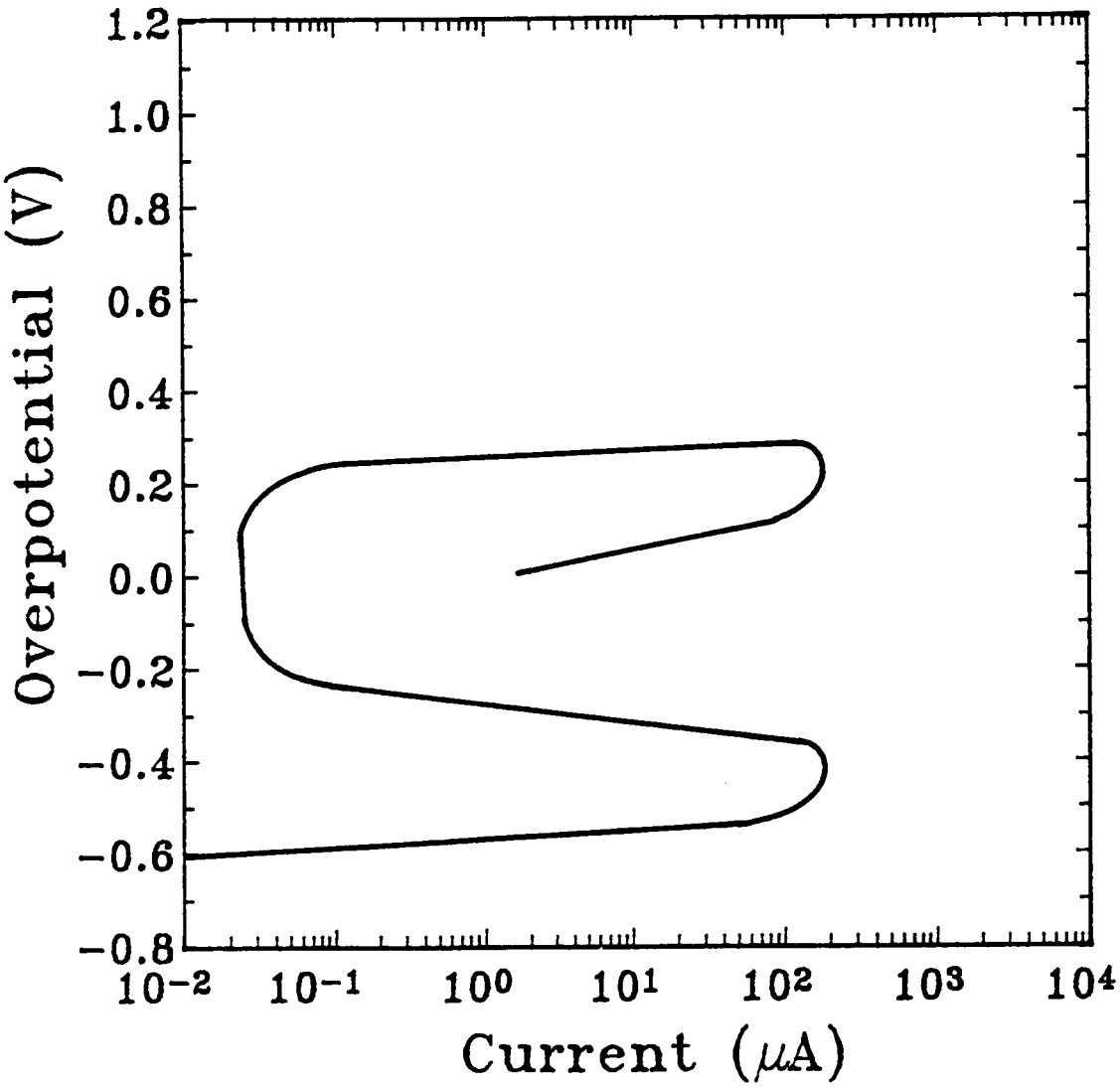

Figure 3. Schematic anodic polarization curve for iron in NaCl solution at pH 9.

or water to form insoluble precipitates by reactions such as (36):

$$Fe^{2+} + H_2O \rightarrow FeOH^+ + H^+ \quad (8)$$

and

$$FeOH^+ + H_2O \rightarrow Fe(OH)_2 + H^+ \quad (9)$$

The hydrolysis of ferrous ions leads to the acidification of the electrolyte within the pits. In order to maintain electroneutrality in the pits anions, including chloride, will migrate to the pits. The lowering of the pH in the pits and the migration of aggressive ions can cause the pits to propagate. The cathodic reaction of oxygen with electrons can produce hydroxide ions, causing an increase in pH over the cathodic areas. Brown (13) introduced the idea of occluded cell corrosion, where the formation of the precipitate over the anodic sites causes the increased acidification within the pits. Using a liquid nitrogen freezing technique, Brown was able to measure pH of 3.8 within pits (12). This phenomenon was also studied by Pourbaix (101) who used an electrochemical cell where the anodic and the cathodic reactions were separated by plexiglass, and the solutions in the two compartments of the cell were connected by a salt bridge. When the small compartment was deaerated and the large compartment was aerated, the small metal in the small compartment became the anode. The measured pH between 4.7 and 2.7 in the medium over the anode, and 10 over the cathode compartment (101).

The potential and the pH of the anodic area are in the area of general corrosion on the Pourbaix diagram. Thus, these conditions should lead to propagation of the pits.

Several aspects of localized corrosion are important with regards to mechanisms of MIC. First the nonuniform colonization of metal by bacteria and respiration of those bacteria could lead to local areas of anaerobiosis. These local sites could become anodic, similar to the deaerated part of Pourbaix's dual cell (101). Second the bacteria, via formation of a biofilm, could cause occlusion of the anodic site, and thus cause the propagation of pits by maintaining the aggressive environment formed in the pitting process (this mechanism is discussed further in Chapter 7).

CORROSION KINETICS

Corrosion kinetics are used to describe the rate at which corrosion reactions proceed, and in particular the rate at which metal dissolution occurs. As the name microbiologically influenced corrosion implies, microorganisms do not necessarily cause corrosion, but rather accelerate the rate of corrosion. Therefore, in any comparative study of MIC it is necessary to compare the rates of corrosion of metal in sterile media to the rates in media containing bacteria. Thus, an understanding of corrosion kinetics is fundamental to the study of MIC. A brief review of corrosion kinetics and a description of the techniques used in this study are described below.

Corrosion kinetics are based on the rate of the half-cell electrochemical reactions occurring on a corroding metal. A current is associated with each half-reaction.

$M \rightarrow M^{n+} + e^-$ (oxidation reaction, $i_{o,m}$) (10)

$M^{n+} + e^- \rightarrow M$ (reduction reaction, $i_{r,m}$) (11)

$Z^+ + e^- \rightarrow Z$ (reduction reaction, $i_{r,z}$) (12)

$Z \rightarrow Z^+ + e^-$ (oxidation reaction, $i_{o,z}$) (13)

With no applied potential the oxidation and the reduction reaction rates must be equal, and no net current flows (129). Therefore;

$$i_{o,m} + i_{o,z} = i_{r,m} + i_{r,z} = i_{corr} \quad (14)$$

where i_{corr} is the exchange current. For most corrosion reactions the $i_{o,z}$ and the $i_{r,m}$ reactions are insignificant. The exchange current, i_{corr}, is directly related to the amount of metal lost to solution by Faraday's law.

$$N/t \quad I_{corr}/nF \quad (15)$$

where N/t is the moles of metal lost per time, n is the

number of electrons involved in the reaction, and F is the Faraday constant. Polarization techniques are used to determine this exchange current, i_{corr}, and thus the corrosion rate. In 1957, Stern and Geary (119) published interpretations of polarization curves which are still used.

At the corrosion potential the anodic current density, $i_{o,m}$, and the cathodic current density, $i_{r,z}$, are equal. However if the sample is polarized sufficiently far from the corrosion potential, the potential is directly proportional to the log of the current by the Tafel equation;

$$n = -\beta_c \log \frac{i_{r,z}}{i_{corr}} \quad \text{(for the cathodic reaction)} \qquad (16)$$

$$n = \beta_a \log \frac{i_{o,m}}{i_{corr}} \quad \text{(for the anodic reaction)} \qquad (17)$$

where n is the overpotential (potential applied minus the open circuit potential (OCP), β_c and β_a, are the Tafel constants for the cathodic reaction and for the anodic reaction, respectively, and i_{corr} is the corrosion current density. I_{corr}, can be determined from the intersection of the cathodic and the anodic reactions at the OCP. In actual experiments, the Tafel lines do not intersect, and polarization curves like Figure 4 are usually obtained. Figure 4 again is simplified in that it assumes no passive film forms on the surface. In Figure 4, i_{corr}, can be determined by extrapolating the Tafel slopes to the OCP.

Figure 4 shows that the measured current deviates from linear Tafel behavior at very high applied potentials and at low applied potentials. The reasons for these deviations are discussed by Stern and Geary (119). Briefly, at high applied potential the deviations can be due to concentration

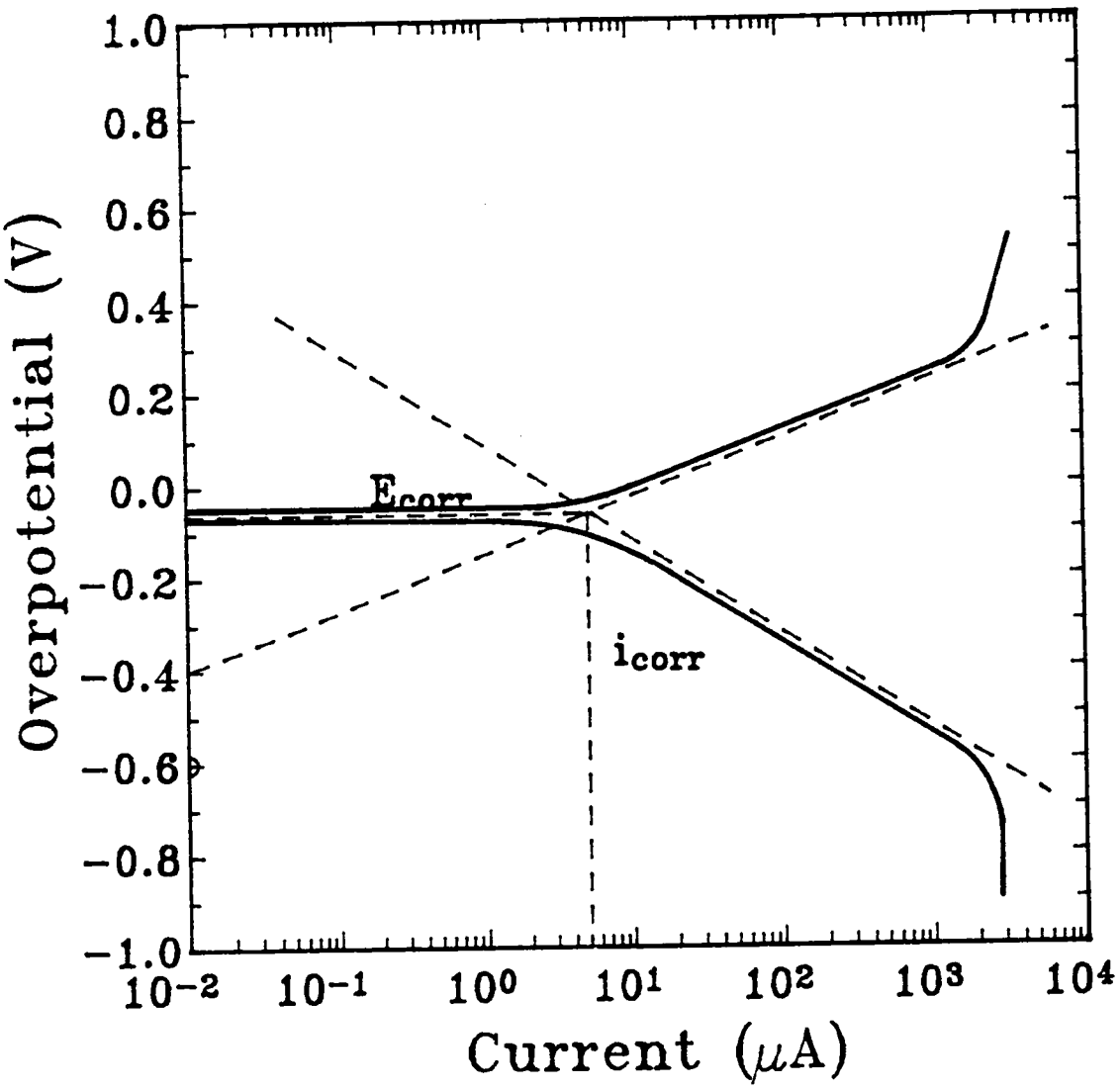

Figure 4. Schematic anodic and cathodic polarization curves for a corroding metal sample.

polarization, where the reacting species in solution, such as hydrogen ions for the cathodic reaction, are consumed at the electrode surface faster than they diffuse to the surface. The deviation at high applied potential can also be due to the potential drop in solution, caused by the solution resistance. The deviation from Tafel behavior at low applied potentials is due to the fact that each half reaction cannot be measured independently. At these low potentials the reverse reaction contributes to the measured current. For example, if the sample is polarized anodically, the cathodic reaction contributes to the measured current, i_{meas}, such that;

$$i_{meas} = i_{o,m} - i_{r,z} \qquad (18)$$

This is true until the sample is anodically polarized sufficiently so that the cathodic reaction becomes insignificant with respect to the anodic reaction. The region of polarization close to the open circuit potential, approximately OCP $\pm$ 20 mV, is termed the linear region, since a plot of current versus potential gives a linear or Ohmic response.

Stern and Geary (119) derived an expression where analysis of the linear region could be used to estimate the corrosion rate. Rearranging equations 16 and 17 and substituting those equations into equation 18 yields;

$$i_{meas} = i_{corr}[10^{-n/\beta c} - 10^{n/\beta a}] \qquad (19)$$

For simplification the following estimates can be made (since the overpotential applied is low)

$$10^{n/\beta a} = 1 + 2.3n/\beta a \qquad (20)$$

$$10^{-n/\beta c} = 1 - 2.3n/\beta c \qquad (21)$$

Substituting these expression into equation 19 gives

$$i_{meas} = 2.3 i_{corr} n(\beta_a + \beta_c/\beta_a\beta_c) \qquad (22)$$

n/i_{meas} is the resistance, which is the sum of the polarization resistance (R_p) and the solution resistance. Therefore, assuming negligible contribution from the solution resistance;

$$R_p = \frac{\beta_a\beta_c}{2.3\ i_{corr}\ (\beta_a + \beta_c)} \qquad (23)$$

From equation 23 it can be seen that the polarization resistance is inversely proportional to the corrosion rate, i_{corr}. Since the Tafel constants rarely deviate much from a value of 0.1, the polarization resistance can be used to estimate the corrosion rate (118). This is advantageous since the Tafel method requires high applied currents and is destructive to samples, whereas the polarization resistance technique (termed linear polarization) does not require high currents. Using linear polarization, Stern (118) found a linear relationship between the inverse of the polarization resistance and the weight loss of various iron samples in sulfuric acid.

ELECTROCHEMICAL IMPEDANCE SPECTROSCOPY

The linear polarization method developed by Stern and Geary (119) uses very low scan rate, which is equivalent to one low frequency. At low frequencies the total resistance, R_p plus the solution resistance, R_s, impedes the flow of current, and therefore the sum of these values can be obtained as described above. However, the resistance is not the only factor which can impede the flow of current. The impedance to applied potential can be visualized as an electrical circuit as shown in Figure 5A. This simple circuit consists of the solution resistance, the polarization resistance, and the double layer capacitance in parallel with the polarization resistance. Epelboin et al. (27,28) applied alternating signals at a wide range of frequencies to corroding iron to obtain information with regards to the mechanisms of iron dissolution. In this way a spectrum of response to the alternating potentials at a range of frequencies could be determined. The technique is now referred to as electrochemical impedance spectroscopy (EIS).

The analysis of corrosion rates by EIS has been reviewed by Mansfeld et al. (80,81) and Lorenz and Mansfeld (77). When a sinusoidal potential is applied to a metal in solution, the resulting current is impeded by the resistance of the solution, the resistance of the metal-electrolyte interface, and the double layer capacitance of the

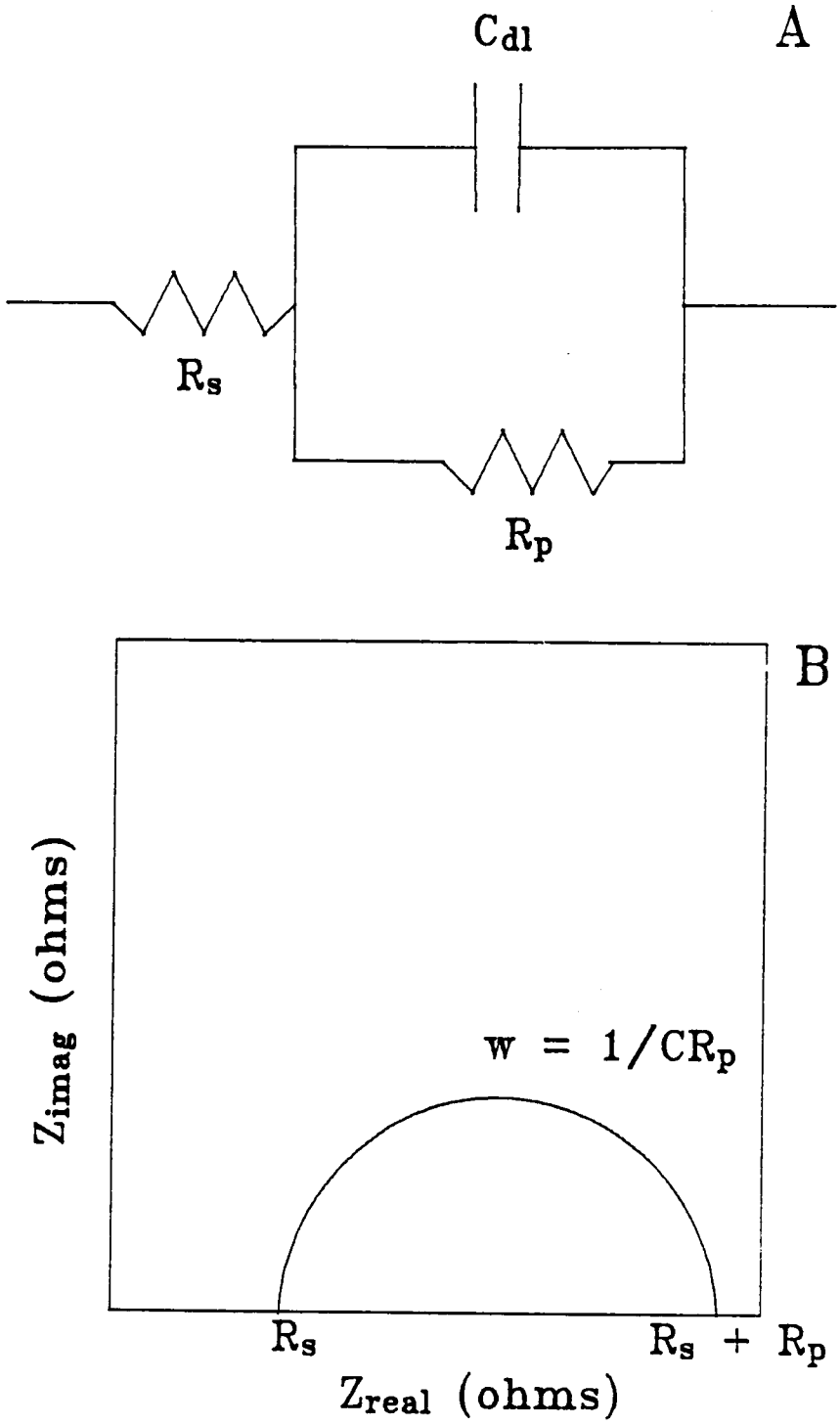

Figure 5. A) Electrical circuit used to model the impedance of a metal in solution. B) Nyquist plot for the impedance at a range of frequencies for the circuit shown in A.

interface. For example as in the circuit shown in Figure 5A. The resistors cause a sinusoidal current to flow which is in phase with the applied potential. This part of the impedance is termed the real impedance, Z_{real}. The capacitors result in the sinusoidal current to be out of phase with the applied potential, termed the imaginary impedance, Z_{imag}. The total impedance is obtained by;

$$Z_{total} = Z_{real} + jZ_{imag} \qquad (24)$$

j is the square root of -1. Expressions for the real and the imaginary component of the impedance have been derived (7,37,77,78). For the simple circuit shown in Figure 5A the equations are;

$$Z_{real} = R_s + \frac{R_p}{1 + w^2C^2R_p^2} \qquad (25)$$

and

$$Z_{imag} = \frac{wCR_{p2}}{1 + w^2C^2R_p^2} \qquad (26)$$

where C is the double layer capacitance, and w is the angular frequency of the applied signal. The admittance, Y, is the inverse of the impedance. The real and the imaginary components of the impedance are related to the admittance as a function of frequency by;

$$Z_{real} = \frac{Y_{real}}{Y_{real}^2 + Y_{imag}^2} \qquad (27)$$

and

$$Z_{imag} = \frac{Y_{imag}}{Y_{real}^2 + Y_{imag}^2} \qquad (28)$$

substitution of 27 and 28 into 24 gives;

$$[Z_{real} - (R_s + 1/2R_p)]^2 + Z_{imag}^2 = (1/2R_p)^2 \qquad (29)$$

Equation 29 is the equation for a semicircle when Z_{imag} is plotted versus Z_{real}. A plot of the semicircle shown for the circuit in Figure 5A is shown in Figure 5B. The difference between the impedance at the high frequencies and the origin is the uncompensated resistance (solution resistance). The diameter of the semicircle (the difference between the impedance at high frequencies and at low frequencies) is the polarization resistance. The double layer capacitance can be determined from the frequency at the maximum phase shift by the expression;

$$w_{max} = \frac{1}{CR_p} \qquad (30)$$

By obtaining this spectrum of response, parameters involved in corrosion reactions in addition to the polarization resistance can be obtained, such as the double layer capacitance and the solution resistance (80,81). As the applied frequency approaches infinity, the double layer capacitance does not impede the flow of current and only the solution resistance contributes to the impedance. As the applied frequency approaches zero, the resistance is analogous to the linear polarization technique. The current is completely impeded by the double layer capacitance, and

the current must flow through the solution resistance and the polarization resistance. At higher frequencies than what are applied in the linear polarization technique, the double layer capacitance of the corroding electrode can impede the flow of current.

If the response is more complicated than the one diagramed in Figure 5, EIS can be used to obtain some mechanistic data with regards to corrosion. In particular, models have been developed to evaluate the EIS response to pitting corrosion (94), and to corrosion where three dimensional deposits (65), such as corrosion products, develop on the surface of corroding electrodes.

EIS has been used in studies of microbial influenced corrosion (25,66). In chapters 1 and 3 of this study, EIS was used to help determine the effects of biofilms on carbon steel corrosion, and to determine the effect of biocide treatments on the biofilms and on the carbon steel corrosion.

SCANNING VIBRATING ELECTRODE TECHNIQUE

The above discussion demonstrates that i_{corr} and R_p can be used to indicate the rates at which metal corrodes in aqueous solutions, and therefore can be used in comparative studies of MIC. However, as mentioned above, much of the corrosion attributed to microbial biofilms and activity is localized. Localized corrosion, although giving low corrosion rates, tends to be more severe than uniform corrosion, since it can cause rapid penetration of metal structures. Therefore, techniques have been developed to study the rates of penetration of metals at localized sites. Post test microscopic analysis of pits is the main technique used to evaluate localized corrosion. Techniques which physically separate local anodic and cathodic sites have been used (101). Physical separation of anodic and cathodic sites have also been used in MIC studies (23,40,73).

In 1967, Rosenfeld and Danilov (109) developed a microelectrode technique, where the local anodic and cathodic sites on a metal sample could be scanned <u>in situ</u>. This technique was further developed by Butler et al. (16) and Isaacs and coworkers (45,46,58,128) to study pitting corrosion of steels and weldments, intergranular corrosion, stress corrosion cracking, and galvanic corrosion. The technique was made more sensitive by using the microelectrode in conjunction with applied sinusoidal potentials to the metal sample under study (57). Analyses by the scanning microelectrode technique were difficult due to the high impedance of the capillary tip electrode, which

caused low signal to noise ratio. Isaacs (55,56) used a technique, developed by Jaffe and Nuccitelli (61) to map ionic currents associated with individual living cells, to scan the anodic and cathodic sites over corroding metal. This technique used a vibrating microelectrode which converted the potential fields associated with localized corrosion into alternating signals. All frequencies except the frequency of electrode vibration could be filtered, thus reducing the noise inherent in the scanning microelectrode technique. This advance increased the signal to noise ratio over 100 fold compared to the scanning capillary electrode technique (61).

Since the scanning vibrating electrode technique (SVET) is nondestructive to the sample (requires no applied current) the technique has found wide use on in situ studies of corrosion. The SVET has been used to study the pitting corrosion of iron and stainless steel (50,51,55,56), galvanic corrosion of lead solder (48), defects in ion vapor-deposited aluminum on steel (47), and corrosion inhibition with dissolved cerium (54).

The SVET makes use of the fact that in localized corrosion the local anodic sites are separated from the local cathodic sites. As mentioned above, current flows within the metal between the anodic and cathodic sites. However, the metal does not provide sufficient resistance to allow measurement of the sites on the metal surface. In addition to the flow of current in the metallic phase, ionic currents flow in solution from the local anodic to the local

cathodic sites. Due to this flow of current and the resistance of the electrolyte, potential fields are established in the electrolyte perpendicular to the flow of current by Ohm's law. The potential fields over a local anodic site are shown schematically in Figure 6 (45). Figure 6 shows an exponential decay in the change in potential field with increasing distance from the anodic site. However, if a microelectrode is sufficiently close to the metal surface the change in potential fields can be mapped, and if the microelectrode is vibrating the potential fields can be converted into an alternating signal. A lock-in amplifier is used to "lock-in" on the sinusoidal signal, filter noise not associated with that signal, and amplify the signal for analysis. Isaacs has discussed the theory for the vibrating electrode analysis, including the SVET applications and limitations (49,52).

A major limitation of the technique is that the SVE is positioned a certain distance in solution above the sample. Therefore the potential field in solution is determined rather than the current density at the surface (which provides the corrosion rate). Therefore, the technique, although providing qualitative information, may not provide quantitative information with regards to the corrosion rate. In addition if the probe is positioned too close to the surface, the probe interferes with the current flow and causes erroneous measurements (52). If the probe is positioned too close to the surface, the field cannot be considered uniform and the AC signal is distorted (52).

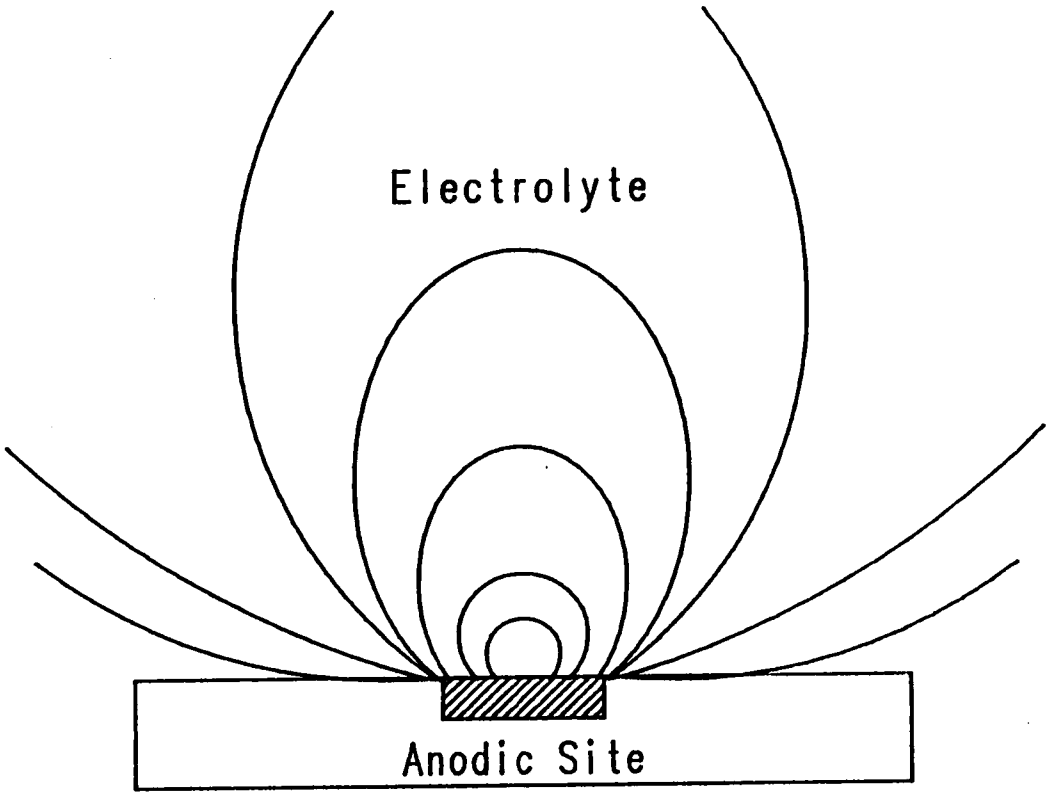

Figure 6. Potential field in solution over local anodic site.

The principles of the vibrating electrode technique, described below, were discussed by Isaacs (52). The potential at any point in solution, V, is related to a point current source, I, by the equation

$$V = \frac{pI}{2\pi r} \qquad (31)$$

where p is the solution resistance, and r is the point in solution for the x position, the y position and the height, z, by the equation $r = (x^2 + y^2 + z^2)^{0.5}$. The normal field, F_z, measured by the vertically vibrating electrode is obtained by partial differentiation of equation 100 with respect to z;

$$F_z = \frac{\delta V}{\delta z} = \frac{pIz}{2\pi(x^2 + y^2 + z^2)^{1.5}} \qquad (32)$$

The equation for the sinusoidal vibrations for the vibrating electrode with vibration amplitude, $2\Delta z$, for a fixed height of z_o, is;

$$z = z_o + \Delta z \sin(wt) \qquad (33)$$

where w is the angular frequency and t is the time. Substituting equation 33 into 31 gives the AC signal produced by the vibrating electrode at any position above a point sources of current. When the vibrating electrode is directly above the point source, the AC signal produced is;

$$V = \frac{pI}{2\pi z_o[1 + (\Delta z/z_o) \sin(wt)]} \qquad (34)$$

Using models of point sources of current, equipotential discs, and uniform current discs, as well as experimentation on sources of current through capillary tubes (to simulate a conducting disc), Isaacs (53) has studied the effect of probe height above a sample on the current distribution measured with the vibrating electrode. From these studies he concluded that "1) the shape of a current source can be determined when the probe height is less than 0.5 times the radius of the perimeter of the current sources. 2) At heights greater than 2 times the radius of the current source the variations in the field approximate those expected from a point current source. 3) The variations in field in solution above an electrode can be simulated by substituting point current sources for the currents from an array of elemental areas of the electrode, with less than 5% error" (53). Based on these studies it is possible in some situations to use the SVET in a nondestructive manner to estimate the current densities at the electrode surface, and thus establish corrosion rates. This procedure was used to estimate the corrosion rates of the galvanic corrosion of soldered copper (48).

In the present studies, the SVET was used to study the pitting corrosion of steel influenced by bacterial biofilms, and to indicate the relationships between the localized corrosion of steel and the localized metabolic activity of bacteria in biofilms.

PROPOSED MECHANISMS FOR MIC

The study of MIC is complicated by the fact that multiple metabolic activities occur in bacteria simultaneously, and these activities within biofilms are not easily studied. Thus, conclusion on the effect of any one activity, such as hydrogenase activity, for the corrosion of metal are probably greatly over simplified. In addition often the media used in MIC studies contains undefined components such as yeast extract, buffers, and higher concentrations of aggressive or inhibiting ions than found in natural environments. The role of the medium components on the observed corrosion is rarely accounted for, although the components can greatly affect the corrosion of the metal. Thus, in addition to the many metabolic activities occurring in bacteria, the components of the electrolytes may directly affect the results of MIC studies.

Corrosion influenced by bacteria was first proposed by von Wulzoger Kuhr and van der Vlugt in 1934 (127). Little work was performed on MIC again until the 1960's with papers by Booth and Tiller (9,10,11) on corrosion by sulfate reducers. In the 1980's work on MIC again initiated, including studies on the effect of biofilms on stainless steel corrosion in seawater and the effect of bacteria other than sulfate reducing bacteria on corrosion. Corrosion influenced by microorganisms is gaining increasing interest at meetings of the National Association of Corrosion

Engineers, and at the recent International Congress on Microbial Influenced Corrosion. Understanding of mechanisms should develop more rapidly with the recent development of electrochemical and analytical microbiological techniques.

Several reviews have recently been written on mechanisms of MIC and on electrochemical evaluation of MIC (26,41,75,82,96,123). Probably the most studied putative mechanism for MIC is the cathodic depolarization theory, proposed by von Wolzogen Kuhr and van der Vlugt (127) as a mechanism of corrosion facilitation by sulfate reducing bacteria under anaerobic conditions. The idea follows that the overall corrosion reaction under anaerobic conditions is as follows;

$$Fe + 2H_2O \rightarrow Fe^{2+} + H_2 \qquad (35)$$

The hydrogenase containing sulfate reducing bacteria should be able to "pull" the thermodynamic equilibrium of this reaction to the right by removing the hydrogen and thus accelerate corrosion. However, the Pourbaix diagram for iron in water demonstrates that the reaction of iron with water does not reach a thermodynamic equilibrium under normal conditions (101) (less than 1 atm of H_2, and greater than 5 M ferrous ions), and is therefore not a reversible reaction. Pourbaix states that "contrary to copper, metallic iron may never be thermodynamically stable in the presence of water under the usual conditions of temperature and pressure. Among the many reactions which may occur

inside iron pits, some may not reach a state of equilibrium (corrosion of active iron, hydrogen evolution)" (101). Thus, the "cathodic depolarization" theory ascribes thermodynamic processes to a system which likely never reaches thermodynamic equilibrium. In any event, the rate of the metal oxidation is dependent on the corrosion kinetics, not on the concentration of end products, such as hydrogen. The only way in which hydrogen utilization may speed up a corrosion reaction is if mass transport of hydrogen from the surface becomes the rate limiting step. Except when a cathodic current is imposed on metal, such as in cathodic protection, mass transport of hydrogen from a metal is not likely to be the rate-limiting step (21). Crolet (21) pointed out that the theory of cathodic depolarization was formulated prior to our present understanding of corrosion kinetics, and although it was the best explanation at the time (1934), it cannot be used to describe rates of corrosion reactions in terms of our modern understanding of electrochemistry.

Although the cathodic depolarization mechanism is not likely to occur under natural conditions, many papers in the 1960's and as recently as 1988 have provide "direct evidence" in favor of the theory. In 1960 Booth and Tiller (9), using polarization curves, showed that sulfate reduction by both the hydrogenase positive Desulfovibrio vulgaris and the "hydrogenase negative" Desulfotamaculum

orientus resulted in a sulfide film on the electrode which accelerated the anodic reaction, but only D. vulgaris was able to depolarize the cathodic reaction. Recently it was shown that D. orientus does contain intracellular hydrogenase, and is able to grow autotrophically at the expense of hydrogen, sulfate, and CO_2. Thus, it is apparent that other properties of the organisms must be considered in order to describe the observed results, and not merely the presence or absence of hydrogenase. Similar experiments comparing corrosive effects of hydrogenase positive and hydrogenase negative sulfate reducers have been performed (10,11) and as recently as 1988 (23). In some studies benzyl viologen or fumarate were used as electron acceptors for the sulfate reducers rather than sulfate in order to eliminate the corrosive effects of the sulfide produced during sulfate reduction (23,59). However, the corrosive effects of these compounds was not evaluated. In addition all of these studies used rich media with high concentrations of phosphate. Phosphate acts as a corrosion inhibitor but becomes less effective in the presence of bacteria (Chapter 6). Changes in the medium components may have led to the observed effects.

Several studies have shown that sulfate reducing bacteria and methanogens utilize hydrogen produced during the cathodic reaction (20,22,95). However, as mentioned

utilization of hydrogen does not necessarily facilitate corrosion rates.

A more likely role for the increased corrosion rates in the presence of sulfate reducers, is in the production of sulfide. This was recognized in the 1960's and 1970's by Booth and Tiller (11) and King et al (68). They showed a correlation between the weight loss of carbon steel and the concentrations of ferrous sulfide. Salvarezza and Videla (111) used polarization curves to test the effects of various concentrations of added sulfide, in sterile media, and the effects of sulfate reducing bacteria on the pitting potential of carbon steel in seawater. They found that both the added sulfide and the sulfate reducing bacteria caused a lowering of the pitting potential compared to sterile media without sulfide. Those results demonstrated that the sulfate reducers caused a change of the steel passive film, and that the effects were similar to the addition of sulfide. Ringas and Robinson (104,105) also showed changes in the electrochemical properties of carbon steel and stainless steel in the presence of sulfate reducing bacteria. They showed a decrease in the pitting potential of the steel, suggesting that the sulfide altered the properties of the passive film. They also found that the sulfide induced pits were formed at lower potentials than chloride induced pits. Those results suggested that sulfide may be more aggressive to the steel than chloride.

Sulfide appears to be particularly aggressive to steel which is exposed to anaerobic and subsequently to aerobic media (43). Newman et al. (88) demonstrated that sulfide can be particularly aggressive to stainless steel in the presence of oxygen, even at low chloride and sulfide concentrations. They suggested that the sulfide is oxidized to thiosulfate which causes rapid pitting of stainless steel. They proposed that where bulk solutions are aerobic, but where anaerobic environments form within biofilms, sulfide may be produced by the sulfate reducing organisms. As the sulfide diffuses to aerobic zones, the sulfide may be oxidized to the aggressive thiosulfate ion. They suggested that this may account for the rapid pitting which occurs in stainless steel under fresh water conditions.

The role of microorganisms other than sulfate reducing bacteria has received increasing attention in recent years. Among these studies have been the effect of undefined biofilms formed on stainless steel in seawater. Several investigators have observed changes in the open circuit potential (OCP) in the positive direction when biofilms formed on the steel (24,64,87,117). This shift in the OCP could increase the potential of the steel from the region in which the steel is passive to the transpassive region, resulting in pitting corrosion. Mollica et al. (87) have demonstrated that the increase in the OCP caused by the activity of the biofilm increased the probability of

localized corrosion initiation, and pitting propagation. They explained the increase in potential due to the biofilm by the unlikely mechanism that the bacteria in the biofilm increased the oxygen reduction kinetics at the cathode (87). More recently, Little et al. (76) have used microelectrodes to provide a more plausible mechanism for the increase in potential. They demonstrated that the potential of the steel increased in the presence of light, but showed a drop in the darkness. They demonstrated that in light the attachment of algae predominated. Using oxygen microelectrodes they showed an increase in oxygen near the surface of the steel correlating to a positive shift in OCP. In the dark, bacterial biofilms predominated and the surface of the steel was essentially anaerobic. In this case the potential dropped. Thus, changes in the OCP on steel in seawater was predominantly due to changes in the dissolved oxygen concentration at the metal-seawater interface.

Another proposed mechanism of MIC is the localized lowering of the pH by the production of organic and inorganic acids. Little et al. (73) have shown, using a dual cell technique where the anodic and cathodic reactions can be physically separated, that a thermophilic bacterium induces anodic activity of nickel electrodes. This anodic activity could also be induced by the addition of isovaleric and isobutyric acid to one side of the cell (73). In addition, Little et al. (74) demonstrated that an acetic

acid producing bacterium could dissolve the calcarious deposit formed on cathodically protected stainless steel, resulting in an increased current demand to maintain the potential at -900 mV/SCE. Phelps et al. (97,98) have demonstrated in situ production of ^{14}C-acetic acid from hydrogen and ^{14}C-CO_2 in gas transmission pipelines by acetogenic bacteria. They have suggested that acid production can be responsible for failures of these pipelines.

Several other proposed mechanisms of MIC have been suggested. These mechanisms include disruption of passive films formed on carbon steel by iron reducing bacteria. In those studies, under sterile conditions in the presence of nitrite a "protective" film formed on carbon steel samples. However when the iron reducing bacterium was added, the film was removed over time. The removal of the film corresponded to an increase in the current densities observed during anodic polarization of the samples. The authors proposed that the bacteria were able to reduce the insoluble ferric ions on the metal to soluble ferrous ions, and thus breakdown the protective film.

Differential aeration on steel surfaces leading to differential polarization of the sample has been proposed as a MIC mechanism (73). This mechanism has been addressed by Little et al. (73), using the dual cell technique. They showed that the nickel electrode on the deaerated side of

the cell can become the anode, while the electrode exposed to aerated solution becomes the cathode. Those results are in agreement with the results of Pourbaix (100).

The effect of bacterial extracellular polymer on the corrosion of metals has also been studied. Nivens et al. (91) showed a direct correlation between the increase in the corrosion current density of stainless steel and the bacterial extracellular polymer, observed by Fourier transform infrared spectroscopy. Removal of the bacteria and the polymer from the surface resulted in a decrease in the corrosion current density. Those results suggested that the production of bacterial polymer either directly accelerated the corrosion rate or indirectly accelerated the corrosion rate by creating differential oxygen cells. Geesey et al. (39) have seen a similar effect in the corrosion of copper. They proposed a model where the accelerated corrosion was due to the binding of copper by the bacterial polymer creating a galvanic corrosion effect.

Most of the mechanistic studies described above used pure cultures of bacteria in rich microbiological media. Jack (60) studied the effects of mixed microbial communities on the corrosion of carbon steel in a low nutrient flowing medium. He showed that biofilms containing sulfate reducers had accelerated corrosion compared to biofilms without sulfate reducers. The differences may have been due to the production of hydrogen sulfide.

SUMMARY

The same concepts used to describe corrosion attributed to chemical corrosion can be used to describe MIC. However two important differences complicate MIC. First, the bacteria which cause MIC are living organisms within biofilms. The processes which occur in biofilms are dynamic and may not resemble the processes which occur in the much easier studied bulk phase. Thus, activities which affect corrosion, either direct enzymatic activities or changes in the environment in close contact with the metal surface, including acid production and sulfide production, are inherently difficult to define within biofilms. In addition, these reactions probably change with time. Second, biofilms tend not to be uniform over surfaces, but are generally arranged in microcolonies. Thus, even if the activities attributed to MIC can be defined, those activities may vary spatially.

The attributes of MIC described above have made the study of MIC difficult. However, if we are to better understand MIC processes and to mitigate MIC problems, specific research approaches will be required. First, studies must include studies of activities of bacteria within biofilms, and preferably these studies should be used to localize activities in time and space. Second, studies must determine the effect of these processes on corrosion, taking into account known corrosion phenomena. Again,

studies would preferably be able to resolve corrosion processes in time and space, since bacterial activities are not uniform or constant on surfaces.

In this research, approaches taking into account these criteria, were used to help address mechanisms of MIC. In Chapter 1, a system for study was developed. Bacteria from failed steel pipes were isolated and characterized. The bacteria were introduced into a laboratory system, to determine if corrosion, similar to that observed in the field, i.e. localized corrosion, with the formation of tubercles, could be achieved under laboratory conditions. Chapters 2 and 4 evaluate the electrochemical techniques used in these studies. In Chapter 2 determination is made as to whether the electrochemical impedance spectroscopy technique (EIS) is destructive to the biofilms. In Chapter 4 determination is made as to whether the scanning vibrating electrode technique (SVET) can be used to resolve MIC processes in time and in space, nondestructively. Chapters 5, 6, and 7 determine the effects of biofilms as well as medium components on the localized corrosion of steel as observed by the SVET. Chapter 8 describes techniques used to spatially and temporally resolve bacterial activity, in this case biosynthetic activity, and compares this activity to the localized electrochemical reactions, observed by SVET. Chapter 3 describes how studies of bacterial viability and activity, as well as the electrochemical

activity can be used to test the effectiveness of certain countermeasures, in this case biocide treatment, on the biofilms and on the corrosion of the metal.

LITERATURE CITED

1. Absolom, D.R., F.V. Lamberti, Z. Policova, W. Zingg, C.J. van Oss, and A. W. Neumann. (1983) Surface thermodynamics of bacterial adhesion. Appl. Environ. Microbiol. **46**:90-97.

2. Alberti, L., and R.M. Harshey. (1990) Differentiation of Serratia marcescens into swimmer and swarmer cells. J. Bacteriol. **172**:4322-4328.

3. Amann, R.I., L. Krumholz, and D.A. Stahl. (1990) Flourescent-Oligonucleotide probing of whole cells for determinative, phylogenetic, and environmental studies in microbiology. J. Bacteriol. **172**:762-770.

4. Bard, A.J., and L.R. Faulkner. (1980) Techniques based on concepts of impedance in Electrochemical Methods pp. 316-369 John Wiley and Sons, New York.

5. Baier, R.E., (1980) Substrata influences on the adhesion of microorganisms and their resultant new surface properties, in Adsorption of Microorganisms to Surfaces, (G. Bitton and K. Marshall, eds.) Wiley-International Publishers, 59-104.

6. Bartlett, D.H., M.E. Wright, and M. Silverman. (1988) Variable expression of extracellular polysaccharide in the marine enviornment bacterium Pseudomonas altlantica is controlled by genome rearrangement. Pro. Natl. Aca. Sci. U.S.A. **85**:3923-3927.

7. Belas, R., M. Simon, and M. Silverman. (1986) Regulation of lateral flagella gene transcription in Vibrio parahaemolyticus. J. Bacteriol.**167**:210-218.

8. Bobbie, R.J., and D.C. White. (1980) Characterization of benthic microbial community structure by high-resolution gas chromatography of fatty acid methyl esters. Appl. Environ. Microbiol. **39**:1212-1222.

9. Booth, G.H., and A.K. Tiller. (1960) Polarization studies of mild steel in cultures of sulfate-reducing bacteria. Trans. Faraday Soc. **56**:1689-1697.

10. Booth, G.H., and A.K. Tiller. (1962) Polarization studies of mild steel in cultures of sulfate-reducing bacteria. Part 3 - halophilic organisms. Trans. Faraday Soc. **58**:2510-2516.

11. Booth, B.F., and A.K. Tiller. (1968) Cathodic characteristics of mild steel in suspensions of sulphate-reducing bacteria. Corrosion Science **3**:583-600.

12. Brown, B.F. (1969) Methods for studying the solution chemistry within stress corrosion cracks. J. Electrochem. Soc. **116**:218-219.

13. Brown, B.F. (1970) Concepts of the occluded corrosion cell. Corrosion **26**:249-250.

14. Bryers, J.D., and W.G. Characklis. (1982) Processes governing primary biofilm formation. Biotech. Bioeng. **14**:2451-2476.

15. Burlage, R.S., G.S. Sayler, and F. Larimer. (1990) Monitoring of naphthalene catabolism by bioluminescence with nah-lux transcriptional fusions. J. Bacteriol. **172**:4749-4757.

16. Butler, G., P. Stretton, and J.G. Beynon. (1972) Initiation and growth of pits on high-purity iron and its alloys with chromium and copper in neutral chloride solutions. Br. Corrosion J. **7**:168-173.

17. Characklis, W.G. (1981) Fouling biofim development: A process analysis. Biotech. Bioeng. **13**:1923-1960.

18. Characklis, W.G., and K.E. Cooksey. (1983) Biofilms and microbial fouling. Adv. Appl. Microbiol. **23**:93-138.

19. Characklis, W.G., and K.C. Marshall (eds.). (1990) Biofilms John Wiley and Sons, Inc. New York.

20. Cord-Ruwisch, R. and F. Widdel. (1986) Corroding iron as a hydrogen source for sulfate-reduction in growing cultures of sulfate reducing bacteria. Appl. Microbiol. and Biotechnol. **25**:169-174.

21. Crolet, J.L. From biology and corrosion to biocorrosion. (submitted Br. Corrosion J.)

22. Daniels, L., N. Belay, B.S. Rajagopal, and P.J. Weimer. (1987) Bacterial methanogenesis and growth from CO_2 with elemental iron as the sole source of electrons. Science **237**:509-511.

23. Daumas, S., Y. Massiani, and J. Crousier. (1988) Microbiological battery induced by sulfate reducing bacteria. Corrosion Science **28**:1041-1050.

24. Dexter, S.C., and G.Y. Gao. (1988) Effect of seawater biofilms on corrosion potential and oxygen reduction of stainless steel. Corrosion **44**:717-723.

25. Dowling, N.J.E., J. Guzennec, M.L. Lemoine, A. Tunlid, and D.C. White. (1988) Analysis of carbon steels affected by bacteria using electrochemical impedance and direct current techniques. Corrosion **44**:869-874.

26. Duquette, D.J., and R.E. Ricker. (1986) Electrochemical aspects of microbiologically induced corrosion.

27. Epelboin, I., and M. Keddam. (1970) Faradaic impedances: Diffusion impedance and reaction impedance. J. Electrochem. Soc. **117**:1052-1056.

28. Epelboin, I., M. Keddam, and H. Takenouti. (1972) Use of impedance measurements for the determination of the instant rate of metal corrosion. J. Appl. Electrochem. **2**:71-79.

29. Findlay, R.H., P.C. Pollard, D.J.W. Moriarty, and D.C. White. (1985) Quantitative determination of microbial activity and community nutritional status in estuarine sediments: evidence for a disturbance artifact. Canad. J. Microbiol. **31**:493-498.

30. Fletcher, M. (1979) A microautoradiographic study of the activity of attached and free-living bacteria. Arch. Microbiol. **122**:271-274.

31. Fletcher, M. (1980) The question of passive versus active attachment mechanisms in non-specific bacterial adhesion. in Microbial Adhesion to Surfaces pp. 197-210. (R. Berkeley, J. Lynch, J. Melling, P. Rutter, and B. Vincent eds.) Horwood, Chichester.

32. Fletcher, M. (1986) Measurement of glucose utiliztion by Pseudomonas fluorescens that are free-living and that are attached to surfaces. Appl. Environ. Microbiol. **52**:672-676.

33. Fletcher, M. (1988) Attachment of Pseudomonas flourescens to glass and influence of electrolytes on bacterium-substratum separation distance. J. Bacteriol. **170**:2027-2030.

34. Ford, T.E., J.P. Black, and R. Mitchell. (1990) Relationship between bacterial exopolymers and corroding metal surfaces. CORROSION/90 paper no. 190, National Association of Corrosion Engineers. Las Vegas, Nv.

35. Ford, T.E., M. Walch, R. Mitchell, M.J. Kaufman, J.R. Vestal, S.A. Ditner, and M.A. Lock. (1989) Microbial film formation on metals in an enriched arctic river. Biofouling **1**:301-311.

36. Galvele, J.R. (1981) Transport processes in passivity breakdown- II Full hydrolysis of the metal ions. Corrosion Science **21**:551-579.

37. Gabrielli, C. (1984) Identification of electrochemical processes by frequency response analysis. Solartron Schlumberger technical report no. 004/83, Farnborough, Hants, UK.

38. Geesey, G.G., R. Mutch, J.W. Costerton, and R.B. Green. (1978) Sessile bacteria: An important component of the microbial population in small mountain streams. Limnol. Oceanogr **23**:1214-1223.

39. Geesey, G.G., M.W. Mittelman, T. Iwaoka, P.R. Griffiths. (1986) Role of bacterial exopolymers in the deterioration of metallic copper surfaces. Materials Performance **25**:37-40.

40. Gerchakov, S.M., B.J. Little, and P. Wagner. (1986) Probing microbiologically induced corrosion. Corrosion **42**:689-692.

41. Hamilton, W.A. (1985) Sulphate-reducing bacteria and anaerobic corrosion. Ann. Rev. Microbiol. **39**:195-217.

42. Hamilton, W.A. (1987) Biofilms: Microbial interactions and metabolic activities. in Ecology of Microbial Communities (M. Fletcher, T. Gray, and J. Jones eds.) Society for General Microbiology. Cambridge University Press, New York.

43. Hardy, J.A., and J.L. Brown. (1984) The corrosion of mild steel by biogenic sulfide films exposed to air. Corrosion **40**:650-654.

44. Hoar, T.P., and W.R. Jacob. (1967) Breakdown of passivity of stainless steel by halide ions. Nature **216**:1299-1301.

45. Isaacs, H.S. (1974) Potential scanning of stainless steel during pitting corrosion. in Localized Corrosion National Association of Corrosion Engineers, Houston.

46. Isaacs, H.S. (1986) Applications of current measurement over corroding metallic surfaces. in Ionic Currents in Development Alan R. Liss, Inc. pp. 37-44.

47. Isaacs, H.S. (1987) The use of the scanning vibrating electrode technique for detecting defects in ion vapor-deposited aluminum on steel. Corrosion **43**:594-598.

48. Isaacs, H.S. (1988) The measurement of the galvanic corrosion of soldered copper using the scanning vibrating electrode technique. Corrosion Sci. **28**:547-557.

49. Isaacs, H.S. (1989) Applications and limitations of in situ current density mapping. CORROSION/89 paper no. 28, New Orleans, La.

50. Isaacs, H.S. (1990) The pitting of iron in dilute chloride and sulfate solutions. Advances in Localized Corrosion, eds. H.S. Isaacs, V. Bertocci, J. Kruger, and Z. Szklarska-Smialowska. NACE.

51. Isaacs, H.S. (1990) The localized breakdown and repair of passive surfaces during pitting. Corrosion Science **29**:313-323.

52. Isaacs, H.S. (1990) Limitations of in situ current density mapping for vibrating electrodes close to metal surfaces. Corrosion **46**:677-679.

53. Isaacs, H.S. (1990) The effect of height on the current distribution measured with the vibrating electrode. (in press J. Electrochem. Soc.)

54. Isaacs, H.S., A.J. Davenport, and A. Shipley. (1990) The electrochemical response of steel to additions of dissolved cerium. (submitted J. Electrochem. Soc.)

55. Isaacs, H.S., and Y. Ishikawa. (1985) CORROSION/85, paper no. 55, National Association of Corrosion Engineers, Boston, Ma.

56. Isaacs, H.S., and Y. Ishikawa. (1985) Current and potential transients during localized corrosion of stainless steel. J. Electrochem. Soc. **132**:1288-1293.

57. Isaacs, H.S., and M.W. Kendig. (1980) Determination of surface inhomogeneities using a scanning probe impedance technique. Corrosion **36**:269-274.

58. Isaacs, H.S., and B. Vyas. (1981) "Scanning Reference Electrode Techniques in Localized Corrosion" Electrochemical Corrosion Testing, ASTM STP 727, (F. Mansfeld and U. Bertocci eds.) ASTM, p. 3-33.

59. Iverson, W.P. (1966) Direct evidence for the cathodic depolarization theory of bacterial corrosion. Science **151**:986-988.

60. Jack, R.F. (1990) The effects of increased bacterial metabolic diversity on the corrosion of carbon steel. Masters Thesis, University of Tennessee.

61. Jaffe, L.F., and R. Nuccitelli. (1974) An ultrasensitive vibrating brobe for measuring steady extracellular currents. J. Cell Biol. **63**:614-628.

62. Jeffrey, W.H., and J.H. Paul. (1986) Activity of an attached and free-living Vibrio sp. as measured by thymidine incorporation, p-iodonitrotetrazolium reduction, and ATP/DNA ratios. Appl. Environ. Microbiol. **51**:150-156.

63. Jeffrey, W.H., and J.H. Paul. (1986) Activity measurements of planktonic microbial and microfouling communities in a eutrophic estuary. Appl. Environ. Microbiol. **51**:157-162.

64. Johnson, R., and E. Bardal. (1985) Cathodic properties of different stainless steels in natural seawater. Corrosion **41**:296-302.

65. Juttner, K., W.J. Lorenz, M.W. Kendig, and F. Mansfeld. (1988) Electrochemical impedance spectroscopy on 3-D inhomogeneous surfaces. J. Electrochem. Soc. **135**:332-339.

66. Kasahara, K., and F. Kajiyama. (1986) Role of sulfate reducing bacteria in the localized corrosion of buried pipes. pp. 171-183 in Biologically induced corrosion (S. Dexter ed.) National Association of Corrosion Engineers, Houston, Tx.

67. King, J.M.H., P.M. DiGrazia, B. Applegate, R. Burlage, J. Sanseverino, P. Dunbar, F. Larimer, and G.S. Sayler. (1990) Rapid, sensitive bioluminescent reporter technology for naphthalene exposure and biodegradation. Science **249**:778-781.

68. King, R.A., A.D. Miller, and D.S. Wakerley. (1973) Effect of ferrous ion concentration on the corrosion of iron in semicontinuous cultures of sulfate reducing bacteria. Br. Corrosion J. **11**:105-107.

69. Lappin-Scott, H.M. and J.W. Costerton. (1989) Bacterial biofilms and surface fouling. Biofouling **1**:323-342.

70. Lawrence, J.R., D.R. Korber, B. Hoyle, J.W. Costerton, and D.E. Caldwell. (1990) Visualization of microbial biofilm architecture using confocal scanning laser microscopy. Abst. Ann. Meeting. of the American Society for Microbiology, Anahiem, Ca.

71. LeChevallier, M.W., C.D. Cawthon, and R.G. Lee. (1988) Factors promoting survival of bacteria in chlorinated water supplies. Appl. Environ. Microbiol. **54**:649-654.

72. Lewandowski, Z., W.C. Lee, W.G. Characklis, and B. Little. (1988) Dissolved oxygen and pH microelectrode measurements at water immersed metal surfaces. CORROSION/88, paper no. 93, National Association of Corrosion Engineers. St. Louis, Missouri.

73. Little, B., P. Wagner, S.M. Gerchakov, M. Walch, and R. Mitchell. (1986) The involvement of a thermophilic bacterium in corrosion processes. Corrosion **42**:533-536.

74. Little, B., P. Wagner, and D. Duquette. (1988) Microbiologically induced increases in corrosion current density of stainless steel under cathodic protection. Corrosion **44**:270-274.

75. Little, B.J., P.A. Wagner, W.G. Characklis, and W. Lee. (1990) Microbial Corrosion in Biofilms (W.G. Characklis ed.) pp. 635-670. John Wiley and Sons, New York.

76. Little, B.J., P.A. Wagner, F. Manseld. (1990) CORROSION/90, National Association of Corrosion Engineers, Las Vegas, Nv.

77. Lorenz, W.J. and F. Mansfeld. (1981) Determination of corrosion rates by electrochemical dc and ac methods. Corrosion Science **21**:647-672.

78. MacDonald, D.D. (1977) AC impedance techniques. in Transient Techniques in Electrochemistry. pp.229-272. Plenum Press, New York.

79. MacDonald, D.D. (1987) Theoretical analysis of electrochemical impedance. paper no. 479, CORROSION 87, National Association of Corrosion Engineers, San Fransisco, Ca.

80. Mansfeld, F. (1981) Recording and anslysis of AC impedance data for corrosion studies. I. Background and methods of analysis. Corrosion **37**:301-307.

81. Mansfeld, F., M.W. Kendig, and S. Tsai. (1982) Recording and analysis of AC impedance data for corrosion studies. II. Experimental approach and results. Corrosion **38**:570-580.

82. Mansfeld, F., and B. Little. (1990) The application of electrochemical techniques for the study of MIC - A critical review. CORROSION/90, paper no 108, National Association of Corrosion Engineers. Las Vegas, Nv.

83. Marshall, K.C., R. Stout, and R. Mitchell. (1971) Mechanism of the initial events in the sorption of marine bacteria to surfaces. J. Gen. Microbiol. **68**:337-348.

84. Meyer-Reil, L. (1978) Autoradiographic and epifluorescence microscopy combined for the determination of number and spectrum of actively metabolizing bacteria in natural waters. Appl. Environ. Microbiol. **36**:506-511.

85. Mittelman, M.W., and D.C. White. (1989) Effects of shear stress on the adhesion, activity, and biofilm constituents of Pseudomonas atlantica on stainless steel. Abst. Annual Meeting of the American Society for Microbiology, p. 356, New Orleans, La.

86. Mittelman, M.W., J.M.H. King, G.S. Sayler, and D.C. White. Light production by a Pseudomonas fluorescens (lux) reporter strain as an endpoint for bacterial adhesion. (submitted Appl. Environ. Microbiol.)

87. Mollica, A., A. Trevis, E. Traverso, G. Ventura, G. De Carolis, and R. Dellepiane. (1989) Cathodic performance of stainless steels in natural seawater as a function of microorganism settlement and temperature. Corrosion **45**:48-56.

88. Newman, R.C., W.P. Wong, and A. Garner. (1986) A mechanism of microbial pitting in stainless steel. Corrosion **42**:489-491.

89. Nichols, P.D., J.M. Henson, J.B. Guckert, D.E. Nivens, and D.C.White. (1985) Fourier transform-infrared spectroscopic methods for microbial ecology: analysis of bacteria, and bacteria-polymer mixtures adn biofilms. J. Microbiol. Methods **4**:79-94.

90. Nivens, D.E., J.Q. Chambers, and D.C. White. (1990) Monitoring microorganisms at solid surfaces using on-line devices. International Congress on Microbial Influenced Corrosion, Knoxville, Tn.

91. Nivens, D.E., Nichols, P.D., Henson, J.M., Geesey, G.G., and White, D.C. (1986) Reversible acceleration of the corrosion of AISI 304 stainless steel exposed to seawater induced by growth and secretions of the marine bacterium Vibrio natriegens. Corrosion **42**:204-210.

92. Obuekwe, C.O., D.W.S. Westlake, J.A. Plambeck, and F.D. Cook. (1981) Corrosion fo mild steel in cultures of ferric iron reducing bacterium isolated from crude oil 1. Polarization characteristics. Corrosion **37**:461-467.

93. Obuekwe, C.O., D.W.S. Westlake, J.A. Plambeck, and F.D. Cook. (1981) Corrosion fo mild steel in cultures of ferric iron reducing bacterium isolated from crude oil II. Mechanism of anodic depolarization. Corrosion **37**:632-637.

94. Oltra, R., and M. Keddam. (1988) Application of impedance techniques to localized corrosion. Corrosion Science **28**:1-18.

95. Pankhania, I.P., A.N. Moosavi, and W.A. Hamilton. (1986) Utilization of cathodic hydrogen by Desulfovibrio vulgaris (Hildenborough). J. Gen. Microbiol. **132**:3357-3365.

96. Pankhania, I.P. (1988) Hydrogen metabolism in sulphate-reducing bacteria and its role in anaerobic corrosion. Biofouling **1**:27-47.

97. Phelps, T.J., N. Dowling, and D.C. White. (1990) Techniques for assessing microbial activities associated with MIC. International Congress on Microbial Influenced Corrosion, Knoxville, Tn.

98. Phelps, T.J., R.M. Schram, D. Ringelberg, N.J.E. Dowling, and D.C. White. (1990) Hydrogen mediated acetogenesis as a possible mechanism for microbially influenced corrosion of natural gas transmission lines. (submitted Biofouling)

99. Pourbaix, M. (1966) Atlas of Electrochemical Equilibria in Aqueous Solutions. Pergamon Press, London.

100. Pourbaix, M. (1970) Significance of protection potential in pitting and intergranular corrosion. Corrosion **26**:431-438.

101. Pourbaix, M. (1971) The electrochemical basis for localized corrosion. in Localized Corrosion National Association of Corrosion Engineers, Houston.

102. Pourbaix, M. (1974) Applications of electrochemistry in corrosion science and in practice. Corrosion Science **14**:25-82.

103. Pourbaix, M. (1976) Some applications of potential-pH diagrams to the study of localized corrosion. J. Electrochem. Soc. **123**:25C-36C.

104. Ringas, C. and F.P.A. Robinson. (1987) Corrosion of stainless steel by sulfate-reducing bacteria - Electrochemical techniques. Corrosion **44**:386-396.

105. Ringas, C., and F.P.A. Robinson. (1988) Corrosion of stainless steel by sulfate-reducing bacteria - Total immersion test results. Corrosion **44**:671-678.

106. Rittmann, B.E., and P.L. McCarty. (1980) Model of steady-state-biofilm kinetics. Biotech. Bioeng. **12**:2343-2357.

107. Rittmann, B.E., and P.L. McCarty. (1980) Evaluation of steady-state-biofilm kinetics. Biotech. Bioeng. **12**:2359-2373.

108. Rosenberg, M. and S. Kjelleberg. (1986) Hydrophobic interactions: role in bacterial adhesion. Adv. Microbial Ecology **14**:353-393.

109. Rosenfeld, I.L., and I.S. Danilov. (1967) Electrochemical aspects of pitting corrosion. Corrosion Science **7**:129-142.

110. Roszak, D.B., and R.R. Colwell. (1987) Survival strategies of bacteria in the natural environment. Microbiol. Rev. **51**:365-379.

111. Salvarezza, R.C., and H.A. Videla. (1980) Passivity breakdown of mild steel in sea water in the presence of sulfate reducing bacteria. Corrosion **36**:550-554.

112. Sato, N. (1987) Some concepts of corrosion fundamentals. Corrosion Science **27**:421-433.

113. Sato, N. (1989) Towards a more fundamental understanding of corrosion processes. Corrosion **45**:354-368.

114. Savage, D.C. and M. Fletcher (eds.) (1985) Bacterial adhesion: mechanisms and physiological significance. Plenum Press, New York.

115. Saye, D.J. O.A. Ogunseitan, G.S. Sayler, and R.V. Miller. (1987) Potential for transduction of plasmids in a natural freshwater environment: effect of donor concentration and a natural microbial community on transduction in Pseudomonas aeruginosa. Appl. Environ. Microbiol. **53**:987-995.

116. Saye, D.J. O.A. Ogunseitan, G.S. Sayler, and R.V. Miller. (1990) Transduction of linked chromosomal genes between Pseudomonas aeruginosa strains during incubation in situ in a freshwater habitat. Appl. Environ. Microbiol. **56**:140-145.

117. Scotto, V., R. Di Cintio, and G. Marcenaro. (1985) The influence of marine aerobic microbial film on stainless steel corrosion behaviour. Corrosion Science **25**:185-194.

118. Stern, M. (1958) A method for determining corrosion rates from linear polarization data. Corrosion **14**:60-64.

119. Stern, M. and A.L. Geary. (1957) Electrochemical polarization I. a theoretical analysis of the shape of polarization curves. J. Electrochem. Soc. **104**:56-63.

120. Strommen, R., and A. Rodland. (1981) Computerized techniques applied in design of offshore cathodic protection systems. Materials Performance **20**:15-20.

121. Sydberger, T. (1983) Evaluation of inspection methods for offshore pipeline cathodic protection systems. Materials Performance **22**:56-64.

122. Tabor, P.S., and R.A. Neihof. (1982) Improved microradiographic method to determine individual microorganisms active in substrate uptake in natural waters. Appl. Environ. Microbiol. **44**:945-953.

123. Tiller A.K. and G.H. Booth. (1961) Polarization studies of mild steel in cultures of sulfate-reducing bacteria. Part 2 - thermophilic organisms. Trans. Faraday Soc. **57**:110-115.

124. Tiller, A.K. (1986) A review of the European research effort on microbial corrosion between 1950 and 1984. in Biologically induced corrosion (S. Dexter ed.) National Association of Corrosion Engineers, Houston, Tx.

125. Van Loosdrecht, M.C.M., J. Lyklema, W. Norde, and A.J.B. Zehnder. (1989) Bacterial Adhesion: A physicochemical approach. Microb. Ecol. **17**:1-15.

126. Van Loosdrecht, M.C.M., J. Lyklema, W. Norde, and A.J.B. Zehnder. (1990) Influences of interfaces on microbial activity. Microbiol. Rev. **54**:75-87.

127. Von Wolzogen Kuhr, C.A.H., and L.S. van der Vlugt. (1934) De grafiteering van gietijzer als electrobiochemich process in anaerobe gronden. Water **18**:147-165.

128. Vyas, B. and H.S. Isaacs. (1978) Detecting susceptibility to intergranular corrosion of stainless steel weld heat-affected zones. in Intergranular corrosion of stainless steel, ASTM STP 656, (R.F. Steigerwald, ed.) American Society for Testing and Materials, pp. 133-145.

129. Wagner, C. and W. Traud. (1938) On the interpretation of corrosion phenomena by superposition of electrochemical partial processes, and on the potential of mixed electrodes. Z. Electrochem. **44**:391-402.

130. White, D.C. (1984) Chemical characterization of films. in Microbial Adhesion and Agglutination (K.C. Marshall, ed.) pp. 159-176. Dahlem Konferenzen Life Sciences Research Report 31, Springer-Verlag, Berlin.

131. Zobell, C.E. (1943) The effect of solid surfaces upon bacterial activity. J. Bacteriol. **46**:39-56.

CHAPTER III

LABORATORY TESTS OF BIOFOULING AND CORROSION OF CARBON STEEL BY AEROBIC HETEROTROPHIC BACTERIA ISOLATED FROM CORRODED STEEL TUBERCLES

ABSTRACT

A collection of aerobic heterotrophic bacteria have been isolated from pipe tubercles. In batch culture experiments, four of the strictly aerobic isolates and one of the facultatively anaerobic isolates, colonized the surface of C1020 carbon steel coupons and increased the weight loss of the coupons two- to three- fold over sterile controls. The isolates did not lower the pH of the bulk medium, and no ferrous ions were detected in the bulk medium. Scanning electron microscopic analysis and Fourier transform infrared spectroscopy analysis revealed colonization of these isolates on steel surfaces with the production of extracellular polymer. One isolate which produced the most extracellular polymer was chosen for analysis of colonization and corrosion of C1020 carbon steel coupons using a dilute flowing medium. Electrochemical impedance spectroscopy (EIS) was used to determine changes in the steel polarization resistance over time in the flowing system. Four days after inoculation with the isolate, tubercles began to form on the metal. These were not seen in the sterile control. The growth of the tubercles was accompanied by an increase in microbial biomass, a drop in the open circuit potential, and an increase in corrosion rate.

INTRODUCTION

Aerobic bacteria, including strict aerobes and facultative aerobes, are important components of natural biofilms (8). Aerobic bacteria are of interest in biofouling and corrosion studies, since they reduce the concentration of oxygen within a biofilm, allowing colonization by anaerobic bacteria (8,20), including the sulfate-reducing bacteria, which are often implicated in microbially influenced corrosion (MIC) (2,20). Some strictly aerobic bacteria also produce large amounts of acidic extracellular polymer (19), which may enhance adhesion of bacteria to surfaces. Some extracellular polymers may also affect corrosion by disruption of passive films (4).

Recent studies have indicated that bacteria other than sulfate-reducing bacteria can be involved in microbial influenced corrosion (MIC). Among these types of bacteria are iron-reducing bacteria (17), acid producing facultative anaerobes (15), and thermophilic bacteria (9). Mechanisms for corrosion facilitation by these non-sulfate reducing bacteria have included reduction of ferric iron associated with the passive film of carbon steel, production of organic and inorganic acids (9), and production of galvanic cells due to differential colonization and utilization of oxygen over a surface (9).

Our laboratory has been involved in the microbiological analysis of tubercles from failed steel pipes, which transport untreated water. Through these analyses, a large collection of microorganisms of different physiological types, has been obtained from tubercles. Many of the isolates in the collection are strictly aerobic heterotrophic bacteria. The purpose of this study was to determine if these aerobic bacteria were able to colonize and influence corrosion of carbon steel in laboratory tests. Electrochemical impedance spectroscopy (EIS) was used to determine polarization resistances of the samples over time. Biofouling was analyzed over time by phospholipid fatty acid analysis, Fourier transform infrared spectroscopy, and scanning electron microscopy. The results indicated that aerobic bacteria are important in biofouling and can enhance corrosion rates of carbon steel under laboratory conditions.

MATERIALS AND METHODS

Media. The basal salts used in all media contained (mg/L distilled water) 50 NH_4Cl, 50 $Mg_2SO_4 \cdot 7H_2O$, 27 KH_2PO_4, 5 $CaCl_2 \cdot H_2O$, 50 MOPES buffer, and 1 ml Hutner's trace minerals. For enrichment and maintenance media, 1 g/L $FeNH_4$Citrate and 1 g/L tryptic soy broth were added to the basal salts, and 15 g/L agar was added for solid media. For weight loss experiment 100 mg/L NaCitrate and 100 mg/L tryptic soy broth were added to the basal salts. To assay for volatile fatty acid production, bacteria were inoculated into aerobic or anaerobic medium which contained basal salts and 1 g/L glucose. To assay for ferric iron reduction, bacteria were grown in anaerobic medium containing basal salts, with 0.2 g/L succinate, 0.5 g/L tryptic soy broth, 150 mg/L yeast extract, and 0.5 g/L ferric chloride.

For the flowing system 50 mg/L glucose and only 0.1ml Hutner's minerals containing no chelating agents were added to basal salts. The dilution rate for the flowing system was 0.1 h^{-1}. The medium was allowed to flow into the system for one to two days prior to inoculation.

Isolation. Bacteria were isolated by aseptically chipping away the outer portion of the tubercles and extracting the inner portion of tubercles with a sterile razor blade. The inner contents of the tubercle were serially diluted in basal salts solution. The diluents were then inoculated into liquid isolation medium. The highest

dilution tubes which showed bacterial growth were used to inoculate agar plates. Colonies were repeatedly picked from the plates and streaked, until only one colony morphology was observed on each plate (at least three platings).

Volatile fatty acids. Volatile fatty acids were analyzed using a Schimadzu gas chromatograph. The column was packed with Chromosorb WAW with 1% H_3PO_4. The injector detector temperature was 160C, the column temperature was 120C. The flow rates were N_2 60 ml/min, H_2 30 ml/min, and O_2 300 mL/min. The samples were prepared by acidifying 200 μl aliquots with 2 μl of 10% redistilled formic acid solution. The samples were centrifuged for 2 min in a microfuge and 0.2uL of the sample was injected into the gas chromatograph. The peak area was integrated and compared to external standards.

Metal coupons. C1020 carbon steel coupons, obtained from Metal Samples Co. (Munford, Al.), contained C-0.17; Mn-0.42; P-0.009; and S-0.006. The coupons were finished with 600 grit silicon carbide paper.

Weight loss experiments. The coupons were degreased with acetone and sterilized in 4% formaldehyde for 30 min. followed by three rinses in sterile distilled water before placing into flasks containing sterile media. The media were inoculated with bacteria and allowed to incubate on a rotary shaker for five days. The coupons were then removed, lyophilized, and analyzed by Fourier transform infrared

spectroscopy (FT-IR). Following FT-IR analysis the corrosion products were removed with Kimwipes (the corrosion products easily flaked off after lyophilization), and the coupons were weighed. The weight losses were the mean and standard deviation of five replicates. The pH of the spent medium was determined, and the concentration of ferrous ions in the spent medium was determined by the ferrizine assay of Stookey (18).

Fourier transform infrared spectroscopy. FT-IR measurements were obtained as previously described using a Nicolet 60SX FT-IR (14,15). Data were interpreted based on Kubelka-Munk units for reflectance spectroscopy. Total protein on the metal surface was determined by the method of Lowery (10).

Phospholipid fatty acid analysis. Lipids were extracted from the surface of coupons using an O-ring extractor and 2 ml of chloroform:methanol:water (1:0.5:0.4 mL) (16). The solutions were transferred to clean test tubes, and the phase was broken with the addition of 0.5mL water and 0.5mL of chloroform. The chloroform fraction was collected and the ester linked fatty acids were analyzed by gas chromatography as previously described (1). The position and orientation of double bonds were determined by dimethyl disulfide derivatization (13).

Scanning electron microscopy. Samples for SEM analysis were fixed in 0.1M NaCacodylate buffer (pH 7.4) containing

2% glutaraldehyde for 30m. The samples were then dehydrated by exchanging the solution with increasing concentrations of acetone (50%, 75%, then 100% acetone). The samples were critical point dried and sputter coated. The samples were then examined in a ETEC autoscan scanning electron microscope.

Electrochemical analysis. The electrochemical cell used in these studies was described previously (3). The cell consisted of a reaction flask with a working volume of 500 ml, and contained a multiple working electrode assembly, a titanium counter electrode, and a saturated calomel reference electrode, connected to the solution via a salt bridge with a Vicor frit. The cell also contained ports for inlet and outlet of the flowing medium, and a Teflon stir star. The cells were sterilized by ethylene oxide sterilization at the University of Tennessee Medical Center.

Samples were analyzed by electrochemical impedance spectroscopy (11,12). EIS was performed using a Solartron 1250 frequency response analyzer through a Solartron 1286 electrochemical interface. The instruments were controlled by a Hewlett-Packard computer using Solartron 1091 software. The applied voltage amplitude was 5 mV at frequencies between 3 mHz and 1 kHz. Five frequencies were analyzed per decade.

RESULTS AND DISCUSSION

Isolate characterization. Five isolates of aerobic bacteria from the laboratory culture collection were chosen for laboratory tests of colonization and corrosion of carbon steel coupons. The phospholipid fatty acid (PLFA) profiles from stationary phase (48 h) cultures of these isolates are shown in Table 1. Four of the five isolates have similar PLFA patterns and appear to be related to Pseudomonas spp. The isolates have a high ratio of trans monounsaturated fatty acids to the cis isomers. Two of the isolates were analyzed by the Hewlett Packard Microbial Identification System, which compared the lipid profiles with known profiles contained in a computer library. Isolate 3T5 was identified as a Pseudomonas sp. and isolate 3T4 was identified as a Hafnia sp.

The four isolates that had PLFA profiles similar to Pseudomonas were unable to grow or produce detectable levels of volatile fatty acids (less than 0.5 mM) under anaerobic conditions. The isolate which did grow anaerobically, isolate 3T4, produced 5 mM acetic acid under anaerobic growth.

Reduction of ferric iron associated with the passive film of carbon steel to soluble ferrous iron has been suggested as a mechanism for corrosion facilitation by iron reducing bacteria (17). One of the isolates, isolate 3T4, reduced 0.1 μM ferric iron to ferrous iron after 10 days of

Table 1
Phospholipid fatty acid profiles of aerobic heterotrophic isolates[a]

	Isolate						
Fatty acid	11T6	4T6	11T1	3T4	3T5	3T5[b]	3T5[c]
15:0				0.4			
16:1w9c				0.1			
16:1w7c	17.4	20.1	11.6	5.7	21.3	21.2	21.2
16:1w7t	19.7	18.5	14.3		11.3	5.5	3.5
16:0	33.8	34.1	41.3	47.6	41.5	44.0	58.4
cy17:0				41.2			
17:0				0.4			
17:1	0.6	0.5	3.7		4.7		
18:1w7c	21.6	21.2	19.9	2.1	18.2	25.2	12.9
18:1w7t	4.5	3.6	4.9				
18:0	1.7	1.6	3.4	1.0	2.1	4.0	3.1
Br19:1		0.2	0.2				
cy19:0				1.6			

[a]Data are expressed in mole% of each fatty acid. Data represent the mean of two or three samples.
[b]Data for isolate 3T5 attached to steel samples after five days of exposure to flowing medium.
[c]Data for isolate 3T5 attached to steel samples after eight days of exposure to flowing medium.

growth in iron reduction medium described above. The remaining isolates did not reduce detectable levels of ferric iron after ten days (less than 0.05 μM).

Colonization of steel by isolates in batch cultures. Colonization of the steel was determined by scanning electron microscopy (SEM) and Fourier transform infrared spectroscopy FT-IR. Figure 1 shows the colonization of the corrosion products by isolate 3T5 after five days of growth. Bacterial exopolymer can be seen in association with the bacteria and the corrosion products. When the corrosion products were removed from the surface, bacteria could be seen attached to the metal surface (Figure 2). Figure 3 shows the sterile control. Most of the control coupons remained shiny after five days of exposure to sterile medium. Small amounts of corrosion products or precipitated salts were associated with the surface of the sterile coupons, but the surface shows little corrosion.

FT-IR analysis showed that the organism associated with the metal surface and corrosion products, produced material which absorbed at 1080 cm^{-1} (CHO) (Figure 4). The ratio of CHO to amide 1 as determined by FTIR for each of the isolates is shown in Table 2. The ratios are based on the peak height of the band centered at 1080 cm^{-1} and 1648 cm^{-1}. In bacteria, the peak at 1080 cm^{-1} has been correlated with material composed of carbohydrates (14), which is the

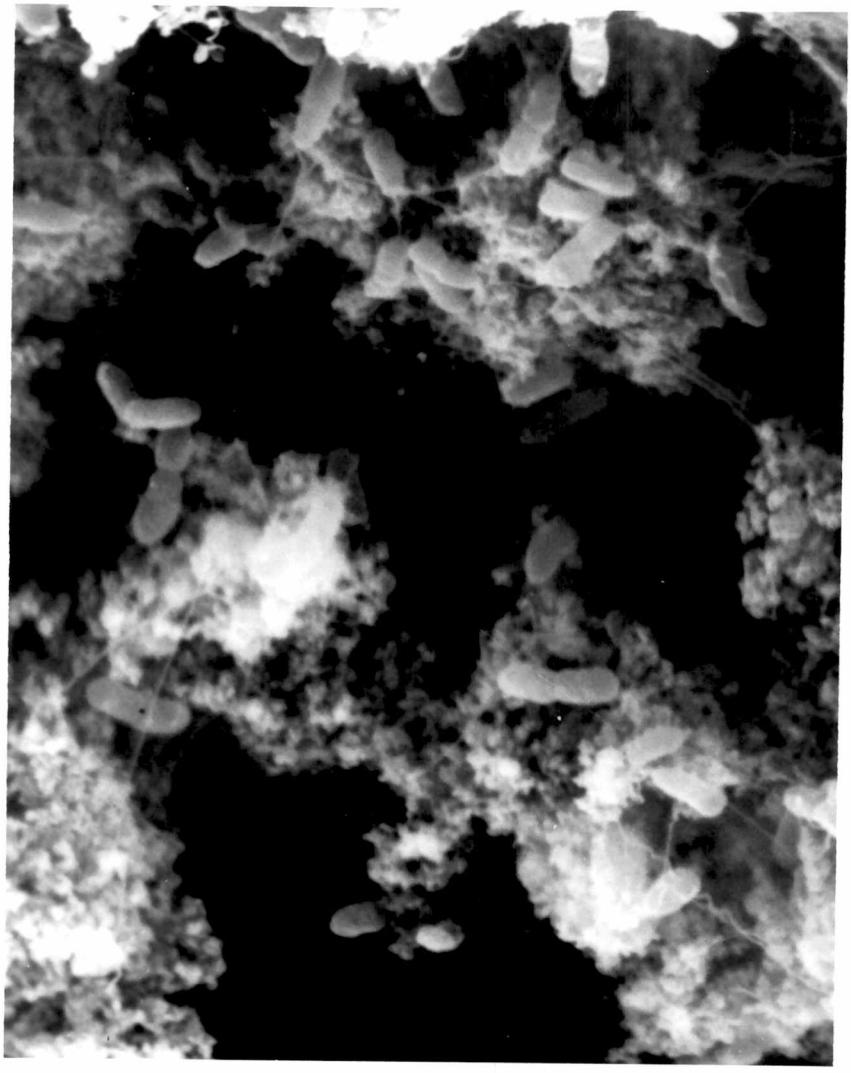

Figure 1. Bacteria (isolate 3T5) and bacterial exopolymeric material associated with the corrosion products of carbon steel coupon after five days of exposure to medium in a batch culture system.

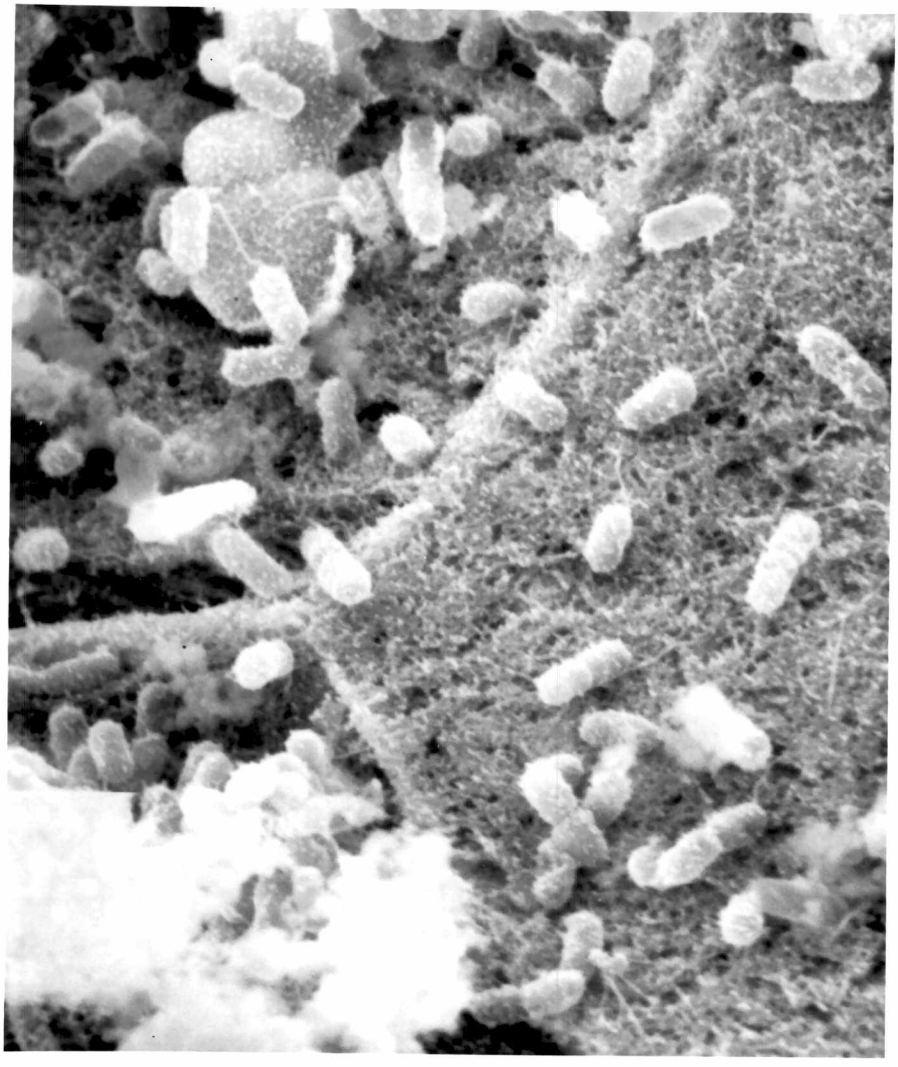

Figure 2. The surface of the carbon steel exposed to bacteria, after removal of corrosion products.

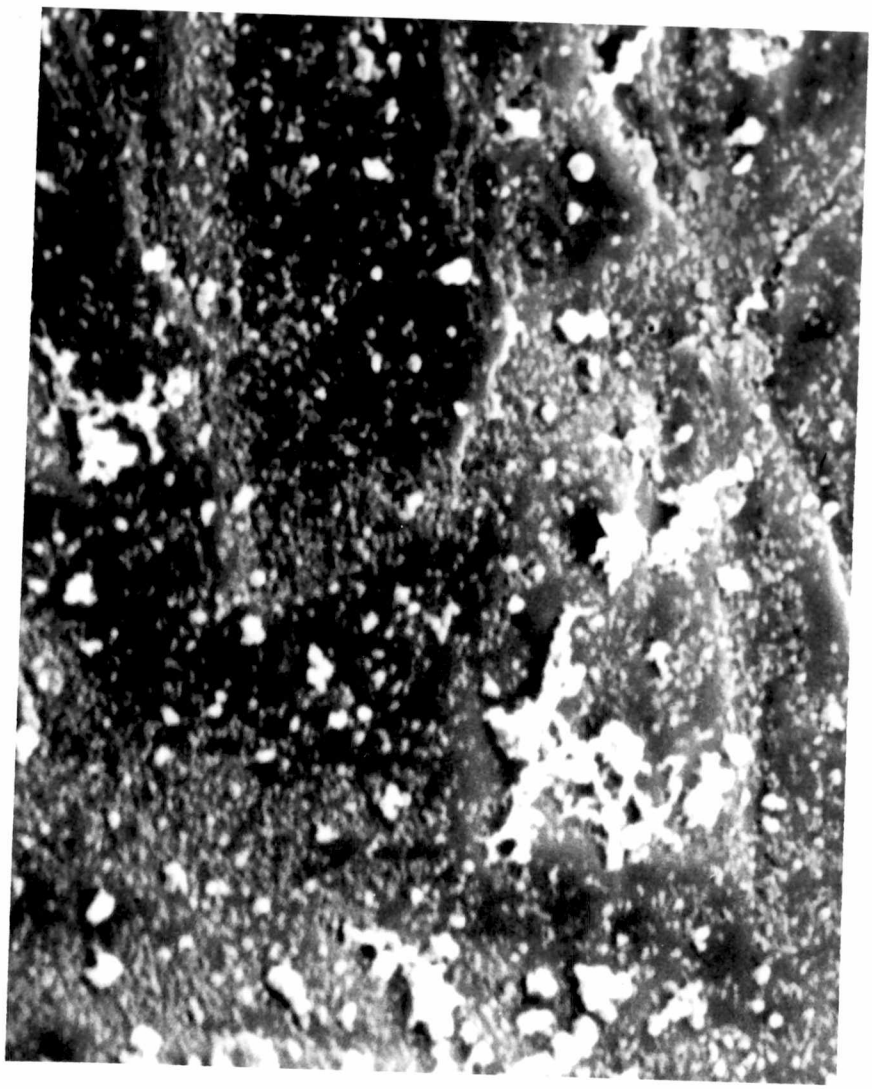

Figure 3 Surface of carbon steel exposed to sterile medium for five days.

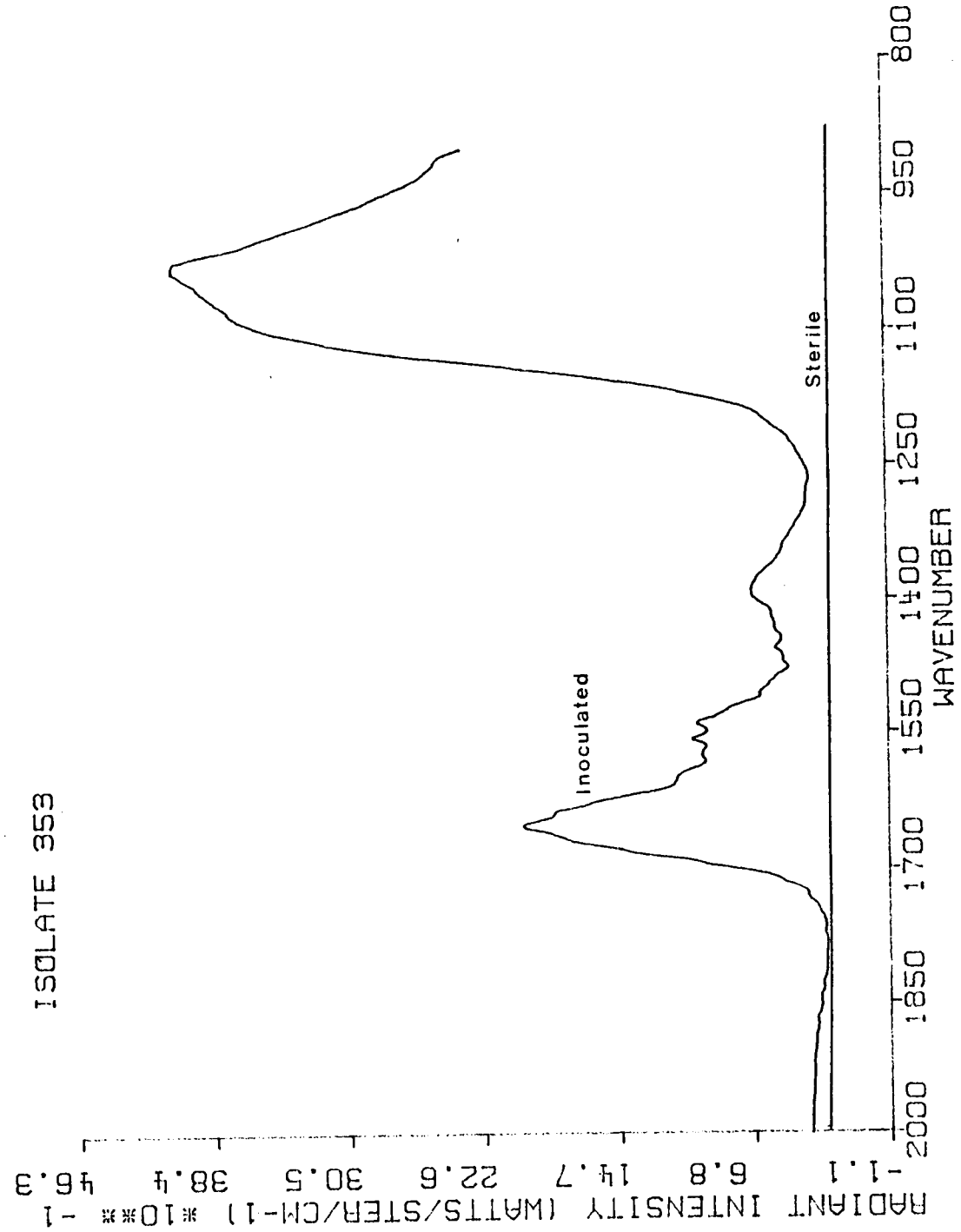

Figure 4. Fourier transform infrared spectra of biofilm (isolate 3T5) on carbon steel coupon after five days exposure of the steel to a batch culture of bacteria.

Table 2
Colonization of carbon steel by bacteria, and weight loss

Isolate	Weight Loss[a]	Final pH	Fe^{2+}	CHO/Amide 1[b]
3T5	69±6	8.0	bd[c]	2.7
11T2	80±9	8.0	bd	2.6
4T6	95±6	8.0	bd	1.7
11T1	77±1	8.0	bd	2.5
3T4	78±7	8.0	bd	1.9
Sterile control	30±20	7.7	bd	bd

[a]Weight losses are in units of $mg \cdot cm^{-2} \cdot day^{-1}$ (mdd). Data were calculated after five days of exposure of steel coupons to bacteria. The data represent the mean and standard deviation of five samples.
[b]Ratio of CHO to Amide 1 determined by FTIR.
[c]Below detection

primary constituent of bacterial exopolymer. The peaks at 1648 cm^{-1} have been correlated with bacterial protein.

Extracellular polymer may be produced to enhance the strength of adhesion of the cells to the surface. The isolates all had higher ratios of CHO to amide 1 than previously reported cultures (14). Isolate 3T5 produced the highest ratio of CHO to amide, and was chosen for additional studies.

Weight loss in batch cultures. The five isolates induced weight loss of the coupons two to three fold in excess of the sterile controls (Table 2). The pH of the bulk media following the five days exposure rose from 7.3 to 8.0 in flasks with bacteria and 7.3 to 7.7 in the flasks not containing bacteria. Since only one of the five cultures tested produced detectable levels of volatile fatty acids under conditions which stimulate fermentative metabolism, and since the pH rose in these experiments, bacterial production of volatile fatty acids is likely not the cause of the increased weight loss.

No detectable concentration of ferrous iron was found in the weight loss experiments. In addition only one of the five isolates reduced detectable levels of ferric iron to ferrous iron, in ten days, under conditions designed to facilitate iron reduction. These results suggested that bacterial reduction of iron associated with passive films is not the mechanism responsible for the increased weight loss

of the samples. These results are in contrast to the results of Obekwe et al. (17). However, the conditions used in this system were different from the conditions used by Obekwe et al. In their study, a rich medium was used to grow the bacteria, and the experiments were performed under microaerophilic conditions. Those conditions are more likely to stimulate iron reduction than the low nutrient, aerobic system used in this study.

Open circuit potential of steel in flowing system. In most environments, nutrients are limiting and bacterial endproducts, such as organic acids and alcohols are washed out or are utilized by other organisms as carbon sources. To better simulate these conditions, flowing systems were used in these studies. One isolate, isolate 3T5, was selected for further studies on biofilm formation and corrosion in a dilute flowing system. After approximately two days following inoculation, turbidity in the medium could be seen due to bacterial growth. Following the increase in turbidity, tubercles began to form on the metal surfaces (Figure 5A). The carbon steel exposed to sterile medium in the flowing system remained shiny over the course of the experiment, with only some darkening of the metal surfaces at the edges next to the epoxy coating (Figure 5B). As the tubercles grew on the steel exposed to bacteria, the open circuit potential dropped from approximately -200 mV/SCE to -650 mV/SCE. The open circuit potential of

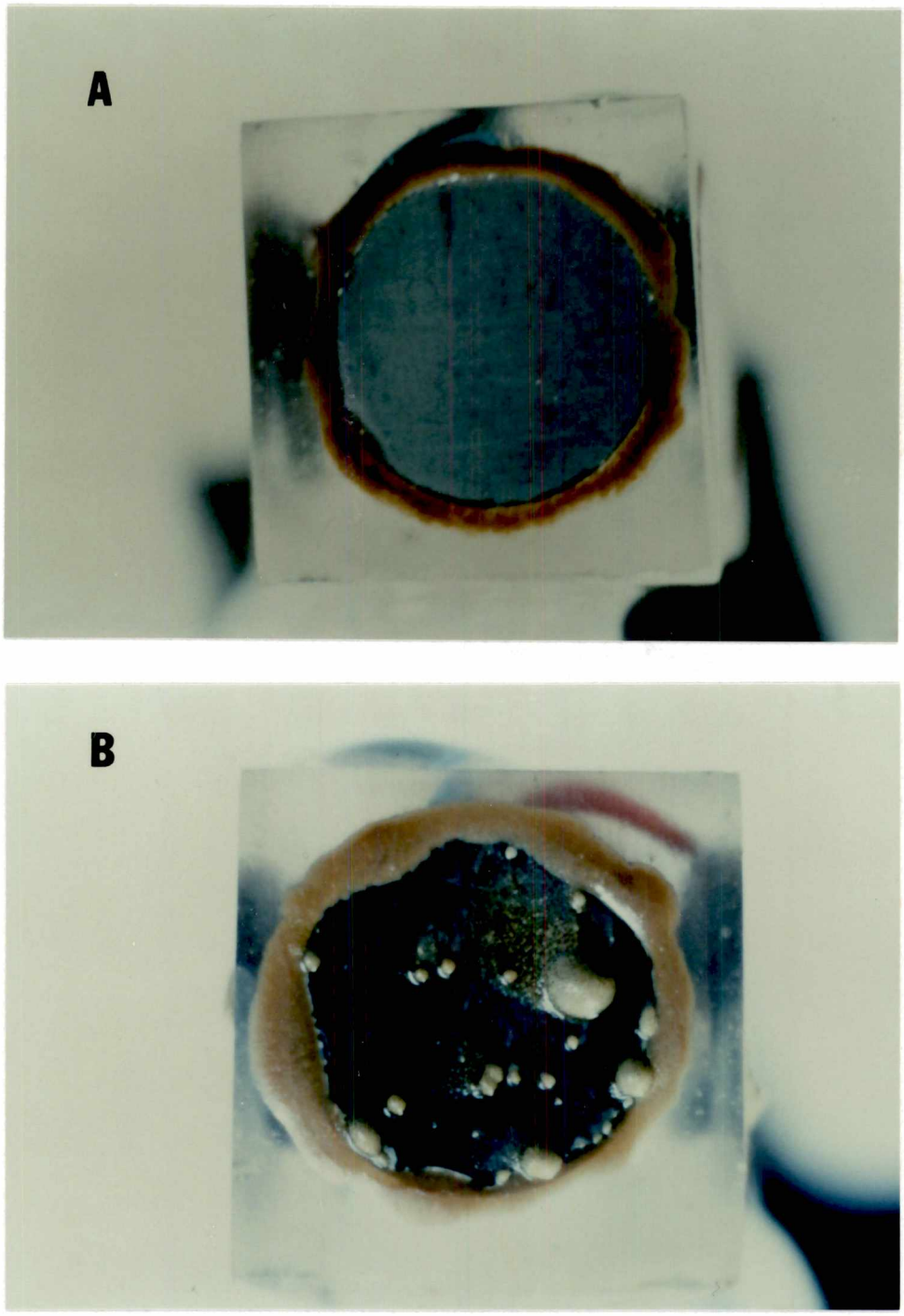

Figure 5. Photograph of carbon steel samples after nine days of exposure to flowing medium. A) Sterile sample. B) Sample exposed to isolate 3T5.

the sterile control remained at approximately -200 mV/SCE over the course of the experiments.

Impedance analysis in flowing system. The polarization resistances were determined by EIS. The impedance spectra of the steel after eight days of exposure to sterile medium or medium inoculated with bacteria are shown in the Nyquist format in Figure 6. The impedance spectra for the inoculated system showed a single capacitive loop, as tubercles were forming. The impedance spectra for the sterile samples often did not approach the real axis in the Nyquist format. In these cases the polarization resistances were estimated by extrapolation to real axis in the Nyquist format or the Y-axis in the Bode format.

The inverse of the polarization resistance for the sterile samples increased very slowly to $2x10^{-2}$ mMho·cm^{-2} of the course of eight days (Figure 7). The carbon steel exposed to bacteria gave values similar to the sterile samples prior to bacterial inoculation. Following inoculation and growth of tubercles the inverse of the polarization resistance increased to 1 mMho·cm^{-2} after six days of exposure to bacteria.

EIS provided a means for estimating the corrosion rate without altering the progression of the corrosion (2, Chapter 2). The results of the flowing system experiment showed that the presence of the pure culture of bacteria was

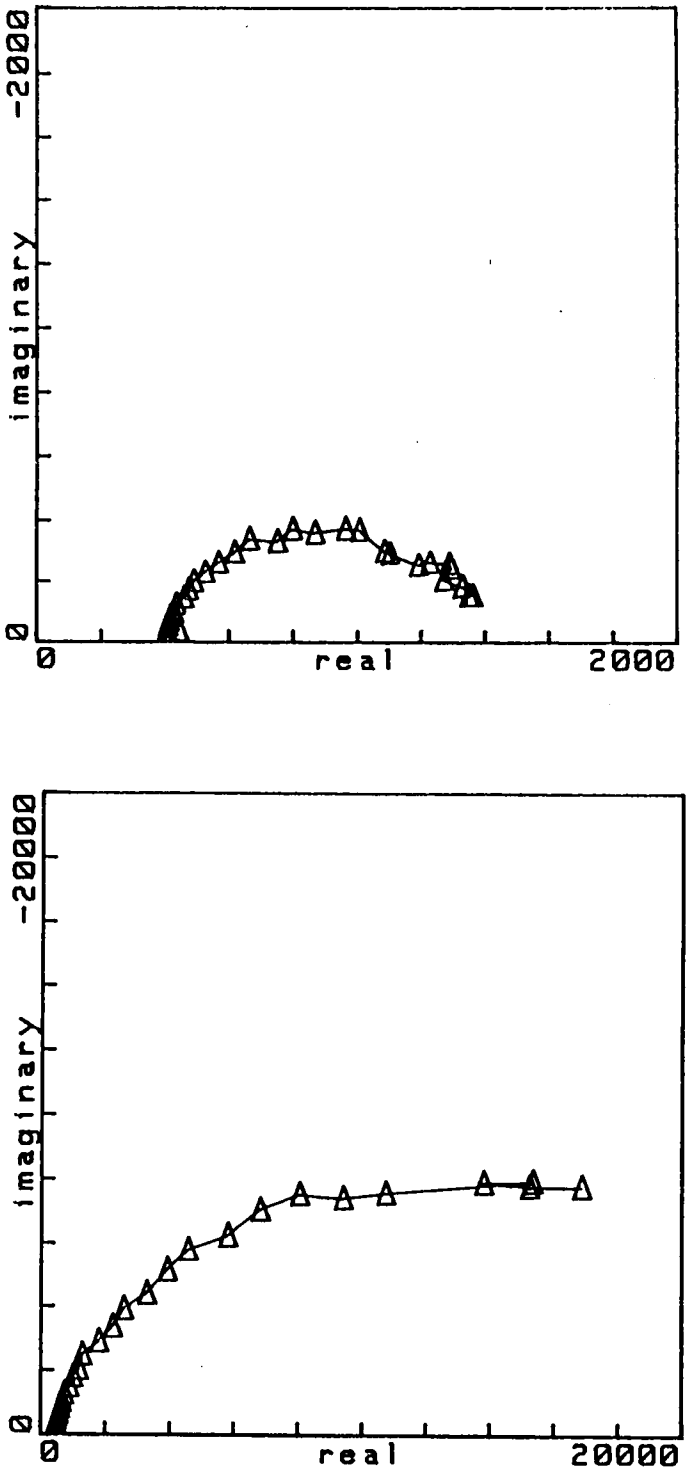

Figure 6. Electrochemical impedance spectroscopy of carbon steel electrodes after eight days of exposure to medium. A) inoculated with isolate 3T5. B) sterile control.

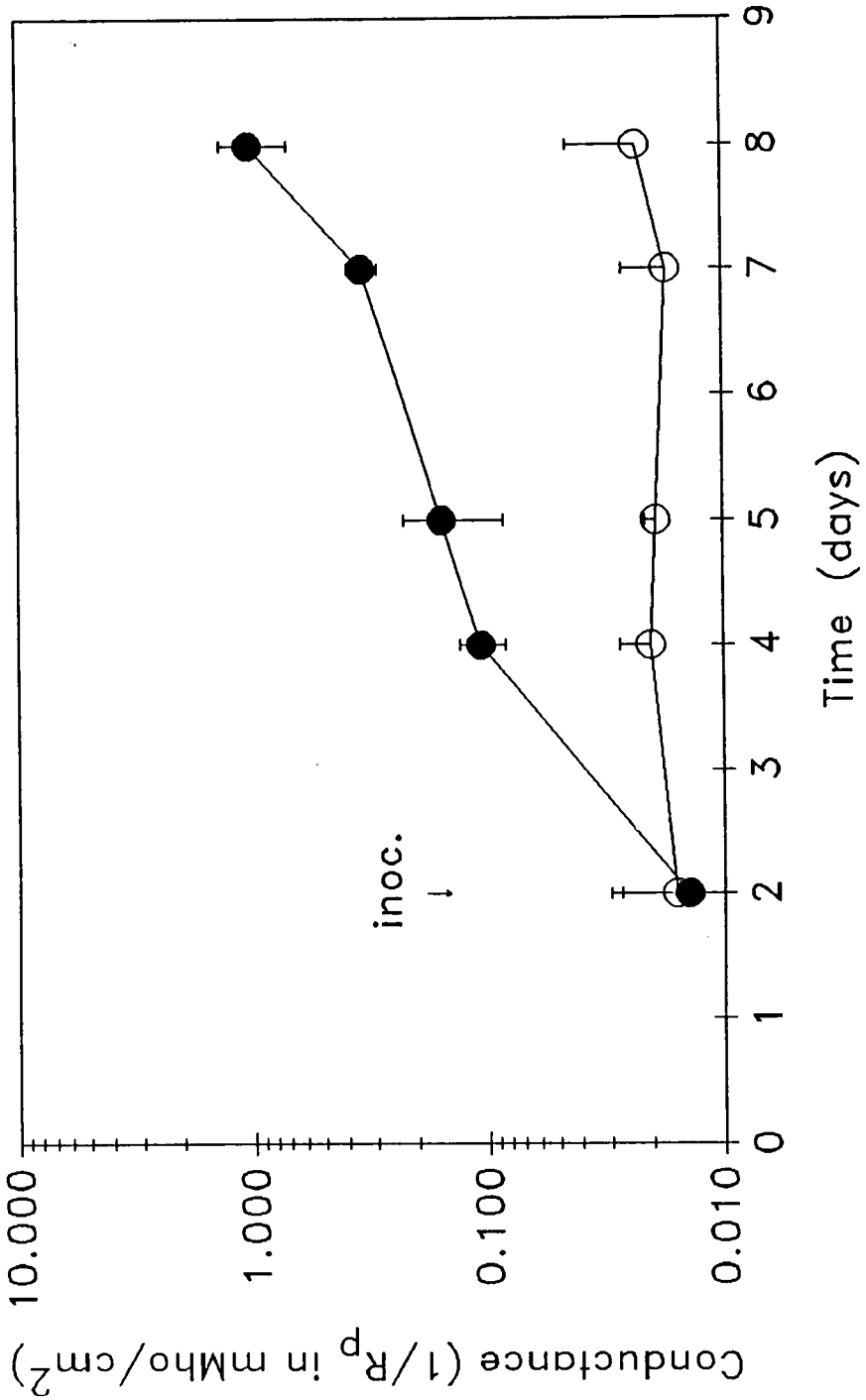

Figure 7. Inverse of the polarization resistance, determined by electrochemical impedance spectroscopy, for the carbon steel samples over time. Samples were exposed to sterile medium for two days prior to inoculation with isolate 3T5. Closed circles represent steel exposed to bacteria. Open circles represent sterile samples. Error bars represent the standard deviations of three samples.

able to accelerate the corrosion rate of the steel compared to the sterile control.

Biofouling in flowing system. The increase in corrosion rate was accompanied by an increase in microbial biomass on the surface of the steel. Ancillary flasks containing removable epoxy embedded carbon steel samples were used to sample biofilm formation in the flowing system. The samples were analyzed by FT-IR, Lowry protein assay, and PLFA analysis, as well as by scanning electron microscopy. Prior to formation of tubercles, the radiant intensity of the amide 1 band was 5 x 10^{-2}. The protein determined by the Lowery method was 1.5 μg protein$\cdot cm^{-2}$ and the total PLFA was 620 pmol PLFA$\cdot cm^{-2}$, corresponding to approximately $3x10^{7}$ cells$\cdot cm^{-2}$. After the tubercles began to form the microbial biomass also increased. The SEM of a sample after six days of exposure to the bacteria in the flowing system is shown in Figure 8. The SEM reveals a large number of bacteria attached to the steel surface. The total protein extracted from coupons after four and six days of exposure to bacteria were 16 and 19 ug$\cdot cm^{-2}$. The total PLFA was 3500 and 8700 pmol$\cdot cm^{-2}$ corresponding to approximately $2x10^{8}$ and $5x10^{8}$ cells$\cdot cm^{-2}$. The sterile controls had less than detectable levels of protein and PLFA and showed little IR absorbance ($<1x10^{-2}$ K-M units for any peak).

The fatty acid profiles for the attached bacteria after four and six days of exposure to bacteria in the flowing

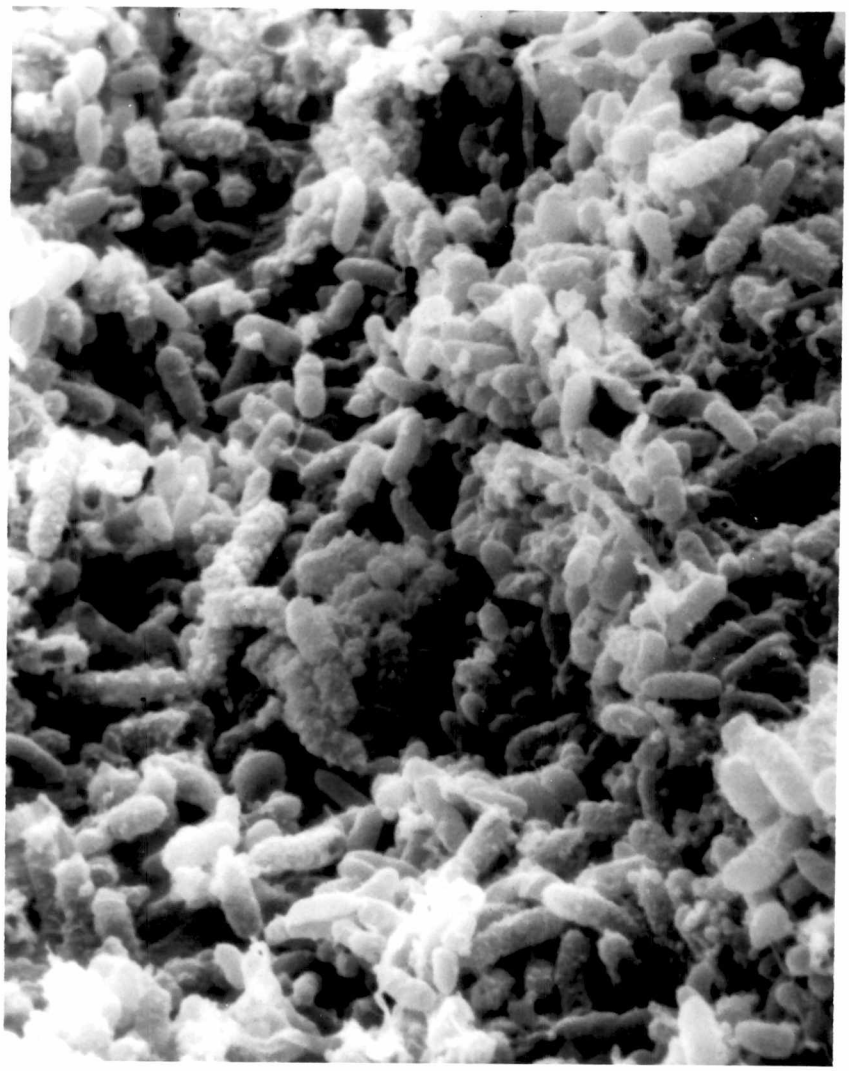

Figure 8. Scanning electron micrograph of isolate 3T5 on the surface of the carbon steel after eight days of exposure in a flowing system.

system are shown in Table 1. The ratio of 16:1w7t to 16:1w7c was less than in the batch cultures (Table 1). Certain marine bacteria have been shown to produce trans fatty acids. The ratio of trans to cis monounsaturates has been correlated to nutrient stress (6,7). Thus, the bacteria in the flowing system appear to be less nutritionally stressed than those in batch culture systems.

The results of this study demonstrated that aerobic heterotrophic bacteria isolated from steel pipe tubercles were capable of colonizing steel surfaces with the production of extracellular polymer, under laboratory conditions. The bacteria induced tubercle formation on the steel samples, and increased the corrosion rates, as determined by the polarization resistances. Although the mechanism for corrosion facilitation was not determined, the production of volatile fatty acids, and the reduction of ferric iron are not likely mechanisms. The production of extracellular polymer has been implicated in the binding of passive films associated with copper (4). In this study, the binding of the extracellular polymer to the passive film may have resulted in an acceleration of the corrosion rate. Alternatively the creation of differential aeration cells by aerobic respiration of the bacteria may have accelerated the corrosion rate.

LITERATURE CITED

1. Bobbie, R.J., and D.C. White (1980) Characterization of benthic microbial community structure by high-resolution gas chromatography of fatty acid methyl esters. Appl. Environ. Microbiol. **39**:1212-1222

2. Dowling, N.J.E., J. Guezennec, M. L. Lemoine, A. Tunlid, and D.C. White (1988) Analysis of carbon steels affected by bacteria using electrochemical impedance and direct current techniques. Corrosion **44**:869-874

3. Franklin, M.J., D.E. Nivens, M.W. Mittelman, A.A. Vass, R.F. Jack, N.J.E. Dowling, R.P. Mackowski, S.L. Duncan, D.B. Ringelberg, and D.C. White. (1989) An analog MIC system with specific bacterial consortia, to test effectiveness of materials selection and countermeasures. CORROSION/89 paper no. 513.

4. Geesey, G.G., M.W. Mittelman, T. Iwaoka, P.R. Griffiths (1986) Role of bacterial exopolymers in the deterioration of metallic copper surfaces. Materials Performance **25**:37-40

5. Guckert, J.B., C.P. Antworth, P.D. Nichols, and D.C. White (1985) Phospholipid, ester-linked fatty acid profiles as reproducible assays for changes in prokaryotic community structure of estuarine sediments. F.E.M.S. Microbiol. Ecology **31**:147-158

6. Guckert, J.B., M.A. Hood, and D.C. White (1986) Phospholipid, ester-linked fatty acid profile changes during nutrient deprivation of Vibrio cholerae: increases in the trans/cis ratio and proportions of cyclopropyl fatty acids. Appl. Environ. Microbiol. **52**:794-801

7. Hood, M.A., J.B. Guckert, D.C. White, and F. Deck (1986) Effect of nutrient deprivation on lipid, carbohydrate, DNA, RNA, and protein levels in Vibrio cholerae. Appl. Environ. Microbiol. **52**:788-793

8. Lappin-Scott, H.M., and J.W. Costerton (1989) Bacterial biofilms and surface fouling. Biofouling **1**:323-342

9. Little, B., Wagner, P., Gerchakov, S.M., and Mitchell, R. (1986) The involvement of a thermophilic bacterium in corrosion processes. Corrosion **42**:533-536

10. Lowry, O.H, Rosebrough, N.J., Farr, A.L., and Randall, R.J. (1951) Protein measurement with the Folin phenol reagent. J. Biol. Chem. **193**:265-275

11. Mansfeld, F. (1981) Recording and analysis of AC impedance data for corrosion studies. I. Background and methods of analysis. Corrosion **36**:301-307

12. Mansfeld, F., Kendig, M.W., and Tsai, S. (1982) Recording and analysis of AC impedance data for corrosion studies. II. Experimental approach and results. Corrosion **38**:570-580

13. Nichols, P.D., J.B. Guckert, and D.C. White (1986)Determination of monounsaturated fatty acid double-bond position and geometry for microbial monocultures and complex consortia by capillary GC-MS of dimethyl disulfide adducts. J. Microbiol. Methods **5**:49-55

14. Nichols, P.D., J.M. Henson, J.B. Guckert, D.E. Nivens, and D.C. White (1985) Fourier transform infrared spectroscopic methods for microbial ecology: analysis of bacteria, bacteria-polymer mixtures and biofilms. J. Microbiol. Methods **4**:79-94

15. Nivens, D.E., Nichols, P.D., Henson, J.M., Geesey, G.G., and White, D.C. (1986) Reversible acceleration of the corrosion of AISI 304 stainless steel exposed to seawater induced by growth and secretions of the marine bacterium Vibrio natriegens. Corrosion **42**:204-210

16. Nivens, D.E. to be published

17. Obuekwe, C.O., Westlake, D.W.S., Plambeck, J.A., and Cook, F.D. (1981) Corrosion of mild steel in cultures of ferric iron reducing bacterium isolated from crude oil. II. Mechanisms of anodic depolarization. Corrosion **27**:632-637

18. Stookey, L.L. (1970) Ferrozine - a new spectrophotometric reagent for iron. Anal. Chem. **42**:779-781

19. Uhlinger, D.J., and D.C. White (1983) Relationship between physiological status and formation of extracellular polysacchaaride glycocalyx in Pseudomonas atlantica. Appl. Environ. Microbiol. **45**:64-70.

20. White, D.C. R.F. Jack, N.J.E. Dowling, M.J. Franklin, D.E. Nivens, S. Brooks, M.W. Mittelman, A.A. Vass, and H.S. Isaacs (1990) Microbially influenced corrosion of carbon steels. Paper no. 90103 CORROSION 90 NACE.

CHAPTER IV

EFFECT OF ELECTROCHEMICAL IMPEDANCE SPECTROSCOPY ON MICROBIAL BIOFILM CELL NUMBERS, VIABILITY, AND ACTIVITY

ABSTRACT

Electrochemical impedance spectroscopy (EIS) is a useful technique for studying mechanisms of microbially influenced corrosion (MIC). In this study, the assumption that the sinusoidal signals applied during EIS do not destroy the biofilms was tested. Matched pair statistical analysis was used to test the effect of EIS on the total numbers of sessile bacteria, the numbers of viable bacteria, and the lipid biosynthetic activity of the sessile bacteria. The results demonstrated that no statistically significant differences occurred between biofilms where signal was applied (5 mV rms, 10 kHz to 5 mHz) and biofilms where no signal was applied.

INTRODUCTION

Electrochemical techniques are increasingly being used in microbially influenced corrosion (MIC) studies to gain a better understanding of the effects of microorganisms on the corrosion of metals. In order to avoid altering MIC processes by the analyses, it is preferable to use techniques which do not damage the biofilms. Among the techniques being used to study MIC is electrochemical impedance spectroscopy (EIS). Applications of EIS in MIC studies have included monitoring corrosion over time on carbon steel exposed to bacteria (2, Chapter 1), carbon steel exposed to bacteria and treated with biocides (5, Chapter 3), stainless steel weldments exposed to bacteria (1), and stainless steel samples exposed to natural seawater (7).

The advantages of using EIS in MIC studies have been reviewed (6). One of the advantages of using EIS is that small amplitude signals, within the linear response range, and generally 5 mV rms or less, are applied. Repeated EIS analysis on stainless steel samples with biofilms caused no change in the open circuit potential after the analysis, providing indirect evidence that EIS did not damage the metal samples or the biofilms (3). In this study, the effect of applied sinusoidal signal on the numbers, viability, and activities of sessile bacteria on stainless steel samples, were directly tested. Matched pair

statistical analyses showed no significant differences between these properties of the biofilms on experimental samples (samples with sinusoidal signal applied) and control samples (samples with no signal applied).

MATERIALS AND METHODS

Medium. The medium used in this study contained (per liter of deionized water) 50 mg NH_4Cl; 50 mg $MgSO4 \cdot 7H_2O$; 5 mg $CaCl \cdot 2H_2O$; 27 mg KH_2PO_4; 15 mg Mops buffer; 15 mg yeast extract; 15 mg peptone; 15 mg glucose; and 1 ml Hutner's mineral. The pH of the medium was adjusted to 7.2 with NaOH. For analyses of colony forming unit (CFU) agar 15 g/l was added to the media, and the concentration of the carbon sources used in the solid media were increased ten fold to allow visual detection of colonies.

Bacteria. The bacteria used in this study were obtained from our laboratory culture collection of bacteria isolated from tubercles on failed steel pipes. These bacteria were analyzed by the Hewlett-Packard microbial identification system, which compares the profile of membrane fatty acids with those contained in a computer library. The bacteria selected for use in this study were; two physiologically different Pseudomonas spp., a Bacillus sp., an Erwinia sp., and an Acinetobacter sp. Bacteria were incubated for one to two days at 24°C prior to inoculation into test flasks. Two ml, approximately 10^9 cells, of each culture was used as the inoculum.

Experimental flasks. Tall one liter flasks were used as electrochemical cells. The flasks were sealed with rubber stoppers, and draped with aluminum foil to prevent contamination. The rubber stopper contained ports for the

salt bridge, titanium counter electrode, and leads for the working electrodes. In addition the rubber stopper had ports for medium inlet drip tubes and medium exit lines, so that the experiments could be performed under continuous flow conditions (4). The working volume of the flasks was 500 ml, and the dilution rate was 0.5 h^{-1}. This rapid dilution rate allowed wash out of most of the bulk phase bacteria, and formation of thick biofilms. The medium was stirred with magnetic stirrers. Flasks were sterilized by ethylene oxide at the University of Tennessee Medical Center.

Metal samples. The working electrodes were 316L stainless steel coupons. (Metal Samples Co., Munford Al). Electrical leads were soldered to the backs of the coupons, and the coupons were embedded in epoxy. The coupons were finished with 600 grit silicone-carbide paper, and the edges of the coupons were painted with lacquer to minimize crevice corrosion. The electrical leads were insulated from the solution using glass tubes. Four working electrodes were suspended in each flask.

Electrochemical impedance spectroscopy. Each flask contained four working electrodes. Sinusoidal signal was applied to two of the electrodes, and no signal was applied to the other two electrodes. A Solartron 1250 frequency response analyzer, and a Solartron 1091 electrochemical interface, controlled by a Hewlett-Packard series 300

computer were used to generate potentials, and to determine the open circuit potential. Sinusoidal potential of 5 mV rms around the OCP, ranging in frequency from 5 mHz to 10 kHz, was applied to the working electrode. Five frequencies were applied per decade. After the signal was applied to one of the samples, that electrode and another electrode, which remained at open circuit, were removed from the solution and microbiological analyses were performed.

Evaluation of bacterial populations. The procedures for determining the total numbers of bacteria, by acridine orange direct counts (AODC), and the total numbers of viable bacteria, by colony forming units (CFU) were similar to those described previously (5). After removal of the electrodes from the flasks, O-ring sealed tubes were clamped to the coupons (8). Basal salts solution (medium without yeast extract, glucose, or peptone added), 500 μl, was added to each tube. The solution was point sonicated at 20% power three times in five sec pulses to remove bacteria from the surface. The suspension was serially diluted in basal salts. The diluents were filtered on 0.2 μm pore size Nucleopore filters and stained with acridine orange to determine AODC's. The diluents were also plated on agar media to determine the numbers of CFU's. The CFU data represents the average of duplicate plates from individual coupons.

Evaluation of bacterial metabolic activity. The other two electrodes from each flask, one with the sinusoidal potential applied and the other without, were used to determine bacterial metabolic activity, as determined by lipid biosynthetic activity. The procedure for determining biosynthetic activity is the same as previously described (5). Test coupons were removed from the flask, and a modified separatory funnel, with an O-ring base was clamped onto each coupon (8). One-half ml of basal salts solution, containing 2.5 μCi ^{14}C-acetate (55 mCi·mmole^{-1}) was added to each separatory funnel. After 30 min incubation, 5 ml chloroform, 5 ml methanol, and 4 ml of pH 7.4 phosphate buffer were added to the modified separatory funnels. After 2 hours, the solutions were transferred to separatory funnels using two washes of 2.5 ml chloroform each. Five ml of 18 mohm·cm deionized water was added to each solution to cause phase separation. The chloroform phase, containing the lipid fraction, was removed and dried under a stream of N_2. This lipid fraction was then transferred to a scintillation vial by three washes of chloroform. The samples were again dried under N_2 and 7 ml Insta-gel scintillation cocktail was added, and the samples were counted using a scintillation counter.

Statistical analysis. The Students t-test was performed on the matched pair data. The critical t-values at the 95% confidence level were 2.13, 2.02, and 1.94 for

the four, five, and six degrees of freedom, respectively, used in this study.

RESULTS AND DISCUSSION

The effect of EIS on initially colonizing biofilms, and on stable biofilms was determined, by performing analyses after one day and after five days of biofilm growth. The experiments were designed to analyze the sessile bacteria with little contamination of bacteria from the bulk phase. Therefore a flowing system with a rapid dilution rate (0.5 h^{-1}) was used. The numbers of cells in the bulk phase, by AODC, ranged from 2×10^7 to 4×10^7 cells/ml for the one day experiments, and from 4×10^7 to 6×10^7 cells/ml for the five day experiments. If a small volume of the bulk phase was removed with the samples, little effect would have been observed on the numbers of bacteria in the one day biofilms, and no effect on the numbers of bacteria would have been observed in the five day biofilms.

Stainless steel samples were used as working electrodes to avoid the build up of corrosion products. Therefore, analyses could be performed on sessile bacteria associated with the steel surface, and not with the corrosion products.

Matched pair analysis of AODC revealed no significant difference at the 95% confidence level between total numbers of bacteria on electrodes where sinusoidal signal was applied and on electrodes where no signal was applied. No difference was observed for both the one day biofilms ($n=5$, $t=0.60$) and for the five day biofilms ($n=7$, $t=1.43$). Figure 1A shows the data where each matched pair (signal

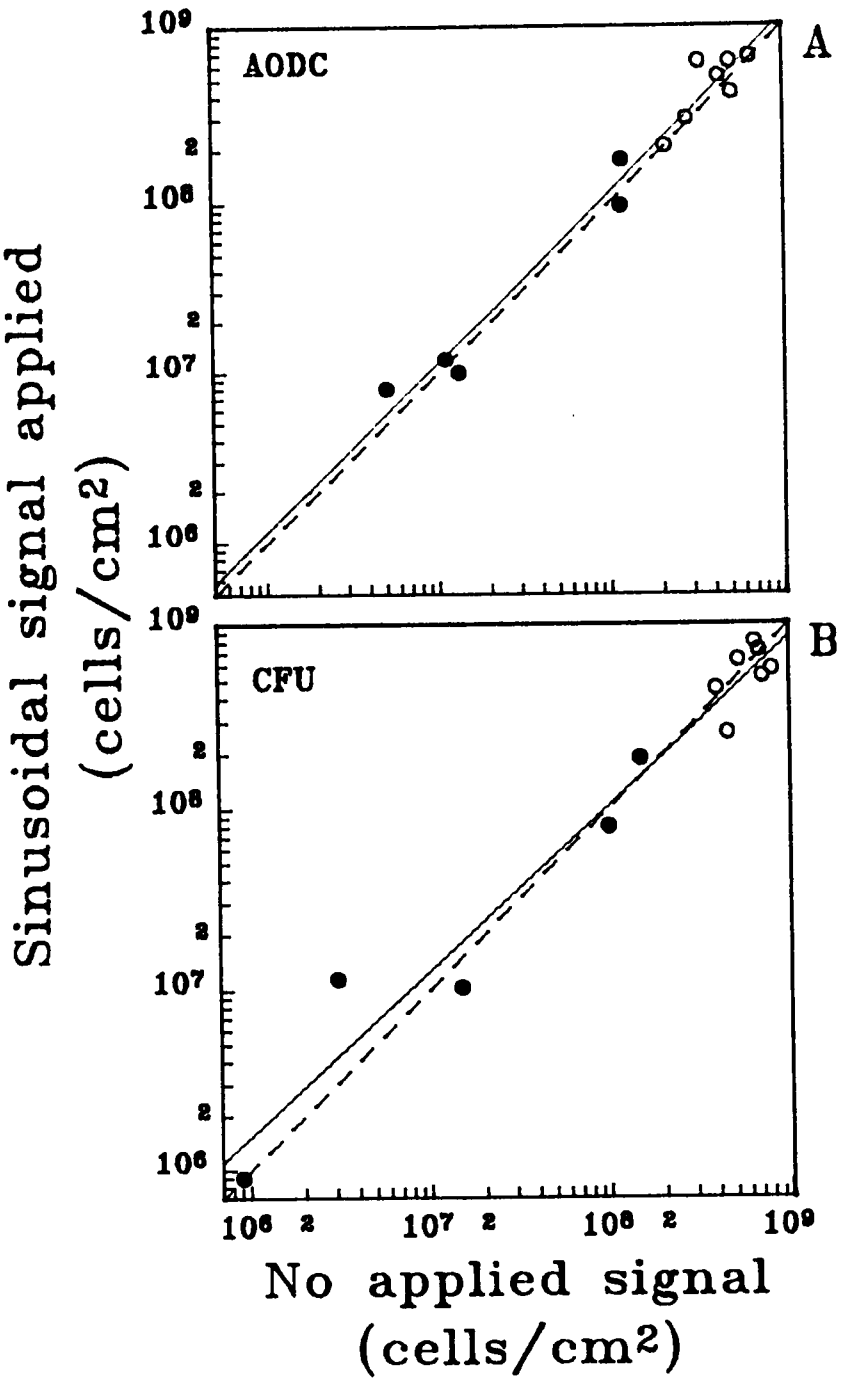

Figure 1. A) Acridine orange direct counts of sessile bacteria for each matched pair, open circles - bacteria from five day biofilms, closed circles - bacteria from one day biofilms. Solid line represents the linear regression. B) Colony forming units of sessile bacteria for each matched pair, open circles - bacteria from five day biofilms, closed circles - bacteria from one day biofilms. Solid Line represents the linear regression. Dashed line represents the ideal 1:1 relationship.

applied versus no signal applied) is plotted on a log-log plot. Regression analysis indicated a linear relationship (r^2=0.86), very close to the ideal 1:1 reponse shown as a dotted line. The results from the matched pair analysis and the linear regression analysis demonstrated that the application of sinusoidal signal did not cause a significant decrease in the total number of cells (viable and nonviable), and therefore did not induce lysis of the sessile bacteria.

The effect of EIS on the numbers of viable bacteria in one day biofilms and in five day biofilms was determined by colony forming units as described in the materials and methods. The matched pair analysis revealed no significant difference at the 95% confidence level between the number of viable bacteria in the EIS treated and the untreated samples for both the one day biofilms (n=5, t=0.05) and for the five day biofilms (n=7, t=1.55). The data for the matched pairs are plotted in Fig 1B. A linear relationship (r^2=0.84) with a slope close to one was observed for the CFU's on samples with EIS input signal applied on samples without applied signal. These data indicated that the applied sinusoidal signal did not cause a decrease in the numbers of viable bacteria in the biofilms.

Figure 2 shows a linear relationship (r^2=0.90) between the AODC's and the CFU's for both the EIS treated samples

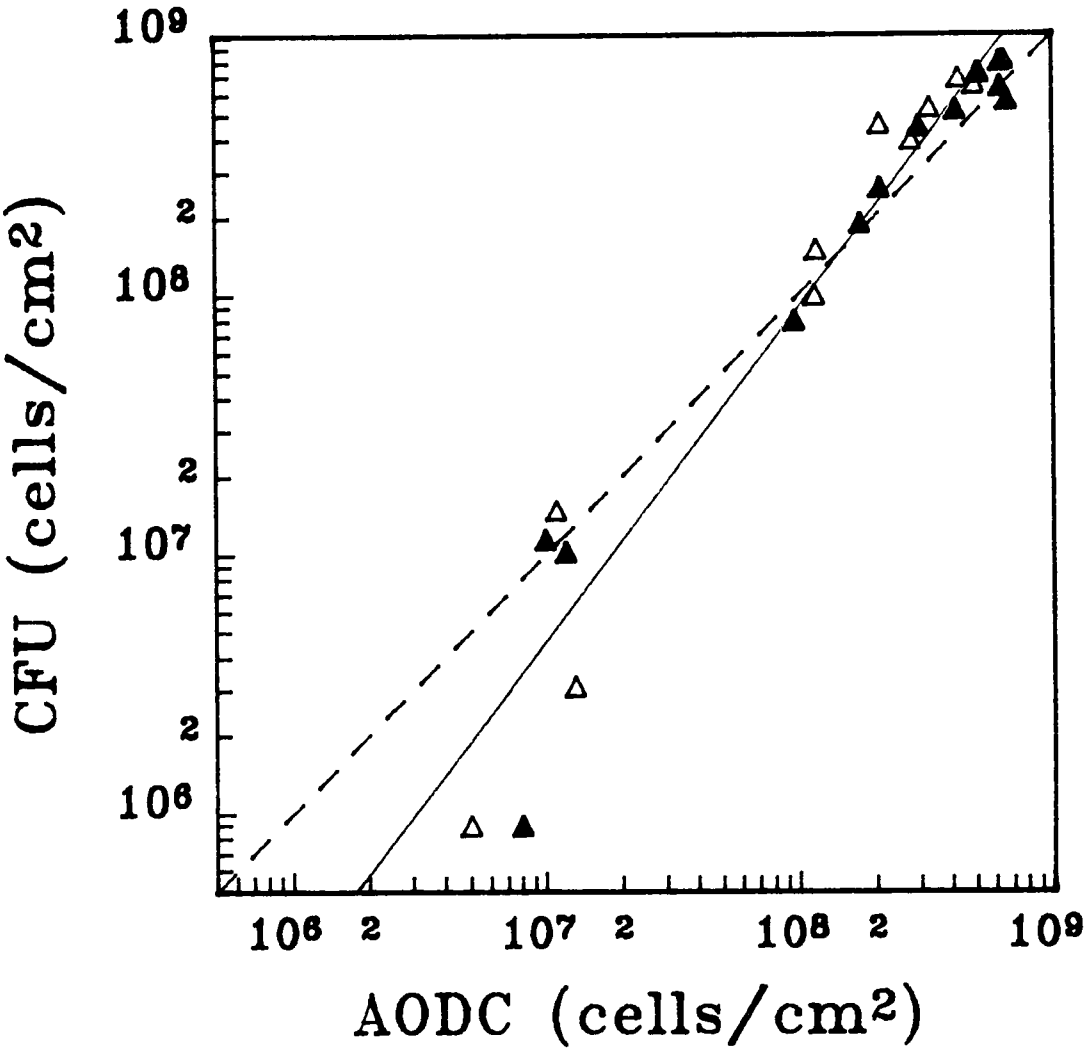

Figure 2. Acridine orange direct counts versus colony forming units, closed triangles - sinusoidal signal applied, open triangles - no applied signal. Solid line represents the linear regression. Dashed line represents the ideal 1:1 relationship.

(closed triangles) and the untreated samples (open triangles). These data indicate that most of the bacteria which were counted by AODC were culturable for the viable counts. This was the case for both the EIS treated samples and the untreated samples. These data also indicate that the procedure for removing the bacteria from the surface (i.e. sonication) did not cause a reduction in the viability of the sessile bacteria.

The effect of EIS on the biosynthetic activity of the sessile bacteria was determined by the incorporation of ^{14}C-acetate into total cell lipids. Matched pair analysis revealed no significant difference at the 95% confidence level for the one day biofilms ($n=5$, $t=1.22$), and for the five day biofilms ($n=6$, $t=1.97$). Figure 3 shows the regression analysis for the activity of the EIS treated biofilms versus the untreated biofilms ($r^2=0.74$). The data indicate that the application of EIS to the samples did not cause a significant change in the biosynthetic activity of the biofilms.

The results of this study indicated that EIS can be used to study mechanisms of MIC with little or no damage to the numbers of viable bacteria in a biofilm or to the activity of the bacteria.

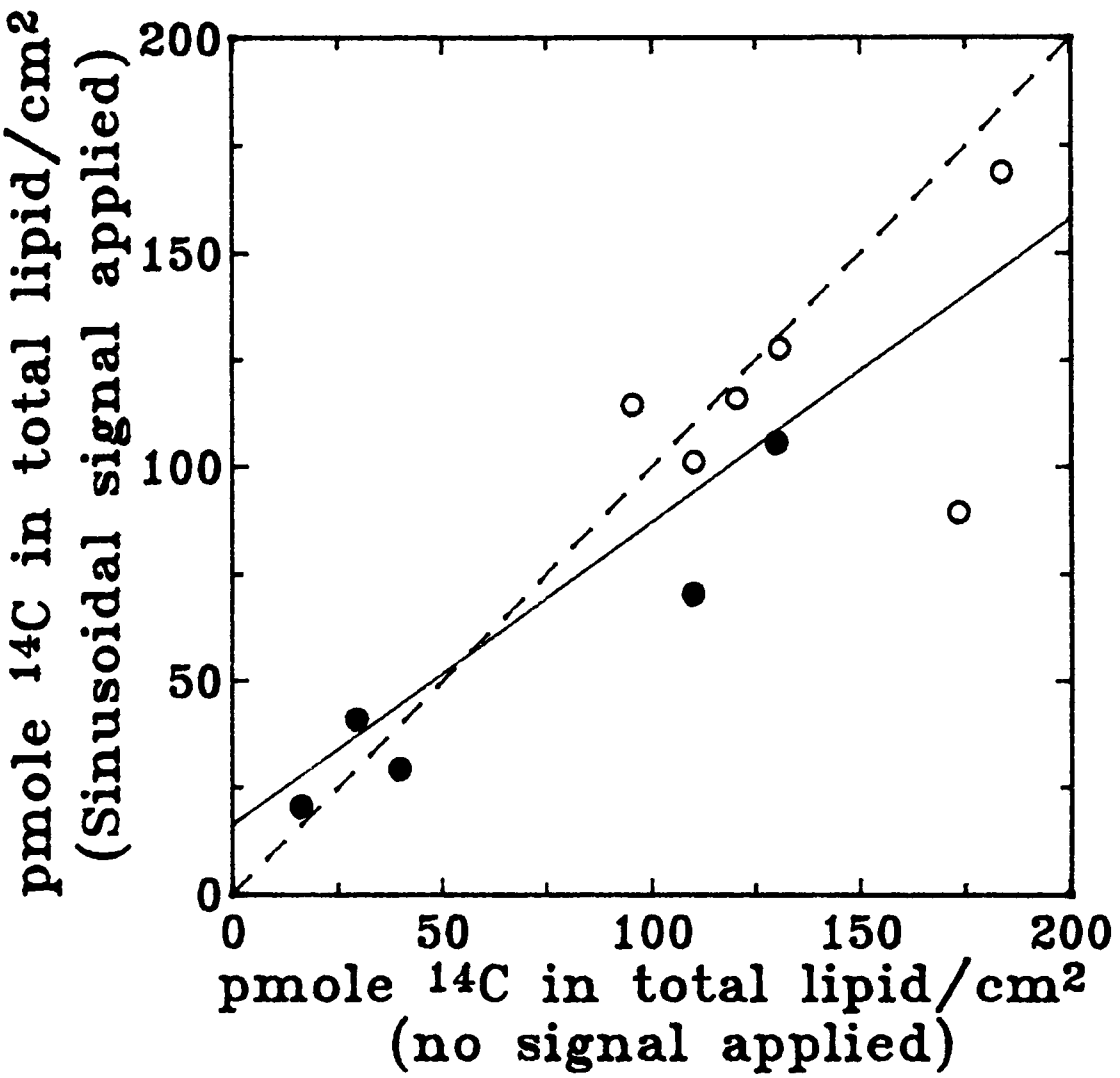

Figure 3. Bacterial activity, measured by incorporation of ^{14}C-acetate into total lipids for each matched pair, open circles - bacteria from five day biofilms, closed circles - bacteria from one day biofilms. Solid line represents the linear regression. Dashed line represents the ideal 1:1 relationship.

LITERATURE CITED

1. Dowling, N.J.E., M. Franklin, D.C. White, C.H. Lee, and C. Lundin. (1989) Effects of microbiologically influenced corrosion on stainless steel weldments in seawater. CORROSION/89, paper no. 187, National Association of Corrosion Engineers (New Orleans, La).

2. Dowling, N.J.E., J. Guezennec, M. L. Lemoine, A. Tunlid, and D.C. White, (1988) Corrosion analysis of carbon steels affected by aerobic and anaerobic bacteria in mono and coculture using AC impedance and DC techniques. Corrosion **44**:869-874.

3. Dowling, N.J.E., E.E. Stansbury, D.C. White, S.W. Borenstein, and J.C. Danko. (1989) On-line electrochemical monitoring of microbially induced corrosion. in: Microbial Corrosion: 1988 Workshop Proceedings (G.J. Licina, ed.) EPRI R-6345, Research Project 8000-26, Electric Power Research Institute, Palo Alto, Ca. pp 5-1 5-17.

4. Franklin, M.J., D.E. Nivens, M.W. Mittelman, A.A. Vass, R.F. Jack, N.J.E. Dowling, R.P. Mackowski, S.L. Duncan, D.B. Ringelberg, and D.C. White. (1989) An analogue MIC system with specific bacterial consortia to test effectiveness of materials selection and countermeasures. CORROSION/89 paper no. 513 National Association of Corrosion Engineers (New Orleans, La).

5. Franklin, M.J., D.E. Nivens, A.A. Vass, M.W. Mittelman, R.F. Jack, N.J.E. Dowling, and D.C. White. Effect of chlorine and chlorine/bromine biocide treatments on the number and activity of biofilm bacteria and on carbon steel corrosion. Corrosion (in press).

6. Mansfeld, F., and B. Little (1990) The application of electrochemical techniques for the study of MIC - A critical review. CORROSION/90, paper no 108, National Assosiation of Corrosion Engineers. Las Vegas, Nv.

7. Mansfeld, F., C.H. Tsai, H. Shih, B. Little, R. Ray, and P. Wagner. Corrosion/90, paper no. (Las Vegas, Nv: NACE, 1990).

8. Nivens, D.E., J.B. Guckert, K. Kroeger, J.Q. Chambers, and D.C. White. Microbial biofilm isolation device for off-line analysis. J. Microbiol. Methods, submitted.

CHAPTER V

EFFECT OF CHLORINE AND CHLORINE/BROMINE BIOCIDE TREATMENTS ON THE NUMBER AND ACTIVITY OF BIOFILM BACTERIA AND ON CARBON STEEL CORROSION

ABSTRACT

The ability of NaOCl and a mixture of NaOCl and NaBr to reduce the numbers and metabolic activity of sessile bacteria on carbon steel in a moderately alkaline test medium were evaluated. The polarization resistances, measured by electrochemical impedance spectroscopy (EIS) of the carbon steel coupons were evaluated prior to and during biocide treatments. Corrosion tubercles were observed on the carbon steel samples four days after inoculation with a consortia of five different physiological types of bacteria. NaOCl or NaOCl/NaBr was then added to the vessels containing the steel samples. Exposure to 2 ppm of residual chlorine or of residual chlorine/bromine for two hours had little effect on the numbers of sessile bacteria, or the bacterial metabolic activity, as measured by ^{14}C acetate incorporation into total lipids. Treatment for two hours with 16 ppm of residual chlorine or of residual chlorine/bromine, followed by a 24 h treatment with 2 ppm of residual biocide, decreased sessile aerobic bacteria two orders of magnitude, and decreased sessile sulfate reducing bacteria by three orders of magnitude. Bacterial metabolic activity was decreased to the levels of the sterile controls following the 16 ppm treatment. Bacteria in the bulk solution were reduced from approximately $5x10^7$ cells per ml to less than one cell per ml, following the 16 ppm treatments. The carbon steel admittance increased when samples were treated

with the high concentrations of biocides, compared to untreated controls. These results indicated that low levels of halogen biocide treatments may be ineffective at reducing sessile bacterial populations in moderately alkaline systems. Treatments with high concentrations of halogen biocide, although effective at reducing bacterial numbers and activities, increased the corrosion rate of the carbon steel.

INTRODUCTION

Biofouling and biodeterioration by microorganisms can lead to premature failures of metallic pipelines (7). As a result, biocide treatments are often used as countermeasures to decrease the biofouling and microbially influenced corrosion (MIC) of steel pipes. Evaluation of biocide efficacy against sessile bacteria at industrial plants is often a difficult task. Often only the planktonic bacterial populations are evaluated, since planktonic bacteria are more easily sampled than sessile bacteria. Sessile bacteria tend to be more resistant to biocide treatment than are planktonic bacteria (8,9,10).

In addition to the difficulties in microbiological evaluation of biocide efficacy, the effect of the biocide on the metal corrosion is also difficult to assess in industrial plants. Halogen biocides, such as hypochlorous acid and hypobromous acid are strong oxidizing agents, and can be corrosive to metals (18). Low level use of these biocides is often recommended for treatment of cooling water systems in order to minimize the corrosive effects of these biocides (17). Since low level treatment may not be effective against the sessile bacteria, evaluation of the effectiveness of these treatments based on planktonic cells may provide a false sense of security.

Often biocide efficacy studies are performed on monocultures, rather than consortia of bacteria. It is

possible that biocide efficacy is not only dependent upon number and biomass parameters, but also on consortial make-up. In the present study, the biocidal activities of NaOCl and a mixture of NaOCl and NaBr against a consortium of five different physiological types of bacteria, which were isolated from failed steel pipes, were evaluated. The rate of corrosion influenced by bacteria appears to be dependent on the metabolic activities of the microbes, and not merely on the amount of microbial biomass (6). Therefore, in addition to evaluation of the numbers of sessile bacteria present during biocide treatments, the activity of the biofilm, as determined by ^{14}C-acetate incorporation into lipids was evaluated.

Primarily due to high photosynthetic activity, the pH of lake water can rise. The acid form of halogen biocides is more effective than the salt (8). Hypobromous acid is considered to be more effective in alkaline environments than is hypochlorous acid, since the pKa of hypobromous acid, 8.8, is higher than hypochlorous acid, 7.2. A dilute flowing medium at pH 8.5 system was used in this study.

In the present study, a test system was developed to evaluate the biocidal effects of biocide treatments against sessile bacteria, and the effects of the biocide on the carbon steel corrosion rates.

MATERIALS AND METHODS

Media. The basal salts used for all media contained (per liter of deionized water) 50 mg NH_4Cl; 50 mg $MgSO4 \cdot 7H_2O$; 5 mg $CaCl \cdot 2H_2O$; 27 mg KH_2PO_4; 142 mg Na_2SO_4; 121 mg Tris·HCl buffer; and 1 ml Hutner's mineral. The pH of all media were adjusted to 8.5 with NaOH. The following carbon sources were added to the media used in the flowing system (per liter of deionized water) 20 mg glucose; 10 mg calcium lactate; 10 mg sodium citrate; 5 mg yeast extract. For analyses of colony forming unit (CFU) agar 15 g/l was added to the media, and the concentration of the carbon sources used in the solid media were increased ten fold to allow visual detection of colonies. Most probable number (MPN) tubes for sulfate reducing bacteria (SRB) contained (per liter of basal salts) 100 mg calcium lactate, 100 mg yeast extract, and 1 g ferric ammonium sulfate. MPN tube media were made anaerobic by boiling under a stream of O_2-free nitrogen. Anaerobic media were dispensed into rubber stopper sealed pressure tubes as described by Balch et al., (9). Sulfate reduction was assayed by the production of black FeS after a one week incubation period.

Bacteria. The bacteria used in this study were obtained from a laboratory culture collection of bacteria isolated from tubercles on failed steel pipes. These bacteria were analyzed by the Hewlett-Packard microbial identification system, which compares the profile of

membrane fatty acids with those contained in a computer library. The bacteria selected for use in this study were; two physiologically different Pseudomonas spp., a Bacillus sp., an Erwinia sp., an Acinetobacter sp., and a lactate utilizing sulfate reducing bacterium. Sterile microbiological medium was allowed to flow into the flasks for one day prior to inoculation with bacteria. Bacteria were incubated for one to two days at 24C prior to inoculation into test flasks. Two ml, approximately 10^9 cells, of each culture was used as the inoculum.

Test system. Two flasks were used for each treatment, one flask for performing electrochemical analysis, and one flask for performing microbiological analysis. The complete experimental system was described (5). This arrangement was used so that the electrochemical measurements would not be disturbed during the removal of coupons for microbiological evaluation. The working electrodes were C1020 carbon steel coupons embedded in epoxy (Metal Samples Co., Munford Al). Electrical leads were soldered to the back of the samples. The composition of the steel by weight percent was C, 0.17; Mn, 0.42; P, 0.009; and S, 0.006. The electrochemical flasks also contained a salt bridge for connecting a saturated calomel reference electrode (SCE) to the solution, and a titanium counter electrode. The flasks had medium inlet and outlet ports. The liquid volume of the flasks was 500 ml and the dilution rate for the medium was 0.1 per

hour. The medium was constantly stirred using magnetic stir bars.

The flasks for microbiological analyses contained epoxy embedded C1020 carbon steel coupons, ten to 16 coupons were used per flask. Stainless steel hooks were used to suspend the embedded coupons in the medium. All carbon steel samples were finished to 600 grit with silicon carbide finishing paper. Flasks were sterilized by ethylene oxide sterilization at the University of Tennessee Medical Center. All experiments were performed under aeseptic conditions in a class 100 laminar-flow hood.

Biocide additions. Biofilms were allowed to develop on the metal surfaces for four days prior to biocide addition. NaOCl was prepared immediately prior to use as a 100x stock solution. The solution was added to the medium until the appropriate level of total residual biocide was obtained, as measured by the DPD Cl_2 test (1). For studies using the continuous treatment of NaOCl and NaBr, NaBr, 4 mg/l, was added to the medium reservoir, and a stock solution of NaOCl was continuously pumped into the flasks using peristaltic pumps (Cole-Parmer Co. Chicago, Il.). The total residual biocide was monitored over the course of the experiments to allow adjustment of the biocide level to the appropriate levels.

Evaluation of bacterial populations. Coupons were removed from the flasks, and flanged tubes containing O-ring

seals were clamped to the coupons (15). One ml of anaerobic basal salts solution was added to each tube. The solution was point sonicated three times in three sec pulses to remove bacteria from the surface. Prior tests comparing total cell counts using acridine orange direct counts (AODC) and viable counts using colony forming units (CFU) showed that this sonication treatment had no significant effect on bacterial viability. The suspension was serially diluted in anaerobic basal salts, and the diluents were plated on agar media or inoculated into most probable number (MPN) tubes. The numbers of aerobic and facultatively anaerobic bacteria, associated with the steel surfaces, were determined by aerobic plate counts of CFU's. The numbers of sulfate reducing bacteria were determined by MPN analysis of anaerobic broth tubes. The CFU data represent the average of duplicate plates from individual coupons. Three tube MPN's were used to obtain values for sulfate reducers.

Evaluation of bacterial metabolic activity. Test coupons were removed from the flask, and a modified separatory funnel, with an O-ring base was clamped onto each coupon (15). One-half ml of basal salts solution, containing 2.5 μCi ^{14}C-acetate (55 mCi·mmole^{-1}) was added to each separatory funnel. After 30 min incubation, 5 ml chloroform, 5 ml methanol, and 4 ml of pH 7.4 phosphate buffer were added to the separatory funnels. After 2 hours, the solutions were transferred to separatory funnels using

two washes of 2.5 ml chloroform each. Five ml of 18 mohm·cm deionized water was added to each solution to cause phase separation. The chloroform phase, containing the lipid fraction, was removed and dried under a stream of N_2. This lipid fraction was then transferred to a scintillation vial by three washes of chloroform. The samples were again dried under N_2 and 7 ml Insta-gel scintillation cocktail was added. Radioactivity was counted in a LKB Wallac model 1212 liquid scintillation counter.

Scanning electron microscopy. Metal coupons were removed and fixed for 30 min in 0.1 M sodium cacodylate buffer, pH 7.4, containing 2% (v/v) glutaraldehyde. The samples were then dehydrated by exchanging the solution with increasing concentrations of acetone (50%, 75%, 100%). The samples were critical point dried and sputtercoated with gold/palladium. The samples were then analyzed using a ETEC autoscan scanning electron microscope.

Electrochemical impedance spectroscopy. A Solartron 1250 frequency response analyzer, and a Solartron 1091 electrochemical interface, controlled by a Hewlatt-Packard series 300 computer were used to generate signals and analyze the magnitude and phase shift of the resulting currents. Sinusoidal potentials of 5 mV rms, ranging in frequency from 5 mHz to 10 Hz, were applied to the working electrode. The resulting impedances were plotted, using the Nyquist format. A single depressed semicircle was obtained

for most of the impedance analyses. Therefore, estimates of solution resistance (R_s), polarization resistance (R_p), and double layer capacitance (C_{dl}) could be obtained (12,13).

RESULTS

Bacterial colonization of carbon steel. Bacteria colonized the steel surface for four days prior to biocide treatment. Loosely adhered corrosion products, due to localized corrosion, formed on the metal surfaces over this time. Figure 1A shows several morphological types of bacteria as well as dehydrated bacterial extracellular polymer associated with the corrosion products in the nontreated metal sample. When the biofilm and the corrosion products were removed from the metal surface, localized corrosion of the surface was observed (Fig. 1B).

Effects of 2 ppm biocide treatments on numbers and activities of sessile bacteria. After four days of biofilm growth, 2 ppm of residual chlorine or a total of 2 ppm of residual chlorine/bromine (3:1), was maintained in flasks for two hours. Treatment was stopped for 22 hours, then continued for two additional hours. Figure 2 shows the colony forming units of heterotrophic bacteria for the two 2 ppm treatments. No significant decrease was observed in the chlorine or the chlorine/bromine treated samples. The scatter in the data is likely due to sampling variation, since the nontreated control shows a slight decrease in CFU's and the treated sammples show a slight increase after the first 2 ppm treatment. In addition to the CFU's, no significant decrease in the numbers of sulfate reducing bacteria or the lipid biosynthetic activity was observed for

Figure 1. A) Scanning electron micrograph showing a consortium of bacteria, and their extracellular polymer associated with the corrosion products of a carbon steel sample. Bar represents 1 μm. B) scanning electron micrograph of the surface of the sample, after the biofilm and corrosion products were removed. Bar represents 10 μm.

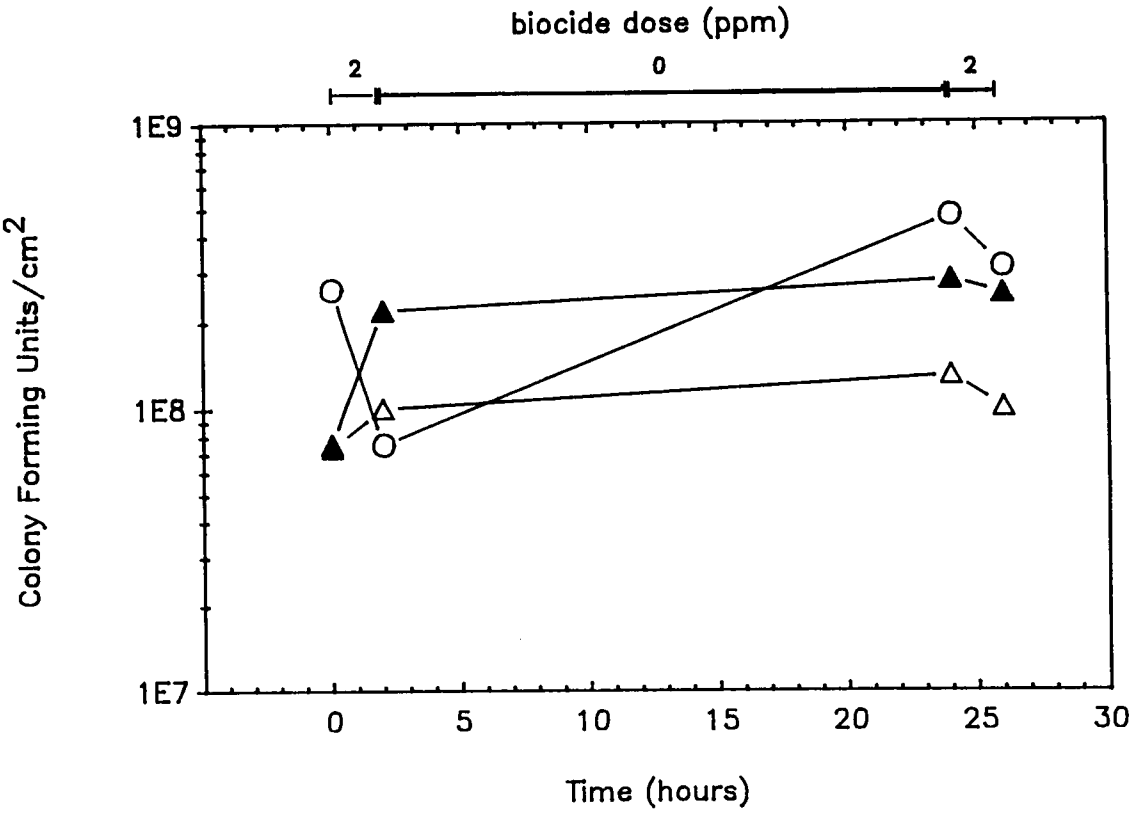

Figure 2. A) Total colony forming units of heterotrophic bacteria per cm^2. Values represent the mean of two CFU platings. Time zero is after four days of biofilm development. Open circles- no biocide treatment, open triangles- 2 ppm NaOCl treatments. Closed triangles- 2 ppm NaOCl/NaBr treatments.

either treatment compared to the nontreated controls. Approximately 10^4 sulfate reducers/cm^2 were observed after the 2 ppm treatments and for the nontreated controls. The lipid biosynthetic activity remained above 50 pmole ^{14}C acetate incorporation/cm^2 for all samples.

Figure 3 shows a scanning electron micrograph, following the final 2 ppm treatment with NaOCl. The micrograph shows similar microbial biomass to that of the untreated control. As with the untreated control, dehydrated extracellular polymer could be seen in association with the biofilm.

16 ppm biocide treatment followed by 2 ppm treatment. Since the 2 ppm biocide treatments showed no decrease in bacterial numbers or metabolic activity, large biocide doses, followed by continuous low doses were evaluated. As with the previous experiments, the biofilm was allowed to develop for four days prior to treatment. The 16 ppm residual biocide was injected into the flasks for a contact time of two hours. Biocide was then continually pumped into the vessels for 24 hours, to maintain a 2 ppm residual biocide. In order to prevent dilution of the medium with the biocide, and to prevent mixing of the NaBr with the NaOCl prior to addition to the flasks in the chlorine/bromine experiments, 4 ppm NaBr was added directly to one medium reservoir. From the previous experiment, the biocide demand of the flasks was estimated to be 8 ppm.

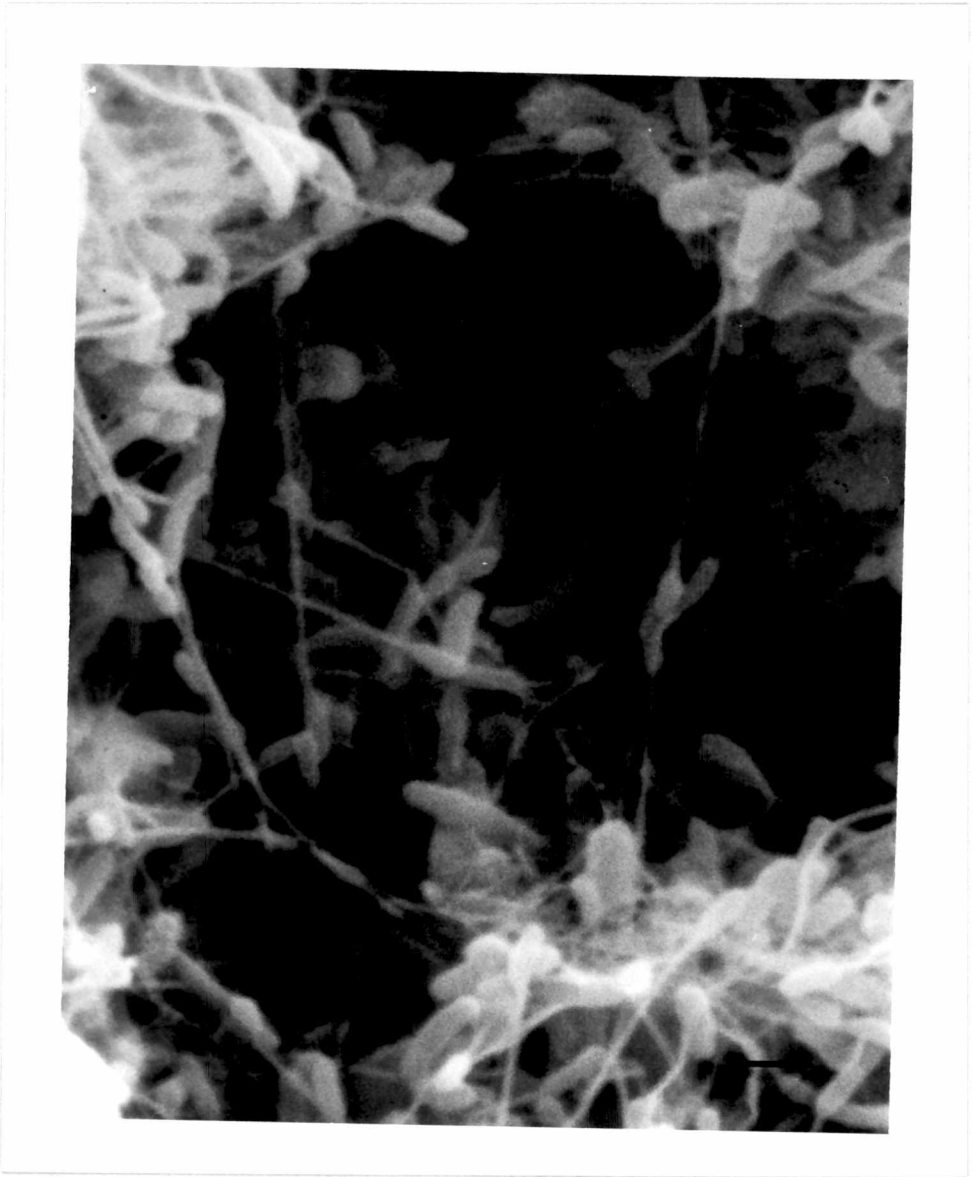

Figure 3. Scanning electron micrograph showing the biofilm associated with the carbon steel sample after the second treatment of 2 ppm NaOCl for two hours. Bar represents 1 μm.

Therefore a stock solution containing 36.9 ppm NaOCl was prepared. The stock solution was pumped into the treated flasks at a rate of 8.3×10^{-4} l/min for the 24 hour period. The level of biocide was assayed every 30 minutes during the 16 ppm treatment, and additional biocide was injected when the level of free residual chlorine or chlorine/bromine fell below 16 ppm. The level of biocide was assayed five times throughout the 24 hour 2 ppm treatment. Additional biocide was added when the residual biocide fell below 2 ppm. The residual biocide level ranged from 0.5 ppm to 3.0 ppm throughout the remainder of the experiment.

Figure 4 shows the effects of the 16 ppm followed by the 2 ppm treatments on the numbers and activities of the surface associated bacteria. The two hour 16 ppm treatment with NaOCl resulted in a decrease in aerobic heterotrophs of two orders of magnitude (Fig. 4A). The NaOCl/NaBr treatment resulted in a decrease in aerobic heterotrophs by one order of magnitude. Continuous treatment with 2 ppm of either biocide resulted in approximately 10^5 cells/cm^2 following 24 hours of treatment. The bacteria rapidly increased to the original numbers when the treatment was discontinued.

After four days of biofilm growth, 10^5 to 10^6 sulfate reducers/cm^2 could be recovered from the surface (Fig. 4B). The 16 ppm treatment of either biocide reduced the level of sulfate reducers by three orders of magnitude. The

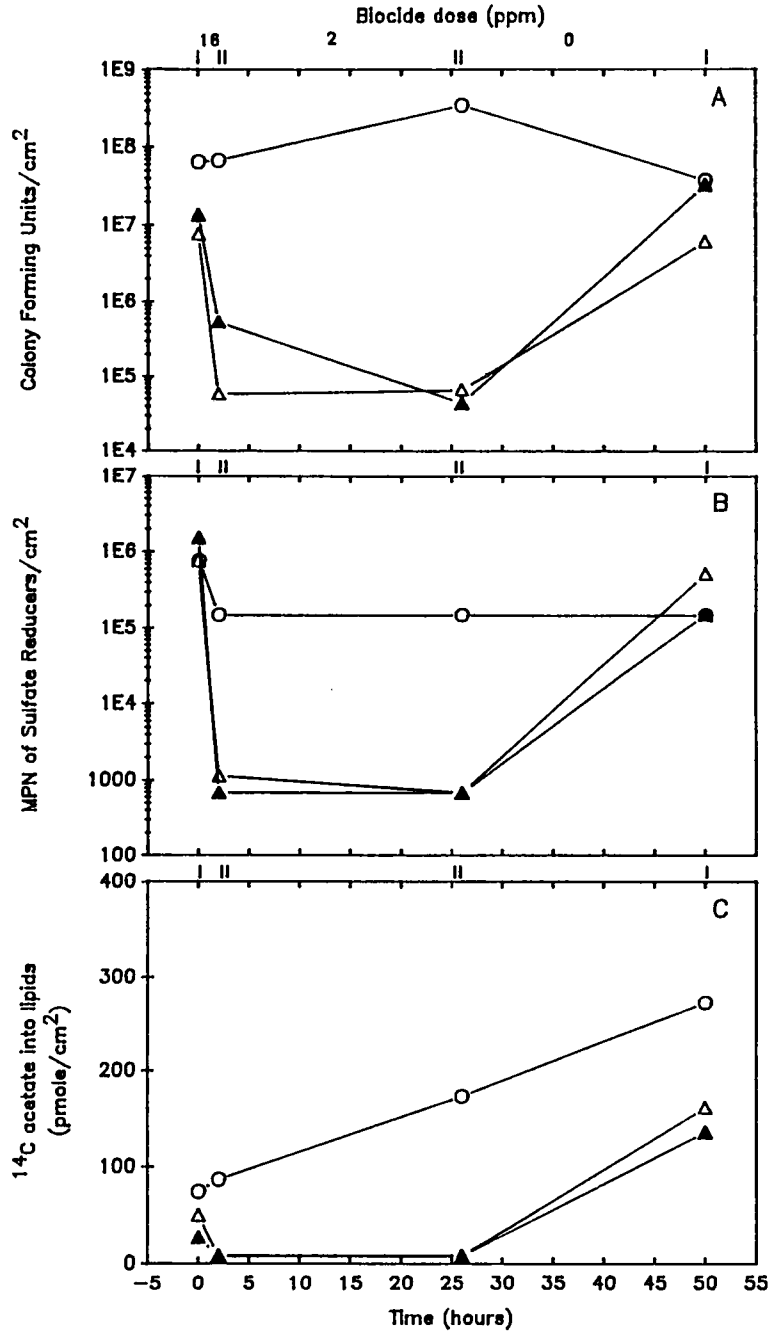

Figure 4. A) Total colony forming units of heterotrophic bacteria per cm^2. Values represent the mean of two CFU platings. B) Three tube most probable numbers of sulfate reducing bacteria per cm^2. C) Bacterial metabolic activity as measured by ^{14}C acetate incorporation into total lipids. Values represent the means of three samples. Time zero is after four days of biofilm development. Open circles- no biocide treatment, open triangles- 16 ppm followed by 2 ppm NaOCl treatment. Closed triangles- two hour 16 ppm followed by 2 ppm NaOCl/NaBr treatment.

continuous 2 ppm treatment maintained the level of sulfate reducing bacteria at 10^3 cells/cm^2.

The lipid biosynthetic activity was reduced to the level of the sterile controls, following treatment with 16 ppm of either biocide (Fig. 4C). This level was maintained by the continuous treatment with 2 ppm biocide. The activity rapidly rebounded following cessation of the treatment. Figure 5 shows an electron micrograph of the biofilm following treatment with NaOCl/NaBr. Few bacteria were observed associated with the corrosion products. Electron micrographs following the NaOCl treatment also showed few bacteria.

Bulk phase effects. The 16 ppm treatment with NaOCl reduced the number of aerobic heterotrophs from approximately 10^7 cells/ml to less than one cell/ml. Treatment with NaOCl/NaBr reduced the number of planktonic aerobic heterotrophs to 10^3 cells/ml. After 26 h treatment with 2 ppm of either biocide, no bacteria could be cultured from the solution.

Effect of treatments on the corrosion rates. The impedance, which is inversely proportional to the corrosion rate, of the C1020 carbon steel coupons was analyzed over the course of the experiment by EIS. Figure 6 shows the impedance in the form of the Nyquist format for one sample prior to treatment with NaOCl (Fig. 6A), after 2 hour treatment with 16 ppm NaOCl (Fig. 6B), and after 24 hour

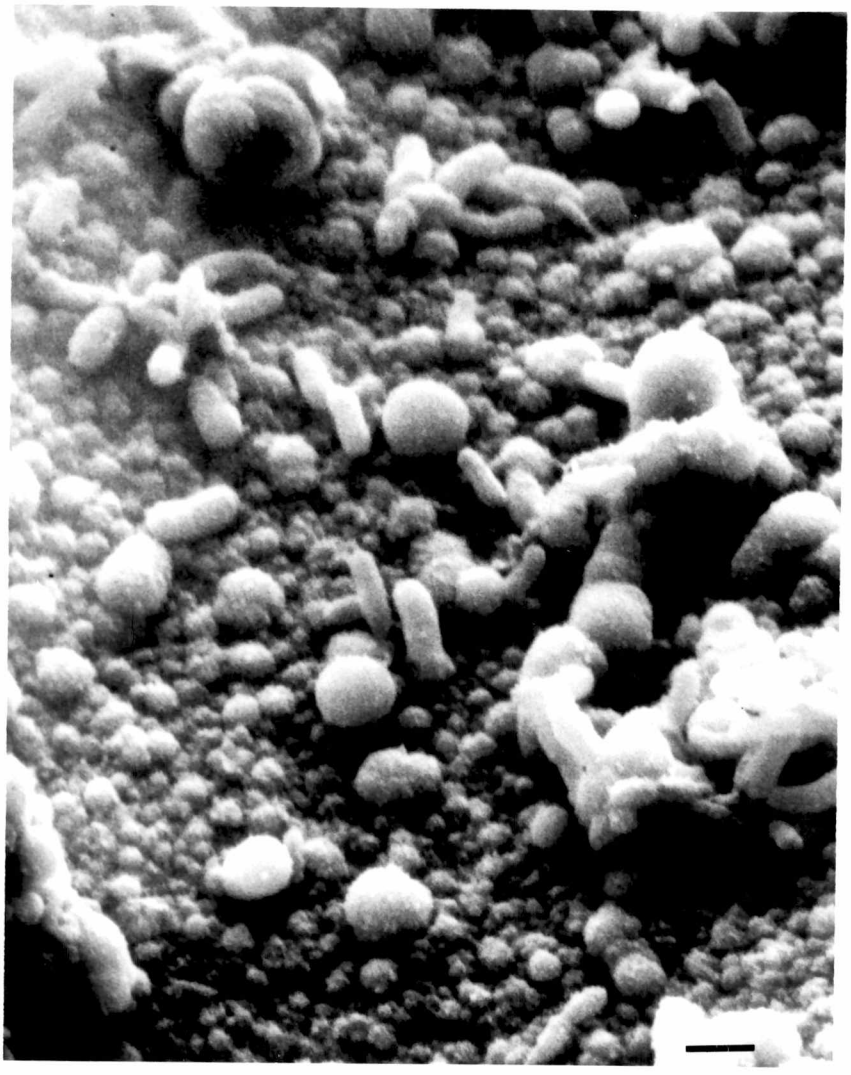

Figure 5. Scanning electron micrograph of biofilm on carbon steel coupon after treatment with 16 ppm NaOCl/NaBr for two hours and 2ppm NaOCl/NaBr for 24 hours. Few rod shaped bacterial cells were seen. Bar represents 1 μm.

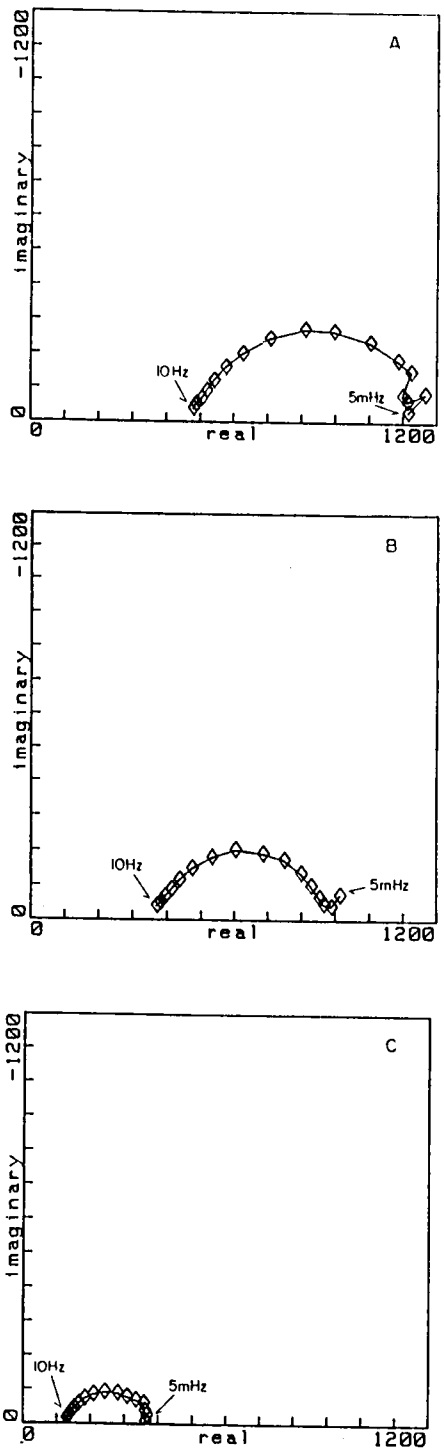

Figure 6. Electrochemical impedance spectroscopy analysis of carbon steel electrode in the Nyquist format. The units for the real and imaginary axes are ohms. A) EIS of the sample after biofilm was allowed to form for four days. B) EIS after exposure of the same sample to 16 ppm for two hours. C) EIS of the sample after additional exposure of the sample to 2 ppm for 24 hours.

treatment with 2 ppm treated with NaOCl. The units for the real and the imaginary axis are in ohms. The impedance analyses reveal a single depressed semicircle, from which the polarization resistance could be determined. Figure 6A-C demonstrates that the polarization resistance of the carbon steel decreased following treatment with NaOCl, indicating an increase in the corrosion rate. A similar decrease in polarization resistance was observed for the NaOCl/NaBr treatment.

The inverse of the polarization resistance, the admittance, are summarized in Table 1. Initially, the admittance was two- to three-fold greater in the presence of the biofilm than in the sterile control. The treatments with 16 ppm biocide followed by the continuous treatment with 2 ppm biocide showed an increase in the admittance in both the inoculated flasks and the sterile controls. The admittance increased in the inoculated flasks from 1.6 to 5.0 mMhos/cm^2 after the 16 ppm followed by the 2 ppm treatment with biocides. The sterile samples increased from 0.6 to 2.5 mMhos/cm^2 after the NaOCl treatment, and from 0.4 to 4.0 mMhos/cm^2 after the NaOCl/NaBr treatment. The nontreated controls increased from 0.4 to 0.5 mMhos/cm^2 for the sterile samples, and 1.2 to 1.6 mMhos/cm^2 in the biofilm containing samples. The two hour 2 ppm treatments with either biocide showed no effect on the corrosion rate of the metal, compared to the nontreated controls.

Table 1[a]
Carbon steel admittance for samples treated with 2 h 16ppm followed by 24 h 2 ppm biocides

Treatment		Pre-treatment	After 2h 16 ppm	After 24h 2 ppm
Sterile	no biocide	0.4[b]	0.4	0.5
Inoculated	no biocide	1.2	1.2	1.6
Sterile	NaOCl	0.6	0.7	2.5
Inoculated	NaOCl	1.7	2.0	5.0
Sterile	NaOCl/NaBr	0.4	0.4	4.0
Inoculated	NaOCl/NaBr	1.6	0.9	5.0

[a]Polarization resistance values were obtained by electrochemical impedance spectroscopy.
[b]Values are given in mMho/cm^2.

DISCUSSION

Test system. In this study, a test system was developed to simultaneously study microbial fouling and microbial influenced corrosion over time. This system was used to examine the efficacy of certain countermeasures. Parameters which appear to be important in microbial influenced corrosion include microbial biomass, including numbers of sulfate reducing bacteria, and microbial metabolic activity (6). Therefore, the system was developed to examine these parameters over time. In addition electrochemical impedance spectroscopy was used to examine corrosion rates over time, since this technique does not appear to alter the progression of corrosion (3, Chapter 2).

Flowing media were used in these experiments. Flowing systems have several advantages over batch culture conditions. First, flowing systems with low nutrient input are more characteristic of environmental conditions than are batch culture systems. Second, the influence of environmental factors, such as nutrient limitation and bacterial enproduct accumulation, become less significant in flowing systems than in batch culture systems. For example, Fig. 2 and 4 show little change in the numbers of viable bacteria over time, in the untreated control. Under batch culture conditions, the cell numbers would likely decline as nutrients became limiting and as toxic bacterial endproducts

accumulated. Third, the flowing system allows the dilution of corrosion products, which can affect the corrosion rates.

Sulfate reducing bacteria in an aerobic system. Sulfate reducing bacteria are often found associated with aerobic bacteria within biofilms. Sulfate reducing bacteria in biofilms enhance the corrosion rate of carbon steel, compared to biofilms without sulfate reducers (6). Therefore, in addition to total aerobic bacteria, the numbers of SRB were also determined in these experiments. As many as 10^6 SRB/cm^2 were found in these biofilms, even though the bulk solution was aerobic. These results indicated that the SRB's were able to inhabit and reproduce in anaerobic environments within biofilms in aerobic systems.

The number of SRB's increased following cessation of the 16 ppm followed by the 2 ppm biocide treatments. No SRB's could be cultured from the bulk fluid after the 26 hour treatments. However, sessile SRB's survived to recolonize the metal surface after cessation of the treatment. These results indicated that sessile SRB's may be able to survive exposure to oxygen and halogen biocides for at least 26 hours.

Bacterial metabolic activity. The metabolic activities of bacteria are an important component in MIC. In addition to the hydrogenase and sulfate reduction activities of SRB's, other bacterial metabolic activities have been

implicated in MIC. These activities have included iron reduction (16), acid production (11), differential oxygen utilization, and exopolymer production (14). Bacteria capable of each of these activities were used in this study. Bacterial metabolic activity was measured as lipid biosynthetic activity. Lipid synthesis occurs in all living cells, and acetate is used as a precursor of lipid synthesis. Therefore, ^{14}C-acetate incorporation into lipids has been used in a number of studies to analyze bacterial activities in complex ecosystems (4). In this study, the effects of biocide treatments on the lipid synthetic activity of a sessial bacterial consortium were demonstrated. The results indicated that the two hour 2 ppm treatments had little effect on the consortial lipid synthetic activity. The 16 ppm two-hour treatment was effective at inhibiting metabolic activity, and continuous 2 ppm treatment was effective at maintaining the inhibition. These results suggest that a continuous low dose of biocide is effective at inhibiting the membrane synthesis and recovery of cells, previously treated with high doses of biocides.

Electrochemical impedance spectroscopy.

Electrochemical impedance spectroscopy (EIS) was utilized in these studies, since it has several advantages over direct current techniques. First, EIS enable the evaluation of corrosion rates over time, before and after the biocide

treatments. EIS requires application of 5mV sinusoidal potentials, which are less destructive to the bacteria and to the metal samples, than are Tafel polarizations (3, Chapter 2). In addition, EIS can be used to distinguish solution resistances from the polarization resistances. This was advantageous in this system, since the two resistances were similar. Thus, direct current measurements may have led to an underestimate of the corrosion rates.

Evaluation of the admittance for the two hour 2 ppm treatments showed little effect of the biocides on the polarization resistances. Since the biofilm was not affected by these treatments, the lack of change in the admittance was probably due to the lack of penetration of the biocide through the biofilm. The NaOCl and the NaOCl/NaBr 16 ppm treatments followed by 2 ppm treatments showed an increase in the corrosion rates of both the sterile and the inoculated systems. These results indicated that halogenated biocides were corrosive toward the carbon steel.

Biocide treatments. In industrial plants where lake or river water is transported through pipes, 2 ppm biocide treatments for one to two hours are often used to bulk water (17). Studies have shown that hypochlorous acid at 2 ppm residual is effective at reducing planktonic bacteria, but sessial bacteria can be resistant to this concentration of biocides (8). The results presented here demonstrate that

the 2 ppm treatment of hypochlorite in a pH 8.5 medium was ineffective at inhibiting sessial bacteria. In addition, the chlorine/bromine treatment was also ineffective, even though the pKa of hypobromous acid is higher than that of hypochlorous acid, and thus should be more effective at alkaline pH.

The 16 ppm followed by the 2 ppm treatments were effective at reducing the numbers of bacteria and inhibiting the metabolic activity of the bacteria. However, the treatments resulted in an increase in the corrosion rates of the carbon steel, as measured by EIS. Ventura et al. (18) demonstrated the effects of hypochlorite on stainless steel corrosion in flowing seawater. Their results indicated that hypochlorite treatment increased the short term propensity for pitting of stainless steel, but decreased the long term corrosion rates. The results of this study indicated an increase in the short term corrosion rates of carbon steel by the addition of high doses of biocides.

LITERATURE CITED

1. American Public Health Association. Standard Methods for the Examination of Water and Wastewater sixteenth ed. American Public Health Association, Washington, D.C. p. 309 (1985).

2. Balch, W.E., G.E. Fox, L.J. Magrum, C.R. Woese, and R.S. Wolfe. (1979) Methanogens: reevaluation of a unique biological group. Microbiol. Rev. **43**:260-296.

3. Dowling, N.J.E., J. Guezennec, M. L. Lemoine, A. Tunlid, and D.C. White (1988) Analysis of carbon steels affected by bacteria using electrochemical impedance and direct current techniques. Corrosion **44**:869-874

4. Findlay, R.H., P.C. Pollard, D.J.W. Moriarty, and D.C. White. (1985) Quantitative determination of microbial activity and community nutritional status in estuarine sediments: evidence for a disturbance artifact. Canad. J. Microbiol. **31**:493-498.

5. Franklin, M.J., D.E. Nivens, M.W. Mittelman, A.A. Vass, R.F. Jack, N.J.E. Dowling, R.P. Mackowski, S.L. Duncan, D.B. Ringelberg, and D.C. White. (1989) An analog MIC system with specific bacterial consortia, to test effectiveness of materials selection and countermeasures. CORROSION/89 paper no. 513.

6. Jack, R.F., The effects of increased bacterial metabolic diversity on the corrosion of carbon steel. Masters Thesis, University of Tennessee, (1990).

7. Lappin-Scott, H.M., and J.W. Costerton (1989) Bacterial biofilms and surface fouling. Biofouling **1**:323-342

8. Lechevallier, M.W., T.S. Hassenauer, A.K. Camper, and G.A. McFeters. (1984) Disinfection of bacteria attached to granular activated carbon. Appl. Environ. Microbiol. **48**:918-923.

9. LeChevallier, M.W., C.D. Cawthon, and R.G. Lee. (1988) Factors promoting survival of bacteria in chlorinated water supplies. Appl. Environ. Microbiol. **54**:649-654.

10. Lechevallier, M.W., C.D. Cawthon, and R.G. Lee. (1988) Inactivation of biofilm bacteria. Appl. Environ. Microbiol. **54**:2492-2499.

11. Little, B., Wagner, P., Gerchakov, S.M., and Mitchell, R. (1986) The involvement of a thermophilic bacterium in corrosion processes. Corrosion **42**:533-536

12. Mansfeld, F. (1981) Recording and analysis of AC impedance data for corrosion studies. I. Background and methods of analysis. Corrosion **36**:301-307

13. Mansfeld, F., Kendig, M.W., and Tsai, S. (1982) Recording and analysis of AC impedance data for corrosion studies. II. Experimental approach and results. Corrosion **38**:570-580

14. Nivens, D.E., Nichols, P.D., Henson, J.M., Geesey, G.G., and White, D.C. (1986) Reversible acceleration of the corrosion of AISI 304 stainless steel exposed to seawater induced by growth and secretions of the marine bacterium Vibrio natriegens. Corrosion **42**:204-210

15. D.E. Nivens, J.B. Guckert, K. Kroeger, J.Q. Chambers, and D.C. White. Microbial biofilm isolation device for off-line analysis. J. Microbiol. Methods, submitted.

16. Obuekwe, C.O., Westlake, D.W.S., Plambeck, J.A., and Cook, F.D. (1981) Corrosion of mild steel in cultures of ferric iron reducing bacterium isolated from crude oil. II. Mechanisms of anodic depolarization. Corrosion **27**:632-637

17. Scott, P.J.B., and M. Davies, (1989) Microbiologically influenced corrosion of alloy 904L. Materials Performance **28 (5)**:57-60.

18. Ventura, G., E. Traverso, and A. Mollica. (1989) Effect of NaClO biocide additions in natural seawater on stainless steel corrosion resistance. Corrosion **45**:319-325.

CHAPTER VI

THE USE OF CURRENT DENSITY MAPPING IN THE STUDY OF MICROBIAL INFLUENCED CORROSION

ABSTRACT

The scanning vibrating electrode technique (SVET) was used to map current densities over carbon steel coupons exposed to bacteria. This study was initiated to evaluate the usefulness of the SVET in studies of microbial influenced corrosion (MIC). A comparison was made between current densities, at open circuit potential, of steel exposed to dilute sterile microbiological medium, and steel exposed to medium containing a culture of aerobic heterotrophic bacteria. At specific times during the analysis, small amplitude cyclic polarizations were performed. The SVET was utilized to detect localized resistance to polarization (R_p). After the samples had been exposed to the solutions for 24 hours, anodic and cathodic polarizations were applied. The SVET was used to detect localized changes in applied current. The results indicated that the SVET can be used to obtain qualitative and quantitative information regarding localized corrosion associated with MIC.

INTRODUCTION

Films of bacteria and other microorganisms often form when metal surfaces are exposed to aqueous environments. These biofilms can lead to enhanced localized corrosion of the metal (Chapter 1). Although microbial influenced corrosion (MIC) has been implicated in corrosion processes for more than fifty years (13), the mechanisms for localized corrosion influenced by bacteria have been difficult to define. This lack of mechanistic information is due in part to the difficulties in characterizing corrosion events with spatial resolution similar to the size of bacteria or microcolonies.

Electrochemical techniques, commonly used in determining corrosion rates, are either destructive to bacteria and/or do not provide information on localized corrosion associated with bacteria. Useful techniques for studying MIC have included anodic and cathodic polarizations (10). These analyses can be used to obtain Tafel parameters and polarization resistance values, which can be used in the Stern-Gerry equation to determine corrosion rate (10). In addition, anodic sweeps can be used to detect changes in pitting potential as a result of bacterial activity. However, anodic and cathodic polarizations require high applied currents, which can alter the physiology of bacteria (1). Therefore, the study of changes in corrosion rate over time requires the use of many samples.

Nondestructive techniques for studying corrosion have included potential monitoring (12) and current monitoring through a galvanically coupled cell (2), and electrochemical impedance spectroscopy (1, Chapter 1,3). These techniques only provide indirect indication of localized corrosion.

In order to gain a better understanding of MIC, additional techniques which can detect localized corrosion and do not alter the progression of corrosion are needed. Current density mapping has been used as a nondestructive technique in biological studies (9), and corrosion studies (4). The technique is based on the principle that over corroding metal, the solution resistance produces potential fields between local anodic and cathodic sites. The current densities producing the fields can be detected with either a scanning capillary reference electrode (8) or a scanning vibrating electrode (4). The scanning vibrating electrode technique (SVET) converts fields to an alternating signal. The sign and the magnitude of this alternating signal can be determined using a lock-in amplifier. The SVET is much more sensitive than the capillary reference electrode technique, since noise is filtered by the lock-in amplifier. Only the signal at the vibration frequency is detected.

One limitation of this technique in determining corrosion rates is that current densities are mapped at a certain distance from the metal surface, whereas the corrosion rate must be determined by the current density at

the surface. Several approaches have been used to more accurately determine corrosion rates (3). Cathodic and anodic polarization techniques, have been used in conjunction with the SVET to provide information regarding localized corrosion rates (3).

In this study, the SVET was used to map current densities over carbon steel in a medium containing bacteria. In addition, localized polarization resistances were measured. At the end of the experiment, localized changes in applied current were determined for anodic and cathodic polarizations. The results indicated that the SVET can be used to evaluate localized corrosion, enhanced by bacteria.

MATERIALS AND METHODS

Media and bacteria. A defined microbiological medium, capable of supporting the growth of the bacterium was used. The medium contained (in mg/L) NH_4Cl 50, $MgSO_4 \cdot 2H_2O$ 50, $CaCl_2 \cdot 2H_2O$ 5, KH_2PO_4 27, Glucose 50, 2-morpholinoethane sulfonic acid (MOPES buffer) 50, and trace minerals (in ug/L) $Na_2MoO_4 \cdot 2H_2O$ 0.1, $ZnSO_4 \cdot 7H_2O$ 50, $MnSO_4 \cdot H_2O$ 7.7, $CuSO_4 \cdot 5H_2O$ 2, $CoCl_2 \cdot H_2O$ 1, $NaB_4O_7 \cdot 10H_2O$ 0.8, $NiSO_4$ 0.5. The bacterial culture used, was a pure culture of a Pseudomonas sp., isolate 3T5 (Chapter 1), which was isolated from a tubercle on a steel pipe. The isolate did not grow anaerobically, and did not produce detectable levels of volatile fatty acids when grown on glucose (1g/L). The bacterium produced copious amounts of extracellular polysaccharide when attached to a steel surface (Chapter 1). When bacteria were used in these experiments, the cells were grown to late exponential phase (24 hours) on the medium described above. The cells were then centrifuged and the spent medium was removed. An equal volume of fresh medium was added to the cells, and the suspension was added to the electrochemical cell.

Electrochemical cell. The working electrodes in these experiments were coupons of C1020 carbon steel supplied by Metal Samples (Munford Al.). The steel contained by percentages; C 0.17, Mn 0.42, P 0.009, and S 0.006. The coupons, with a spot welded electrical connection, were

embedded in epoxy and finished with 600 grit silicon carbide finishing paper. Thin, approximately 75 um, pressure sensitive tape (3M Co. no 92) was used to insulate the sample except for an area in the center of the coupon approximately 25 mm^2. Microshield lacquer (Pyramid Plastics, Inc.) was painted at the edge of the tape to reduce crevice corrosion. The cell had a working volume of 15 ml and contained a double junction saturated calomel reference electrode (SCE) and a platinum wire for a counter electrode.

Current Density Maps. The vibrating electrode, used to scan the working electrode, consisted of an insulated platinum wire, 0.1mm in diameter. The technique for current density mapping has been described elsewhere (6). Briefly, the platinum wire was attached to a piezoelectric reed which was activated by applying a 10 V rms signal to the reed at 200 Hz. The peak to peak vibration was 0.04mm. The vibrating electrode was positioned 0.09mm from the working electrode surface. The alternating current was analyzed with a PAR model 116 lock-in amplifier, and a computer controlled data acquisition unit. The surface of the working electrode was scanned by moving the cell in 100 or 200 um increments with computer controlled stepper motors. The vibrating probe was calibrated with a known uniform current field, and the output voltage from the amplifier was

converted into current densities, through the use of a conversion factor.

Local Polarization Resistance. For analyzing polarization resistances (R_p), a 50 mV triangular signal was applied to the working electrode at a rate of 5mV/sec. The vibrating electrode was positioned over the lacquer coating, then stepped in 0.2mm increments across the metal sample. The probe remained at each point in the transect for 40 secs. Twenty-two points were analyzed, including cathodic and anodic sites. The SVET signal from the lock-in amplifier, was monitored with a strip chart recorder. The ratio of applied potential to measured current was determined by the deflection of the pen on the recorder. Local polarization resistance was determined by Ohm's law.

Anodic and Cathodic Polarizations. Cyclic polarizations were performed on some samples at the end of the exposure periods. The potential was changed at a rate of 1 mV/sec, from open circuit potential to -1.2V/SCE then to 0.0V/SCE. The vibrating electrode was positioned first over the lacquer coating. The probe then stepped across the metal sample in 0.2mm increments. The probe then returned to its original position and again stepped across the metal. This process was continued as the potential of the sample was ramped. Each transect across the sample took 20 seconds. Since the potential was ramped at 1mV/sec, each transect represented a 20mV increase in potential.

RESULTS

SVET analysis of sterile medium during free corrosion. The medium used in these studies was continuously aerated by bubbling with air, and contained trace minerals as well as an organic buffer. The medium contained chloride, sulfate, and phosphate ions in concentrations of approximately 1 mM, 0.2 mM, and 0.2 mM, respectively. Upon exposure of the carbon steel to this medium, the open circuit potential (OCP) rose from a value of -300 mV/SCE to approximately -200 mV/SCE. This potential was apparently above the pitting potential of the steel, since sudden drops in potential ranging from 10 to 70 mV, occurred over the course of the experiment. The drops in potential were followed by slow increases in potential to the initial value. These potential transients were characteristic of pit initiation and repassivation (7). Figure 1A shows a current density map over the carbon steel sample, after 22 hours of exposure of the steel to the sterile medium. One pit, with a measured current density of 50 uA/cm^2 is seen in this figure. Figure 1B is a contour map of the same pit, showing the location of the pit on the sample. Figure 1C shows the same sample after 29 hours of exposure. In this figure, the pit seen at 22 hours is not observed. Figure 1C is autoscaled, so that the minimum detectable current density can be plotted. It can be seen that less than 0.5 uA/cm^2

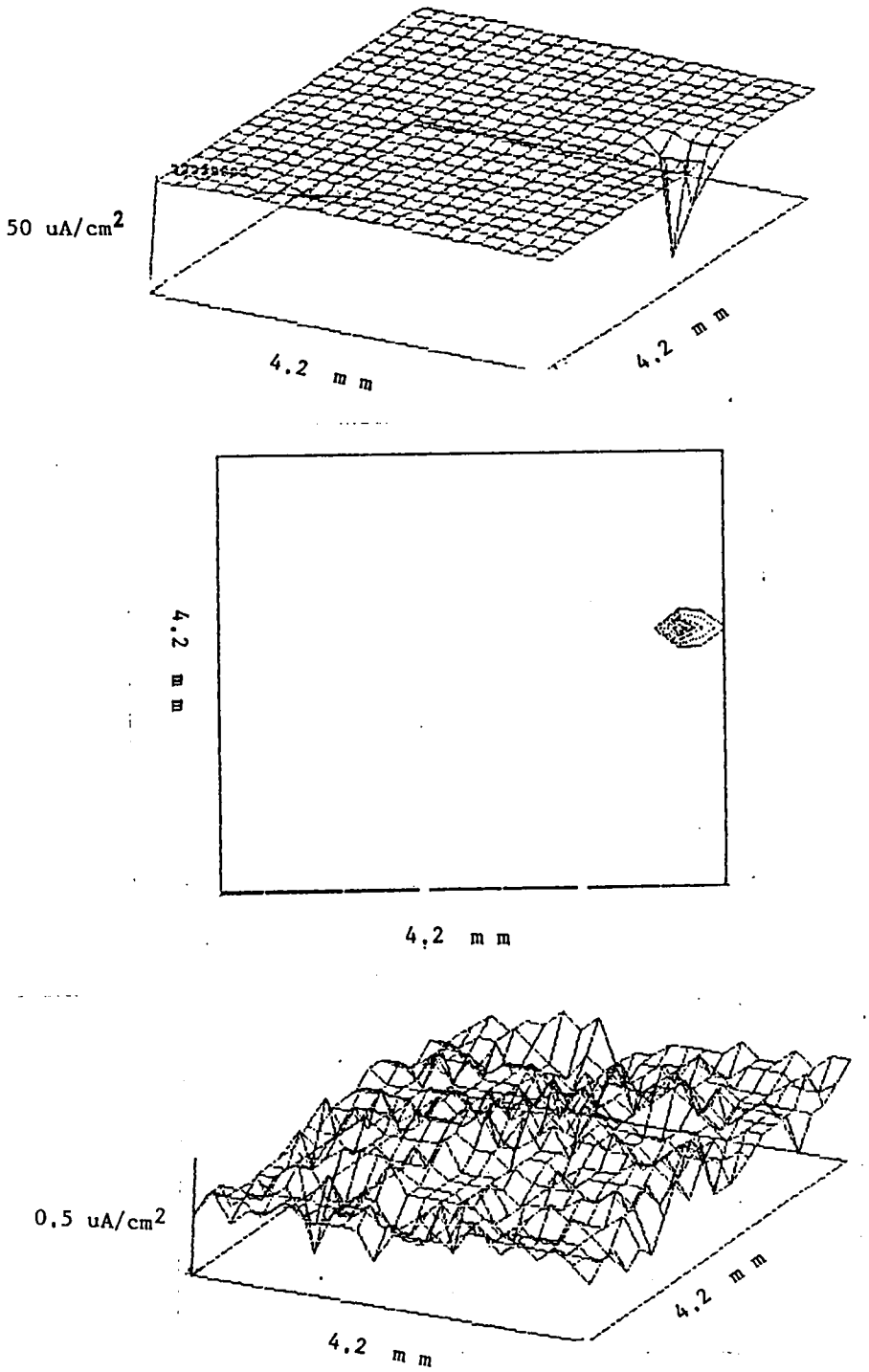

Figure 1. Current density maps over carbon steel sample, obtained with the scanning vibrating electrode technique. A) SVET analysis after exposure of the steel to sterile medium for 22 hours. B) Contour map of the current densities of figure 1A. C) SVET analysis for the same sample after 29 hours of exposure to the sterile medium.

current density was observed over the area formerly occupied by the active pit in Figure 1A,B.

SVET analysis of MIC during free corrosion. A culture of aerobic heterotrophic bacteria, derived from a tubercle on a steel pipe, was added to the same aerated medium described. The initial OCP rose above the pitting potential for the sterile medium. However, as the bacteria colonized the steel surface, the pitting eventually stabilized, and the potential dropped to a value of approximately -620 mV/SCE. The current density map shown in Figure 2 was taken after 23 hours of exposure of the steel to medium containing bacteria. In this experiment, one pit had initiated and did not repassivate. The pit propagated and expanded until a large area of the surface was anodic.

Local polarization resistance. As mentioned, the SVET can be used in conjunction with linear polarization, to analyze localized resistance to polarization. The transect described in the materials and methods is shown in Figure 3A. This plot is a two-dimensional plot of the current densities at open circuit potential. This plot was taken from the three-dimensional plot shown in Figure 2, for a transect 600 um parallel to the X-axis. The points at the far left and far right represent the current densities over the lacquer coating, and serve as reference points. Figure 3B shows the SVET measured local polarization resistances measured for this transect, when a triangular

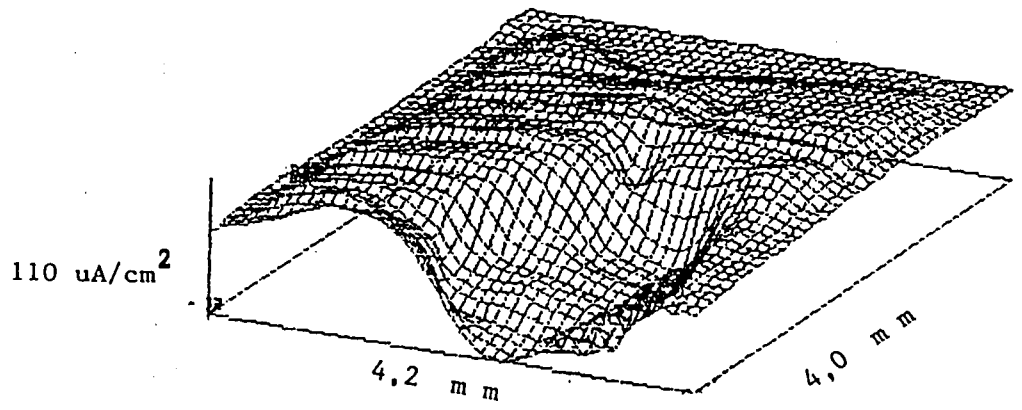

Figure 2. Current density map over carbon steel sample, obtained with the scanning vibrating electrode technique. SVET analysis was obtained after 23 hours of exposure of the steel to medium containing aerobic bacteria.

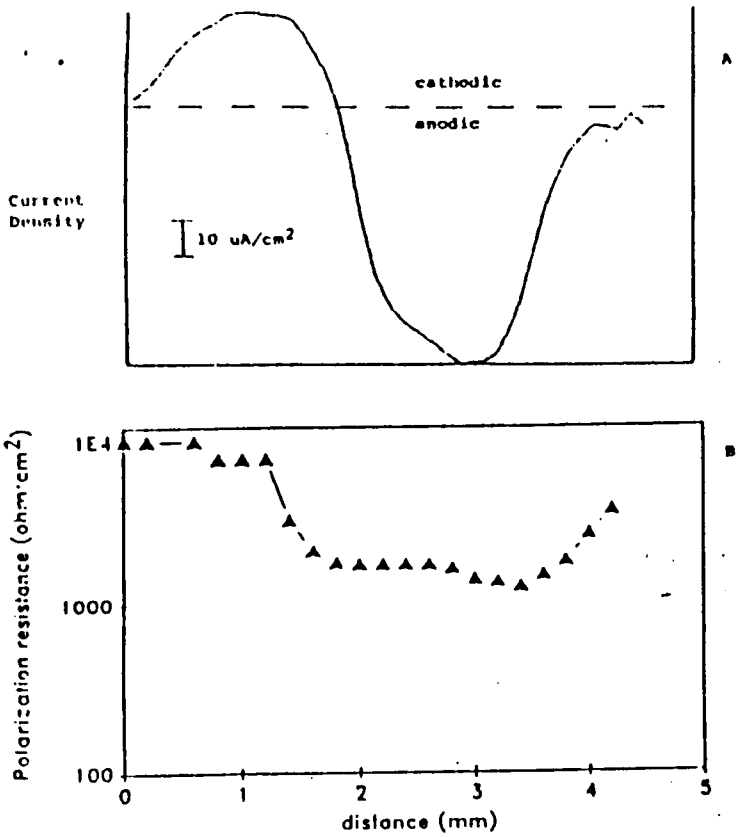

Figure 3. A) Current densities, at open circuit potential, for a transect across the carbon steel sample. Transect was taken from figure 2, 0.6mm parallel to the X-axis. B) Polarization resistance measurements, for the same transect, obtained with the vibrating electrode.

polarization, ± 25mV around OCP was applied to the sample. The local polarization resistances were determined by dividing the magnitude change in local current density by the change in applied potential (50mV). The measured R_p for the whole sample was 1100 ohm·cm^2. The measured values for local R_p was 1200 ohm·cm^2 directly over the anodic area, and 9000 ohm·cm^2 directly over cathodic areas.

Cyclic polarization. After 24 hours of exposure of the sample to medium containing bacteria, cyclic polarizations were performed on the sample. The result of the cyclic polarization is shown in Figure 4. Increase in current due to the anodic processes was observed above -0.4V/SCE, and the increase in current due to the cathodic reaction, was observed below -1.0V/SCE.

SVET analysis of cyclic polarization. The vibrating probe was repeatedly scanned in a transect over the sample while the potential was ramped. The transect was the same as for the polarization resistance measurements (the current densities at open circuit potential for this transect are shown in Figure 3A). Figure 5A shows the change in applied potential, detected by the vibrating probe, when the sample was polarized in the cathodic direction, from -620mV/ SCE to -1.2V/SCE. In this graph, the X-axis is the position of the probe over the sample, the Y-axis is potential, and the Z-axis is measured current density. The results indicated that the area of the sample which produced the largest

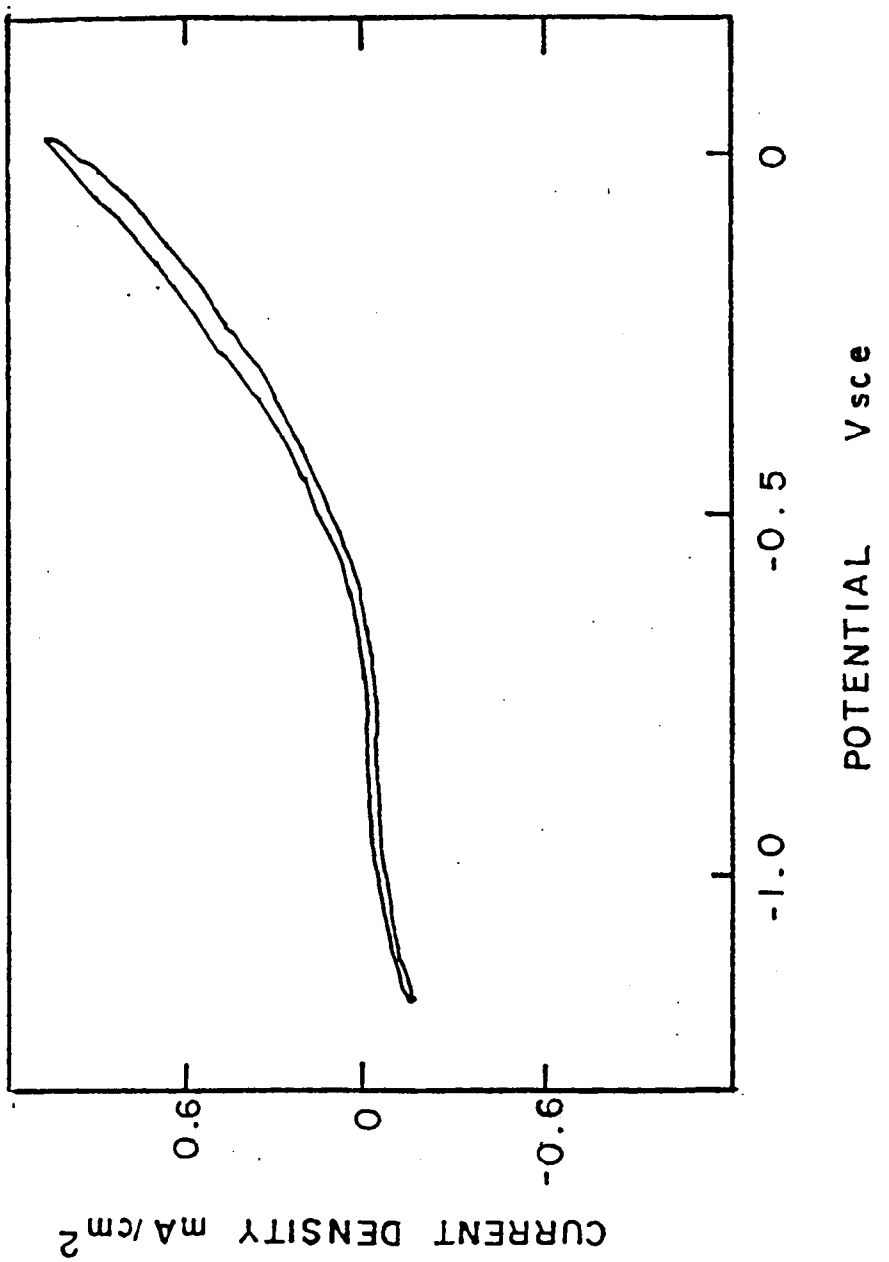

Figure 4. Cyclic polarization for the carbon steel sample after 24 hours of exposure to medium containing bacteria.

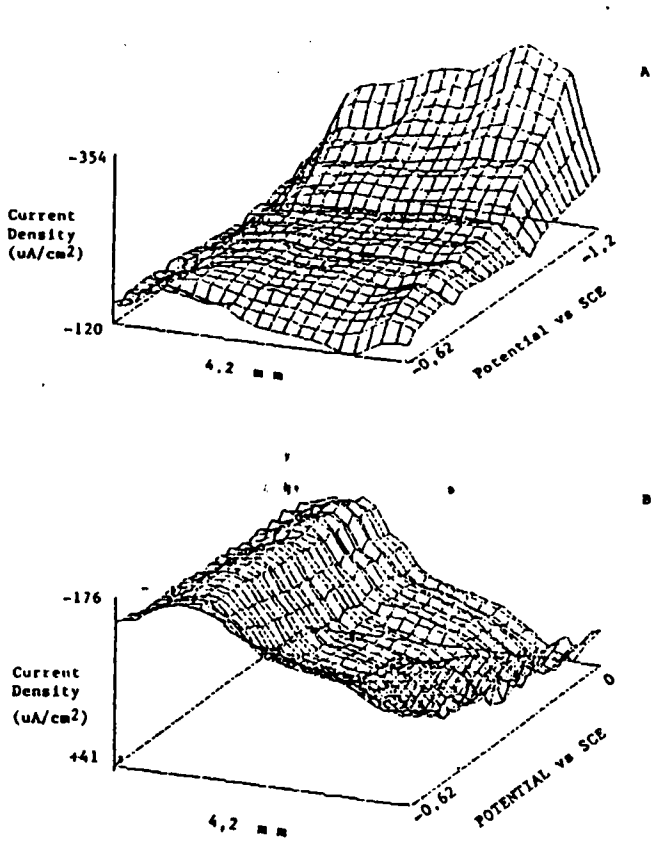

Figure 5. Cyclic polarization for the carbon steel sample after 24 hours of exposure to medium containing bacteria. Changes in applied current, for the transect in figure 3a, detected by the vibrating probe. A) Cathodic polarization, potential ramped from open circuit potential, -620mV/SCE, to -1.2V/SCE at 1mV/sec. B) Anodic polarization, potential ramped from -620mV/SCE to 0.0V/SCE at 1mV/sec.

anodic current density, at open circuit potential, produced the greatest area of change in applied current, when the sample was cathodically polarized.

Figure 5B shows the SVET measured current densities associated with the polarization of the sample in the anodic direction, from -620mV/SCE to 0.0mV/SCE. The current densities in the zones which were cathodic remained at a constant level throughout the polarization. The site which was originally anodic produced the greatest change in applied current.

DISCUSSION

SVET analysis during free corrosion. Current density mapping has been used to study pitting corrosion of stainless steel and iron in aggressive media (8). This study demonstrates that the SVET can be used to nondestructively locate and measure the sign and magnitude of the nonuniform current densities over carbon steel samples, exposed to bacteria. Measurements of current densities at open circuit potential showed differences between the corrosion of the carbon steel, when exposed to sterile medium, and to medium containing bacteria. The results indicated, that in the dilute aerated microbiological medium, propagation but not initiation of pits was inhibited. However, in the presence of colonizing bacteria, an initiated pit propagated, until a large area of the sample was anodic. The bacteria apparently altered conditions which induced pit propagation.

Polarization resistance. The SVET measures current densities in solution, whereas the corrosion rate is determined by current densities at the metal surface. Factors which affect measured current densities include; the height of the probe over the surface, the vibration amplitude, and the resolution of the anodic and cathodic sites. In addition to analysis of potential fields at free corrosion potential, samples can be polarized, and changes in applied potential can be determined with the SVET. This

advance provides additional information regarding the local corrosion rate. Linear polarizations can be performed to determine local polarization resistance. Small amplitude polarizations are less destructive to bacteria than large anodic and cathodic sweeps.

Polarization resistances were used in this study, to better quantitate the pitting reaction. After 23 hours of exposure of the steel to medium containing bacteria the polarization resistance measured for the whole surface was 1100 ohm·cm^2. This value of R_p is consistent with other studies of carbon steel corrosion in this same medium, affected by this same culture of bacteria (Chapter 1). The values of local R_p, for a transect across both anodic and cathodic zones, showed behavior similar to the current density map. The R_p values were lowest over the anodic zones, having measured values of 1000 ohm·cm^2., and the highest values of R_p, 10^4 ohm·cm^2, were measured over the cathodic sites. During the early stages of pit propagation, values showed an even greater discrepancy between the anodic and cathodic sites, ranging from 250 to greater than 10^4, respectively (data not shown). These results indicated that measurements of R_p for whole surfaces can lead to underestimates of penetration rates, when corrosion is highly localized. The SVET offers an advantage in determining localized penetration rates, since the value of local R_p can be measured, and calculated for the area of the

active anodic site. The SVET can be particularly useful in studies of MIC, since MIC is often characterized by localized corrosion.

SVET with anodic and cathodic polarizations. By polarizing samples in combination with SVET analysis, measurements of galvanic corrosion can be made (11). Polarizations are generally destructive to the samples, and are thought to be destructive to bacteria, due to the high applied currents. However, polarization can be performed at the end of experiments, to determine the polarization characteristics of the corroding metal.

The results of the cathodic polarization, shown in Figure 5a, demonstrated that the current densities were nonuniform. As the potential was lowered the current densities became more uniform across the sample. At the very low potentials, the current densities over the site which was anodic at OCP had the greatest change in applied cathodic current. This suggested that at very low potentials, the pits may become more susceptible to hydrogen evolution than the original cathodic sites. The anodic polarization also showed nonuniform current densities during polarizations. The sites originally cathodic showed no change in applied current as the potential was ramped from -620mV/SCE to 0.0V/SCE. The greatest change in applied current was observed over the anodic site. The maximum anodic current density in Figure 4 is much greater than in

Figure 5B. This may be due to the transect of the probe not being positioned over the site of maximum current density. As the potential was ramped in the anodic direction, the anodic sites became more localized. Thus, the likelihood of the probe not being over the maximum anodic site increased. In any event, these results indicated that the SVET can provide better information regarding penetration rates at localized sites.

Use of SVET in MIC studies. Localized corrosion of metals exposed to untreated waters is often attributed to activity of microbes. Studies have suggested that different physiological types of microbes can facilitate the cathodic or the anodic reactions. For example hydrogenase positive sulfate reducing bacteria have been implicated in cathodic depolarization of iron (1), and iron reducing bacteria have been implicated in anodic depolarization of carbon steel (16). This study presents the usefulness of the SVET in characterizing localized corrosion associated with MIC, and demonstrates that the SVET may provide information to test these theories. Studies characterizing microbial physiology and metabolism at localized sites are also progressing (see Introduction). These studies together with in situ analysis of localized metal corrosion may aid in correlating microbial activity to corrosion processes.

LITERATURE CITED

1. Dowling, N.J.E., J. Guzennec, M.L. Lemoine, A. Tunlid, and D.C. White. (1988) Analysis of carbon steels affected by bacteria using electrochemical impedance and direct current techniques. Corrosion **44**:869-874.

2. Gerchakov, S.M., B.J. Little, and P. Wagner. (1986) Probing microbiologically induced corrosion. Corrosion **42**:689-692.

3. Isaacs, H.S. (1988) The measurement of the galvanic corrosion of soldered copper using the scanning vibrating electrode technique. Corrosion Sci. **28**, 547-557.

4. Isaacs, H.S. (1990b) Localized breakdown and repair of passive surfaces during pitting. Corrosion Science

5. Isaacs, H.S. (1989) Applications and limitations of in situ current density mapping. CORROSION/89 paper no. 28, New Orleans, La.

6. Isaacs, H.S., and Y. Ishikawa. (1985a) CORROSION/85, paper no. 55, National Association of Corrosion Engineers, Boston, Ma.

7. Isaacs, H.S., and Y. Ishikawa. (1985b) Current and potential transients during localized corrosion of stainless steel. J. Electrochem. Soc. **132**:1288-1293.

8. Isaacs, H.S., and B. Vyas. (1981) "Scanning Reference Electrode Techniques in Localized Corrosion" Electrochemical Corrosion Testing, ASTM STP 727, (F. Mansfeld and U. Bertocci eds.) ASTM, p. 3-33.

9. Jaffe, L.F., and R. Nuccitelli. (1974) An ultrasensitive vibrating brobe for measuring steady extracellular currents. J. Cell Biol. **63**:614-628.

10. Nivens, D.E., Nichols, P.D., Henson, J.M., Geesey, G.G., and White, D.C. (1986) Reversible acceleration of the corrosion of AISI 304 stainless steel exposed to seawater induced by growth and secretions of the marine bacterium Vibrio natriegens. Corrosion **42**:204-210.

11. Obuekwe, C.O., D.W.S. Westlake, J.A. Plambeck, and F.D. Cook. (1981) Corrosion fo mild steel in cultures of ferric iron reducing bacterium isolated from crude oil 1. Polarization characteristics. Corrosion **37**:461-467.

12. Scotto, V., R. Di Cintio, and G. Marcenaro. (1985) The influence of marine aerobic microbial film on stainless steel corrosion behaviour. Corrosion Science **25**:185-194.

13. Von Wolzogen Kuhr, C.A.H., and L.S. van der Vlugt. 1934. De grafiteering van gietijzer als electrobiochemich process in anaerobe gronden. Water **18**:147-165.

CHAPTER VII

A STUDY OF CARBON STEEL CORROSION INHIBITION BY PHOSPHATE IONS AND BY AN ORGANIC BUFFER, USING A SCANNING VIBRATING ELECTRODE

ABSTRACT

The scanning vibrating reference electrode technique (SVET) has been used to map anodic and cathodic currents in solutions over freely corroding type C1020 carbon steel. All solutions contained millimolar concentrations of chloride, and were sterilized. The effects of phosphate and an organic buffer on the corrosion of carbon steel in liquid media were studied because they were added to promote bacterial growth. Phosphate acted as an anodic inhibitor in the media, causing initiated pits to repassivate. However, if initiated pits did not repassivate, for example in stagnant medium or when crevice corrosion initiated adjacent to the sample coating, the corrosion rates increased and the corrosion remained localized. Increased anodic current resulted in a drop in the open circuit potential and a decrease in the polarization resistance. The results show that phosphate can lead to lower average corrosion rates, than occur in uninhibited steel, but as an anodic inhibitor can also lead to rapid penetration at localized sites.

INTRODUCTION

Pitting corrosion of iron in media containing one millimolar concentrations of chloride and sulfate ions has been studied (1,3,5). The results suggested that in this poorly buffered medium, local pH was an important component in pit propagation and spreading of corrosion around the pit. Many aqueous environments are buffered and contain ions which inhibit or facilitate pit propagation. In a sterile medium containing similar concentrations of chloride and sulfate ions, as well as low concentrations of an organic buffer, glucose and other ions, carbon steel coupons remained passive for the nine days of exposure (Chapter 1). This was in contrast to the rapid pitting and corrosion propagation of pits observed for the pure iron, in the dilute chloride and sulfate containing media (1,3,5). This study was carried out to ascertain the corrosion inhibition by components in the complex medium used previously (Chapter 1), since trace ions can affect the corrosion rates of metals (1,8,9,10), and buffering may be important in preventing the corrosion at pits from spreading.

The scanning vibrating electrode technique (SVET) has been used to obtain current density maps over freely corroding metal samples (2,4,5,6, Chapter 4). With the SVET, the time variations during localized corrosion can be evaluated without altering the progression of corrosion.

Thus, the SVET and other scanning methods (5) provide a useful means for studying corrosion inhibitors.

In this study, the SVET, polarization resistances (R_p), and monitoring the open circuit potential (OCP), were used to study the specific effects of phosphate and an organic buffer on the propagation of pits in carbon steel in sterile solutions. The results indicated that phosphate ions in an air bubbled solution caused repassivation of initiated pits. However, under certain conditions, phosphate addition could lead to highly localized corrosion.

MATERIALS AND METHODS

Electrolyte. The electrolyte used in this study contained (in mg/L) NH_4Cl 50, $MgSO_4 \cdot 2H_2O$ 50, $CaCl_2 \cdot 2H_2O$ 5, KH_2PO_4 27, Glucose 50, 2-morpholinoethane sulfonic acid (MOPES buffer) 50, and trace minerals (in $\mu g/L$) $Na_2MoO_4 \cdot 2H_2O$ 0.1, $ZnSO_4 \cdot 7H_2O$ 50, $MnSO_4 \cdot H_2O$ 7.7, $CuSO_4 \cdot 5H_2O$ 2, $CoCl_2 \cdot H_2O$ 1, $NaB_4O_7 \cdot 10H_2O$ 0.8, $NiSO_4$ 0.5. This medium has been used in a previous study of microbial influenced corrosion (2, Chapter 1,4), and was complex due to the growth requirements for the bacteria. The concentrated components of the medium were omitted as indicated in the results. All solutions were sterilized by autoclaving for 20 min.

Metal samples and electrochemical cells. The metal coupons of C1020 carbon steel were supplied by Metal Samples (Munford Al.). The steel contained; C 0.17, Mn 0.42, P 0.009, and S 0.006, weight percent. The coupons, with a spot welded electrical connection, were embedded in epoxy and finished with 600 grit silicon carbide paper. Thin, approximately 75 um, pressure sensitive tape (3M Co. no 92) was used to insulate the sample except for an area in the center of the coupon approximately 25 mm^2. Microshield lacquer (Pyramid Plastics, Inc., Hope, Ar.) was painted at the edge of the tape to reduce crevice corrosion.

For experiments where only the open circuit potential (OCP) was monitored over time, the working electrode and a salt bridge to a saturated calomel reference electrode imme

immersed in a salt bridge were suspended in a beaker of medium. The media were stirred with a Teflon coated magnetic bar, controlled by a magnetic stirrer. The analog output of OCP from an electrometer was recorded by a strip chart recorder. The electrochemical cell for the SVET experiments had a working volume of 15 ml and contained saturated calomel reference electrode emersed in a salt bridge, and a platinum wire for a counter electrode.

Current Density maps. The vibrating electrode used to scan the working electrode consisted of an insulated platinum wire, 0.1mm in diameter. The platinum wire was attached to a piezoelectric reed which was activated by applying a 10 V rms signal to the reed at 200 Hz, as described previously (6). The peak to peak vibration was 0.04mm. The vibrating electrode was positioned 0.09mm from the working electrode surface. The alternating signal was analyzed with a PAR model 124A lock-in amplifier with a model 116 plug-in unit, and a computer controlled data acquisition unit. The surface of the working electrode was scanned by moving the cell in 0.2 mm increments with computer controlled stepper motors. The output voltage from the lock-in amplifier was calibrated with a known uniform current density.

Polarization Resistance. Polarization resistances were obtained by applying a 25 mV triangular signal, around the open circuit potential, to the working electrode at a rate

of 5mV/sec. Polarization resistance was determined by the slope of the current versus potential line.

RESULTS

OCP in 1mM chloride and sulfate. The carbon steel OCP in a medium containing 1 mM chloride and sulfate is shown in Fig. 1 curve a. The OCP showed a similar behavior to that previously observed for pure iron in this medium (3,5). The OCP decreased rapidly to approximately -510 mV/SCE following immersion of the steel in the medium, and corrosion products were observed as the OCP decreased. The initial rapid decrease in OCP was followed by a slow decrease to approximately -540 mV/SCE, and then by another fairly rapid drop to approximately -620mV/SCE, and then by a slow continual decrease.

OCP in complex medium. In a previous study, using the same sterile complex medium used in this study, the OCP remained at approximately -200 mV/SCE for the nine days of exposure, and little corrosion product was observed on the steel (Chapter 1). Figure 1 curve b shows the results of OCP vs time for the stirred complex medium. The OCP increased from approximately -350mV/SCE to approximately -200mV/SCE. Drops in OCP of approximately 20 mV, followed by increases in OCP were observed throughout the experiment. These potential transients are characteristic of pit initiation, followed by pit repassivations (7). Pit initiation and repassivation in this medium has been characterized by the SVET analysis in the absence and in the presence of active bacteria (Chapter 6).

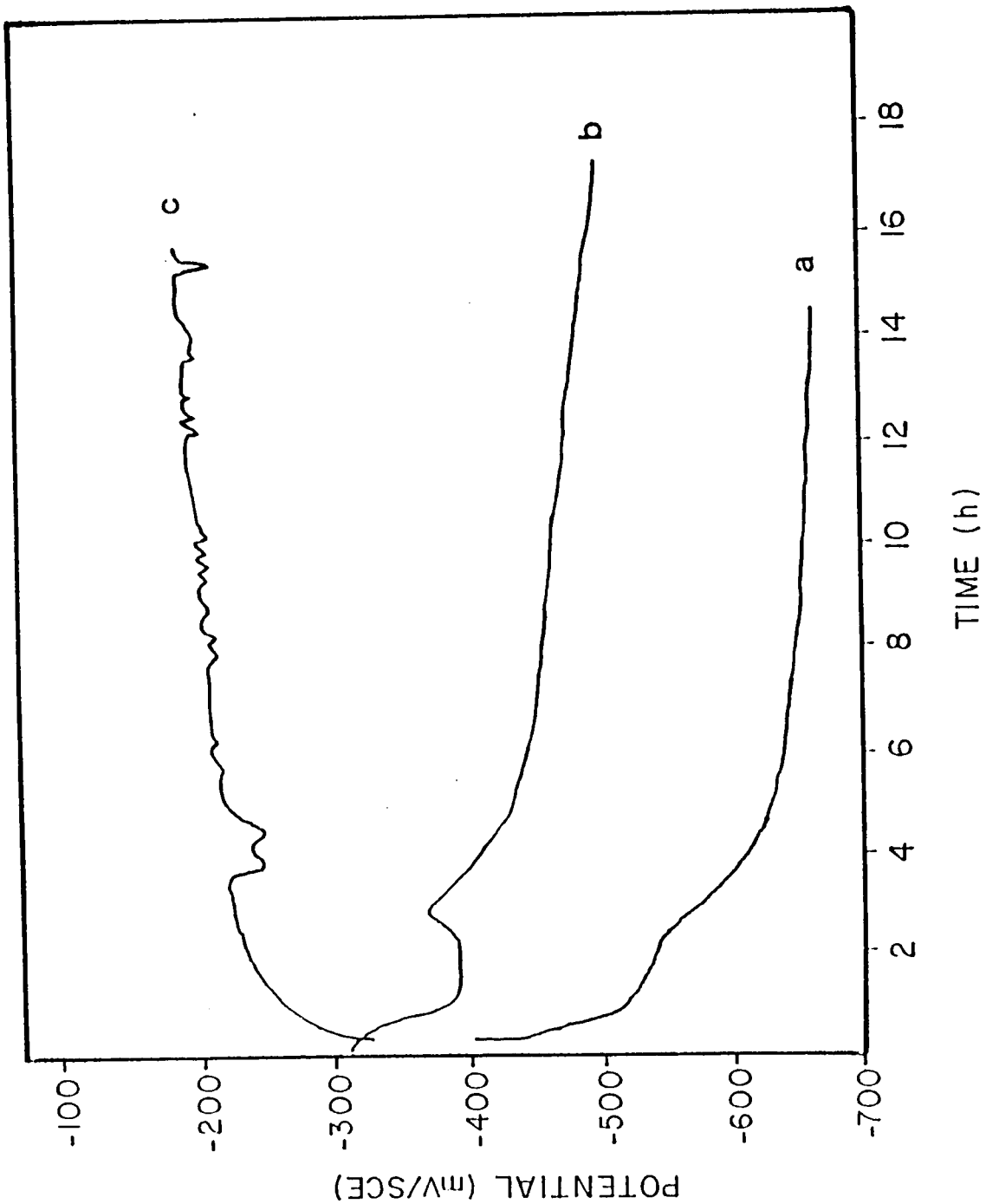

Figure 1. Open circuit potential (mV vs standard calomel electrode) over time for carbon steel electrode. Curve a, carbon steel in 1mM chloride and sulfate solution. Curve b, carbon steel in stirred complex medium containing MOPS, an organic buffer, and ions. Curve c, carbon steel in unstirred complex medium.

Current density maps in unstirred medium. The increase in OCP was not observed when the complex medium was not stirred (Fig. 1, curve c). The OCP decreases rapidly to -400mV/SCE. This rapid decrease was followed by a slow decrease in the OCP. The SVET was used to analyze the carbon steel corrosion in the unstirred complex medium. The results showed that four pits formed after 0.08 h exposure of the steel to the medium (Fig. 2A). After 0.3 h of exposure, all but one pit close to the stop-off became inactive (Fig. 2B). This pit remained active throughout the remainder of the experiment (Fig. 2C). The OCP was monitored throughout this experiment (Fig. 2D). The OCP dropped with time, showing the same trend as curve c, Fig. 1.

Polarization resistance measurements were made at the times indicated by the vertical lines in Fig. 2D. The R_p were 3.5×10^3 ohm·cm^2 and 1.5×10^3 ohm·cm^2 for the two hour and the 3.7 hour measurements, respectively.

Current density maps in stirred complex medium. The medium was continuously bubbled with air to stir the solution during SVET analysis. In all but one experiment, pits initiated and the steel repassivated in stirred or aerated medium. However, in the one experiment, the lacquer coating was undermined and corrosion developed.

The results of the SVET analysis and the OCP vs time for the stirred medium are shown in Fig. 3. Active pits at

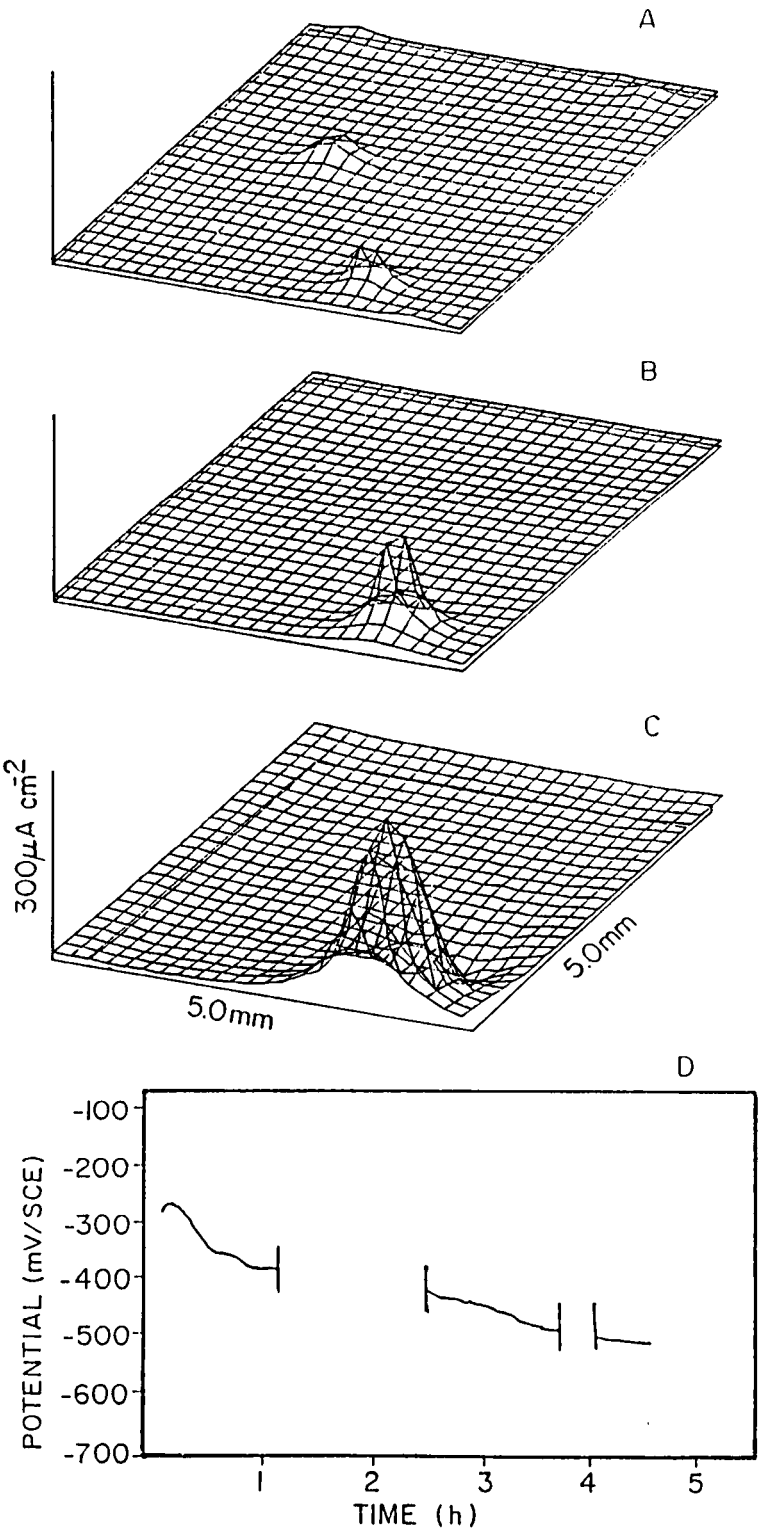

Figure 2. Current density maps over carbon steel in unstirred complex medium. A) 0.08 h B) 0.3 h C) 3.7 h. D) Open circuit potential for carbon steel in unstirred medium. Verticle lines indicate times at which polarization resistance measurements were made.

different locations for limited times were observed during the first nine hours of exposure (Fig. 3A,B). The preferred location of the pits were adjacent to the lacquer. After nine hours of exposure, one pit did not repassivate, but continued to grow over the remainder of the experiment. Figure 3C shows the position of the one anodic site, after 10 h. of exposure. Figure 3D shows the current density map for the same sample after 22 h. of exposure. The anodic site remained active in the same location, however the magnitude of the current density increased. The OCP for this sample is shown in Fig. 3E. The first nine hours of exposure show potential transients due to pit initiation and repassivation (7). After nine hours of exposure the OCP stabilizes at a value of approximately -340mV/SCE, and the fluctuations stopped. The potential drops very slowly over the remainder of the experiment, as the single pitting site remain localized.

The polarization resistance measurements were obtained at the times indicated in Fig. 3E. The R_p was $5x10^4$ ohm/cm^2 at 3.5 hours, when one small pit was observed using the SVET analysis. The R_p for the sample after one pit remained active and after the potential stabilized, at 10 hours, was $9x10^3$ and was $5.9x10^3$ ohms/cm^2 at 20 hours.

Omission of MOPS buffer and glucose, or phosphate. In order to gain a better understanding of the role of the components of the complex medium on the pitting corrosion of

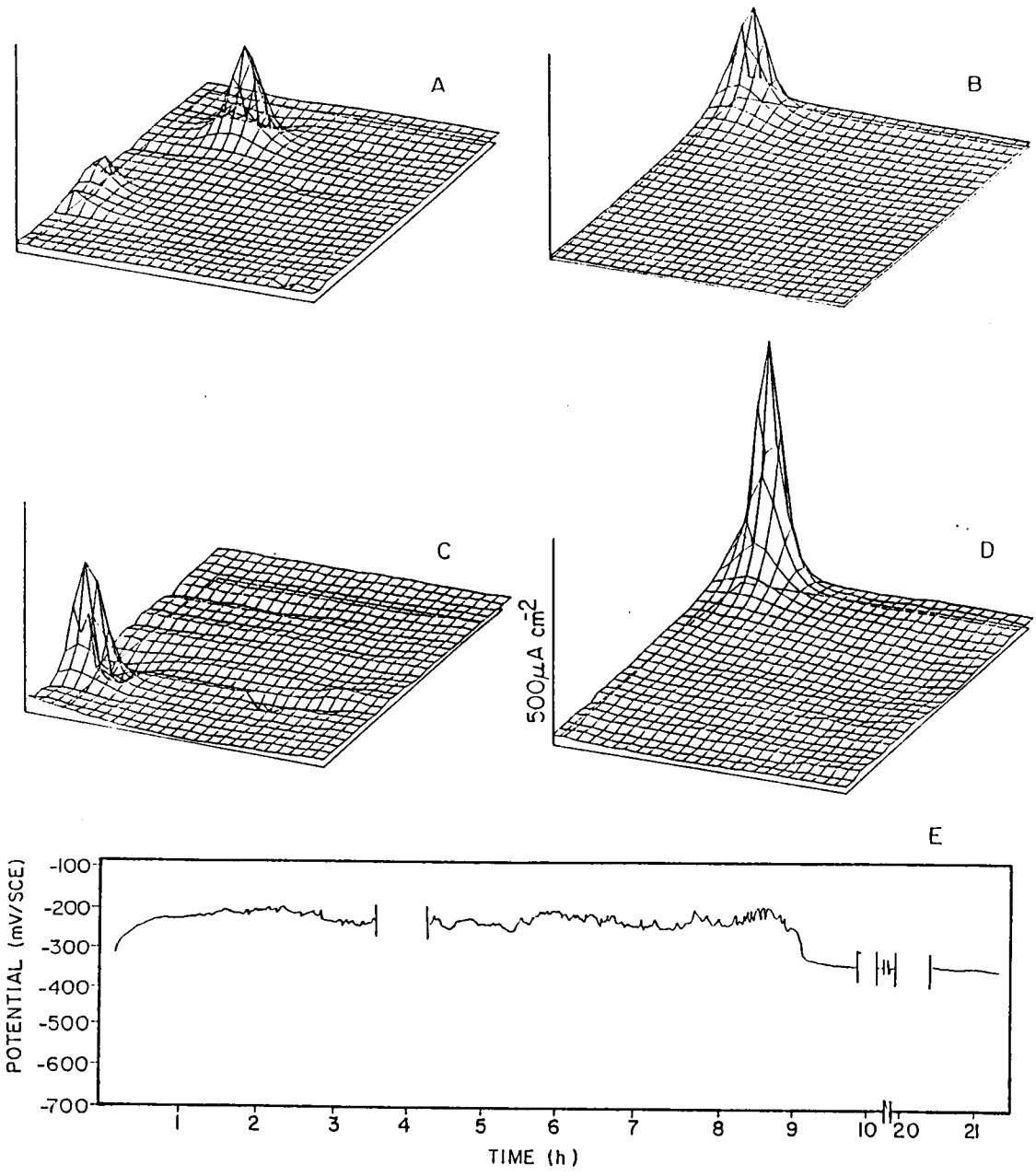

Figure 3. Current density maps over carbon steel in air bubbled complex medium. A) 3 hours. B) 6 hours. C) 10 hours. D) 22 hours. E) Open circuit potential for the sample.

the carbon steel, phosphate and the organic buffer were omitted from the medium in different combinations, and the OCP of the steel was monitored over time. The media were stirred in these experiments. Figure 4, curve a, shows the OCP of the steel when the glucose, MOPS buffer, and phosphate were omitted from the medium. The OCP rapidly dropped to -450 mV/SCE in less than 1 hour and slowly to -590mV/SCE after 16 hours. Figure 4, curve b, shows the OCP of the stirred medium when phosphate was omitted and glucose and MOPES buffer were included. The potential dropped less rapidly after immersion than in case 4a, but also reached -590mV/SCE in about 16 hours. Figure 4, curve c, shows the OCP when the glucose and the MOPS buffer were omitted, but the phosphate was included. The OCP initially increased from -320mV/SCE to -250mV/SCE. The OCP remained around -300mV/SCE and fluctuations due to pit initiation could be observed after 11 hours.

Addition of phosphate to corroding sample. The effect of phosphate addition to freely corroding steel was characterized by SVET analysis (Fig. 5). The steel was allowed to corrode in the medium with the MOPS buffer, glucose, and phosphate omitted. The OCP showed a similar trend to the steel in 1mM chloride and sulfate solution (Fig. 1, curve a). After 4.3 h, when the spreading of corrosion had virtually stopped, as indicated by SVET, and

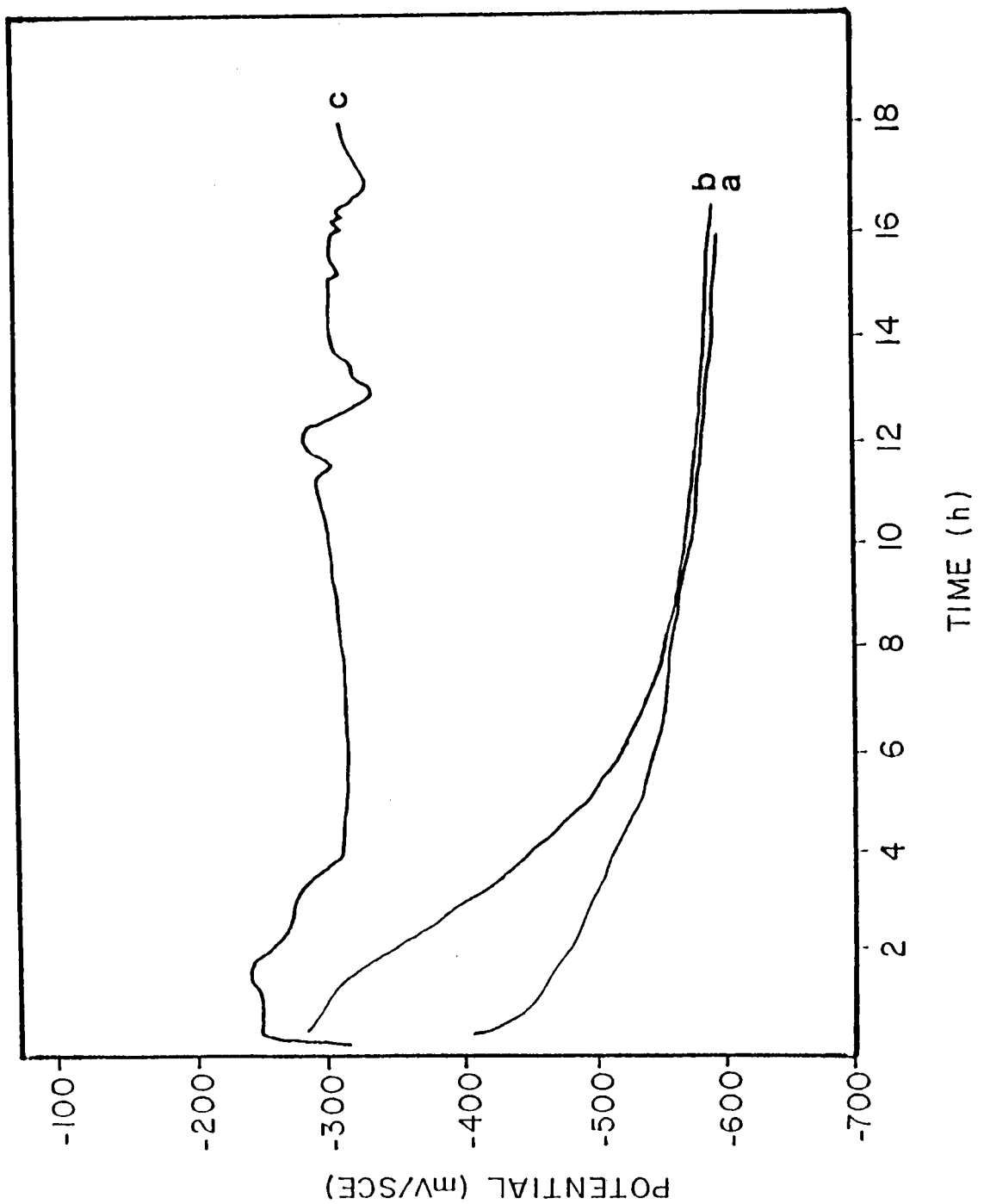

Figure 4. Open circuit potential for carbon steel in stirred incomplete medium. Curve a) carbon steel in medium lacking glucose, MOPES and phosphate. Curve b) carbon steel in medium lacking phosphate. Curve c) carbon steel in medium lacking glucose and MOPES.

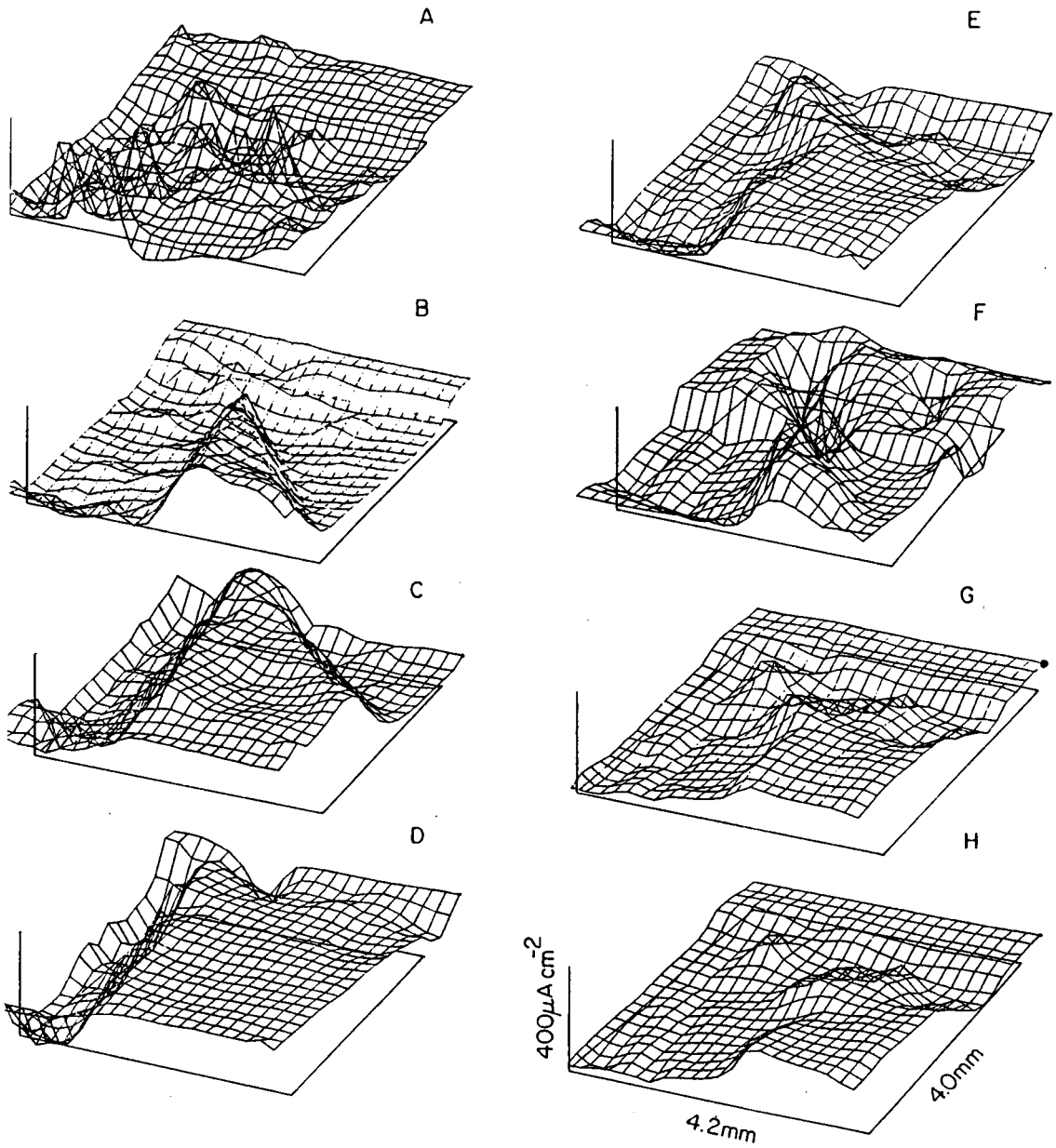

Figure 5. Current density maps over carbon steel in medium lacking glucose, MOPES, and phosphate A) 0.1 h, B) 1 h, C) 2.2 h, D) 4.3 h. Current density maps after addition of phosphate to a final concentration of 0.2mM E) 4.5 h, F) 5.3 h, G) 7.7 h. H) Current density map at 10 h after addition of phosphate to a final concentration of 0.8mM.
by the OCP, -690 mV/SCE, phosphate solution, pH 7.4, was added to bring the final phosphate concentration to 0.2mM.

Figure 5 A-D show the spreading of corrosion from the current density maps over the steel prior to phosphate addition. Initially, after 0.1 h many distinct pits formed (Fig. 5A). After 1 h the anodic zone was confined to one area (Fig. 5B), and this zone spread (Fig. 5C) until approximately 70% of the sample was anodic, at 4.3 (Fig. 5D). At 4.3 h the potassium phosphate solution was added. Upon addition of the phosphate the size of the anodic zone decreased (Fig. 5E). This decrease continued until 5.3 h, after which there were very slow changes in the anodic zone (Fig. 5F,G). Although the changes were very pronounced on first adding the phosphate, the size of the anodic zone was not further decreased by further addition of phosphate to a final concentration of 0.8 mM (Fig. 5H). The decrease in the area of the anodic zone was accompanied by an increase in the OCP from -690mV/SCE to -550mV/SCE. The OCP did not increase above -550mV/SCE, and gradually decreased again with time as the corrosion slowly began to spread again.

DISCUSSION

OCP and corrosion of carbon steel in unbuffered media. The purpose of this study was to determine the effects of the more concentrated solution components on the early stages of corrosion of carbon steel in sterile solutions. The presences of buffers and phosphates are added to assist the growth of bacteria, but may themselves affect corrosion.

The SVET, OCP, and polarization resistance were used to evaluate changes in corrosion processes. The results of the carbon steel corrosion in 1mM NaCl and Na_2SO_4 solution were similar to those observed for pure iron in the same solution, as indicated by SVET and OCP vs time (5). The OCP was also similar in shape to those observed by Gatty and Spooner (3). It therefore is apparent that the shape of the OCP decay curves remain the same but the rates change with many variables including surface preparation (1), steel composition (compare ref 1 and Fig. 1a), and solution composition. With pure iron, the changes in current density distribution, determined by the SVET, were related to the change in OCP (5). The OCP decreased rapidly to approximately -500 mV/SCE, as distinct pits initiated and propagated. After this rapid decrease, the potential decreased slowly to -550 mV/SCE, and distinct pit sites remained localized. Below -550 mV/SCE the anodic sites began to spread rapidly and the potential dropped to approximately -650mV/SCE, where the areas of corrosion began

to stabilize. The SVET study of the carbon steel used in this investigation also showed similar trends and correlations with OCP.

The pH at the cathodic areas is increased by hydroxide formed during oxygen reduction (5). The pH around the anodic areas is decreased by hydrolysis of ferrous or ferric ions. The model proposed for iron corrosion, in the dilute chloride and sulfate solution, assumes that the pH of the cathodic site adjacent to the pit is lower than the remaining cathodic area due to diffusion of hydrogen ions from the pit (5). The spreading of the anodic area occurs as the potential and pH drop to values intersecting the value for the transition of passivity to general corrosion on the pH/potential diagram. A map of pH, 0.04 mm over the iron surface, showed pH values which ranged from less than 6 over the anodic sites to greater than 10 over the cathodic sites (5). Those results suggested that pH is important in spreading of anodic sites. These results suggested that pitting of carbon steel in unbuffered media may not be a serious problem, since the corrosion was fairly uniform over the surface of the sample.

Effect of buffers. The results of this study suggested that buffering may contribute to localized corrosion. The OCP diagrams for steel in medium containing MOPS buffer (Fig. 4) and for steel in medium containing MOPS buffer plus phosphate (Fig. 1) showed a slower drop in OCP than for the

steel in 1mM chloride and sulfate solution. This indicated that the corrosion was more localized for longer periods of time. This effect was more pronounced in the presence of phosphate than in the presence of MOPS, suggesting that phosphate had a greater effect on either pH or dissolution kinetics. The SVET analysis supports the conclusion that corrosion was localized for longer periods of time in the presence of phosphate and MOPS. In Fig. 2 four pits initiated at the beginning of exposure, but after 0.3 h, all but one pit was repassivated. The remaining pit, although slowly increasing in area with time, remained localized over the experiment. This was in contrast to the observation of iron in 1mM chloride and sulfate, where all of the initiated pits propagated, until the anodic sites merged (5). Hence it appears that in medium which was well buffered, the buffering capacity of the medium inhibits the spreading of the pits, by confining the low pH to the pit. This buffering capacity reduces spreading of the actively corroding areas and intensifies localized corrosion, rather than leading to a more general corrosion.

Effect of phosphate and convection. The spread of corrosion on carbon steel was rapid in a solution containing chloride and sulfate as shown by the fall in potential in Fig. 1a. However, with the addition of inhibiting ions, the steel showed characteristics similar to those observed with stainless steels, where pit initiation was followed by

repassivation (Fig. 1, ref 7). The combination of phosphate and convection had the greatest impact on repassivation of pits. This was observed for the OCP diagram in Fig. 1b. The SVET analysis for the first nine hours in Fig. 3 also demonstrated this behavior. However, if conditions were not favorable for a pit to repassivate, aeration and phosphate can lead to enhanced localized corrosion. This was observed in the second twelve hours in Fig. 3. Here, the crevice corrosion formed and the lacquer apparently inhibited repassivation. The crevice remained highly localized through the remainder of the experiment. The OCP dropped very slowly over this time. The magnitude of the anodic current from the localized corrosion increased approximately two-fold over twelve hours, but the area exposed to solution increased only slightly.

The results showing that phosphate can inhibit corrosion of the steel, but can also lead to enhanced localized corrosion as further supported by the SVET analysis in Fig. 5. Phosphate was added to the actively corroding steel sample. The phosphate resulted in a decrease of the corroding areas. However, the smaller anodic site stabilized with time. The presence of four-fold more phosphate did not further decrease the size of the anodic site. These results again indicated that phosphate acted as an anodic inhibitor, but the steel did not completely repassivated following the addition of phosphate.

The increase in anodic current density, determined by SVET, and the drop in OCP correlated to a decrease in the polarization resistance of the samples. Figure 2 shows that when the potential of the steel in the unstirred complete medium fell to approximate -400mV/SCE the Rp was 3500 ohm·cm^2. As the potential fell to approximately -500mV/SCE and the area and the magnitude of the anodic site increased, as determined by the SVET, the Rp decreased to 1500 ohm·cm^2. A similar decrease in Rp was observed in the sample where crevice corrosion occurred on the steel in air bubbled complete medium (Fig. 3). As the size and magnitude of the anodic area increased, the Rp decreased from 40000 ohm·cm^2 after four hours, to 9000 ohm·cm^2 after 10 hours, and 5900 ohm·cm^2 after 20 hours.

These results show that components of complex solutions, such media used for microbially influenced corrosion studies, can affect the corrosion rates and the corrosion propagation of steel samples. The results also suggest that the SVET is useful for evaluating corrosion inhibitors. The current density maps obtained by SVET correlate with measurements of OCP and polarization resistance. In addition the SVET can be used to study corrosion inhibition when corrosion is highly localized. If the corrosion is localized to an area where the inhibitor has difficulty penetrating, such as into a crevice, the inhibitor may cause highly active localized corrosion.

LITERATURE CITED

1. Evans, U.R. The Corrosion and Oxidation of Metals, p. 106, Edward Arnold Ltd. London (1960).

2. Franklin, M.J., D.C. White, and H.S. Isaacs. (1990) The use of current density mapping in the study of microbial influenced corrosion. CORROSION/90, National Association of Corrosion Engineers, Las Vegas, Nv. (1990).

3. Gatty, O. and E.C.R. Spooner, The Electrode Potential Behavior of Corroding Metals in Aqueous Solutions, p. 253. Oxford University Press, Oxford (1938).

4. Isaacs, H.S. (1988) The measurement of the galvanic corrosion of soldered copper using the scanning vibrating electrode technique. Corrosion Sci. **28**, 547-557.

5. Isaacs, H.S. (1990) The pitting of iron in dilute chloride and sulfate solutions. Advances in Localized Corrosion, eds. H.S. Isaacs, V. Bertocci, J. Kruger, and Z. Szklarska-Smialowska. NACE.

6. Isaacs, H.S., and Y. Ishikawa. (1985) CORROSION/85, paper no. 55, National Association of Corrosion Engineers, Boston, Ma.

7. Isaacs, H.S., and Y. Ishikawa. (1985) Current and potential transients during localized corrosion of stainless steel. J. Electrochem. Soc. **132**:1288-1293.

8. Mansfeld, F., S.L. Jeanjaquet, M. Kendig, D.O. Raleigh, and K. Fertig. (1986) Corrosion, **42**:249-255.

9. Matsuda, S., and H.H. Uhlig. (1964) J. Electrochem. Soc. **111**:156.

10. Strehblow, H.H. (1976) Werkst Korros. **27**:792-797.

CHAPTER VIII

PITTING CORROSION BY BACTERIA ON CARBON STEEL, DETERMINED BY THE SCANNING VIBRATING ELECTRODE TECHNIQUE

ABSTRACT

The scanning vibrating electrode technique (SVET) has provided a non-destructive, on-line method for locating the presence and position of anodic electrochemical activity on the surface of carbon steel coupons. Using the SVET, changes in current densities over the steel with time were mapped in the presence and in the absence of bacteria. In sterile liquid medium, the maps showed highly localized anodic current densities, which subsequently became inactive. Analysis of current maps and the open circuit potential (OCP) showed that the potential transients were due to pit initiation and repassivation processes. When in the same bulk fluid, an aerobic bacterium, isolated from a corrosion tubercle, was grown, similar trends of pit initiation and repassivation were observed for several hours. However, after extended exposure to bacteria, local anodic activity did not repassivate. The corrosion then propagated and spread, until a large area of the sample was anodic. Recovery of the spent growth medium after growth of the bacteria, when used as the bulk solution, did not induce this irreversible pitting. These results indicated that the growth of bacteria altered surface conditions and prevented the initiated anodic sites from repassivating.

INTRODUCTION

The role of bacteria in metal corrosion in water is increasingly being considered as an important economic and environmental problem. Various mechanisms relating the activity of microbes and corrosion facilitation have been proposed. For example, the metabolic use of oxygen by non-uniformly colonized aerobic bacteria can lead to differential oxygen cells (8). Local cathodic depolarization by hydrogen consuming bacteria (3,11), or anodic depolarization by iron reducing bacteria (4), has been suggested to accelerate corrosion.

Measurement of corrosion influenced by bacteria, as well as evaluation of the above mechanisms has been difficult, due to the destructive nature of most corrosion measurement techniques. Direct current techniques require high applied currents, and therefore can alter biofilms (1). Non-destructive techniques involving measurement of open circuit potential (OCP), linear polarizations, and electrochemical impedance spectroscopy (EIS) can provide on-line monitoring of corrosion rate, but provide the average corrosion rates for the coupon surface and only indirect indications of localized corrosion caused by MIC (2).

The scanning vibrating electrode technique (SVET) provides a non-destructive means to define the magnitude and sign of current densities in solution over freely corroding metals (6). Current density maps have been utilized to

define localized anodic and cathodic activities of iron and stainless steel (7), the galvanic corrosion of soldered copper (4), and corrosion inhibition by phosphate and organic buffers (Chapter 5). In the present study, the SVET was used to detect localized corrosion of carbon steel in the presence and in the absence of an aerobic bacterium.

MATERIALS AND METHODS

Bacterium and medium. The bacterial isolate used in this study was the same as that used in the previous chapters. The isolate has been identified as a Pseudomonas sp. based on the profile of membrane fatty acids. The isolate rapidly colonized carbon steel (Chapter 1) and did not grow anaerobically, or produce detectable levels of volatile fatty acids when grown on glucose (1g/L). The medium used in these experiments was (in mg/L of glass distilled water) NH_4Cl 50, $MgSO_4 \cdot 2H_2O$ 50, $CaCl_2 \cdot 2H_2O$ 5, KH_2PO_4 27, Glucose 50, 2-morpholinoethane sulfonic acid (MOPES buffer) 50, and trace minerals (in $\mu g/L$) $Na_2MoO_4 \cdot 2H_2O$ 0.1, $ZnSO_4 \cdot 7H_2O$ 50, $MnSO_4 \cdot H_2O$ 7.7, $CuSO_4 \cdot 5H_2O$ 2, $CoCl_2 \cdot H_2O$ 1, $NaB_4O_7 \cdot 10H_2O$ 0.8, $NiSO_4$ 0.5. This medium was the same as used in the previous reports (Chapter 1).

Bacterial cells were grown to late exponential phase (24 hours, at 25°C) in 100 ml of the medium described above. The cells were centrifuged and the spent medium was removed. The bacteria were resuspended 100 ml of fresh medium. Fifteen ml of the suspension was added to the electrochemical cell.

Electrochemical cell. The working electrodes in these experiments were coupons of C1020 carbon steel supplied by Metal Samples (Munford Al.). The elemental composition of the steel from the supplier was given as, C-0.17, Mn-0.42, P-0.009, and S-0.006, weight percentage. The coupons were

MATERIALS AND METHODS

Bacterium and medium. The bacterial isolate used in this study was the same as that used in the previous chapters. The isolate has been identified as a Pseudomonas sp. based on the profile of membrane fatty acids. The isolate rapidly colonized carbon steel (Chapter 1) and did not grow anaerobically, or produce detectable levels of volatile fatty acids when grown on glucose (1g/L). The medium used in these experiments was (in mg/L of glass distilled water) NH_4Cl 50, $MgSO_4 \cdot 2H_2O$ 50, $CaCl_2 \cdot 2H_2O$ 5, KH_2PO_4 27, Glucose 50, 2-morpholinoethane sulfonic acid (MOPES buffer) 50, and trace minerals (in $\mu g/L$) $Na_2MoO_4 \cdot 2H_2O$ 0.1, $ZnSO_4 \cdot 7H_2O$ 50, $MnSO_4 \cdot H_2O$ 7.7, $CuSO_4 \cdot 5H_2O$ 2, $CoCl_2 \cdot H_2O$ 1, $NaB_4O_7 \cdot 10H_2O$ 0.8, $NiSO_4$ 0.5. This medium was the same as used in the previous reports (Chapter 1).

Bacterial cells were grown to late exponential phase (24 hours, at 25°C) in 100 ml of the medium described above. The cells were centrifuged and the spent medium was removed. The bacteria were resuspended 100 ml of fresh medium. Fifteen ml of the suspension was added to the electrochemical cell.

Electrochemical cell. The working electrodes in these experiments were coupons of C1020 carbon steel supplied by Metal Samples (Munford Al.). The elemental composition of the steel from the supplier was given as, C-0.17, Mn-0.42, P-0.009, and S-0.006, weight percentage. The coupons were

RESULTS

OCP in sterile medium. In a previous study, investigating carbon steel corrosion in the same sterile medium used in this study, the OCP remained at approximately -200 mV/SCE for the nine days of exposure (Chapter 1). In this study, the OCP was again monitored. Figure 1d shows the OCP versus time for the carbon steel in the sterile medium which was stirred by air bubbling. The OCP increased from an initial value of approximately -300mV/SCE to approximately -200mV/ SCE. The potential transients seen in Fig. 1d are characteristic of pit initiation followed by repassivation of the pits (7).

SVET analysis in sterile medium. Current density maps over the carbon steel in the sterile, air-agitated medium are shown in Fig. 1a,b,c. Figure 1a shows five pits, that initiated immediately upon exposure of the metal to the medium. Figure 1b shows a single pit at a different location to the five seen in Fig. 1a. The maximum anodic current density, 114 $\mu A/cm^2$, was observed after 25 min of exposure of the steel to the medium. This pit corresponds to a decrease in the OCP to approximately -300mV/SCE (Fig. 1d). This pit subsequently became inactive. Small pits, with measured current densities of less than 20 $\mu A/cm^2$, initiated at different sites. This sequence of pit initiation, repassivation, and initiation at a different sites occurred until the experiment was terminated at 32

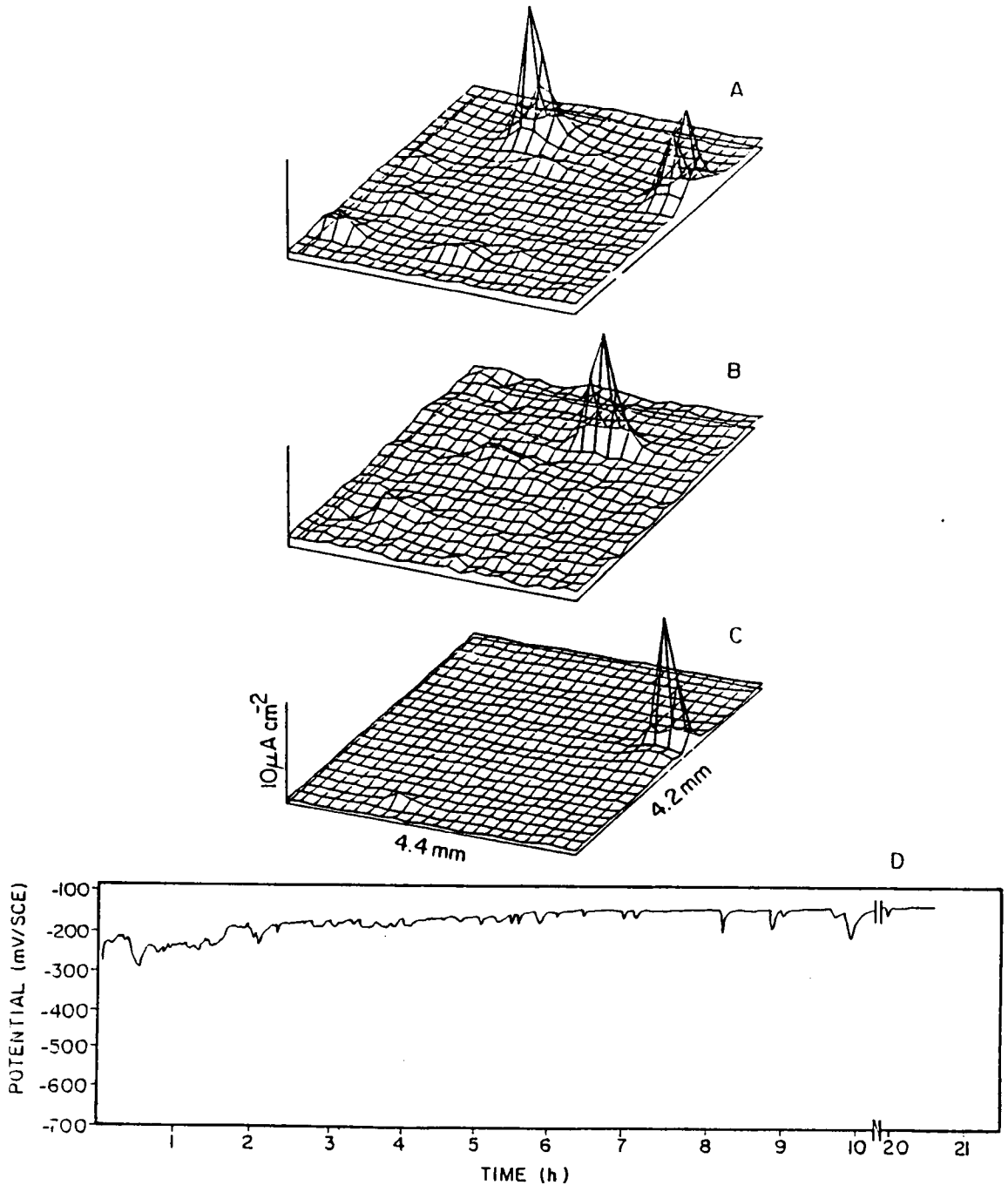

Figure 1. Current density maps over carbon steel electrode in sterile aerobic microbiological medium. A) 1 min. B) 3 hours. C) 32 hours. D) Open circuit potential for carbon steel in sterile medium. Verticle lines indicate times at which polarization resistance measurements were made.

hours. Experiments involving current density mapping in sterile medium were performed twice, and similar results were obtained in both experiments. Measurement of OCP vs time in sterile medium were conducted six times, and similar trends to Fig. 1d were obtained.

OCP in inoculated medium. A comparison was made between pitting of the carbon steel in the sterile medium, and medium containing a culture of an aerobic heterotrophic bacterium. The bacterial culture was prepared, as described in the experimental methods, and added to the electrochemical cell. As with the sterile medium, the inoculated medium was continuously bubbled with air. The OCP for this experiment is shown in Fig. 2e. A trend similar to that observed for the sterile medium was observed for the first four hours of exposure. The OCP, although lower than in the sterile control approximately -300mV/SCE, shows pit initiation and repassivation. However, after six hours of exposure, the OCP slowly dropped, until it reaches a value of approximately -600mV/SCE at 20 hours.

SVET analysis in inoculated medium. The current density maps obtained for the inoculated system are shown in Fig. 2. After five hours (Fig. 2a), two pits were observed. Although one of the pits becomes inactive, the more intensely desolving pit continued to propagate (Fig. 2b). The anodic current density above the active pit, and the area of the pit increased with time. The corrosion

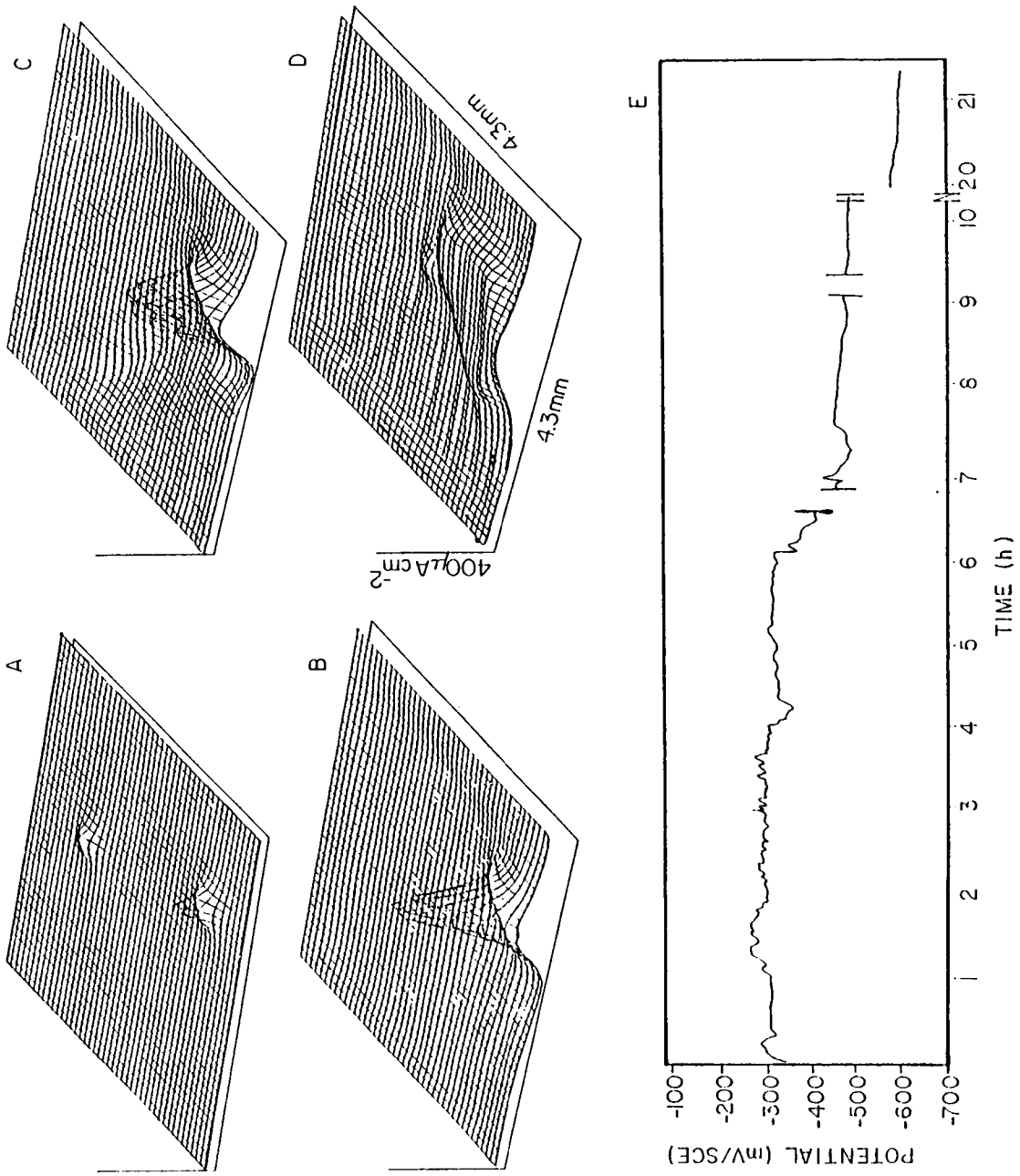

Figure 2. Current density maps over carbon steel in inoculated aerated medium. A) 3 hours. B) 7 hours. C) 11.5 hours. D) 23 hours. E) Open circuit potential for carbon steel in aerated medium inoculated with bacteria.

continued to propagate over the course of the experiment (Fig. 2c,d) until a large area of the coupon was anodic. Although the pit spread to the epoxy coating, the pit did not initiate at the coating.

The experiment containing bacteria was performed three times. Similar trends of pit initiation and repassivation followed by propagation and spreading of one pit was observed in all three experiments. The time required for a single pit to propagate and spread varied from two to six hours for the three experiments.

Polarization resistances. The polarization resistance was measured by cycling the potential (5mV/sec) around the OCP ($\pm$25 mV). The times at which R_p was measured are indicated by the vertical lines in the OCP vs time diagram (Fig. 2e). The values of R_p for the sample exposed to inoculated medium were 4000 ohm·cm^2 at seven hours, 2000 ohm·cm^2 at twelve hours, and 1100 ohm·cm^2 for the 23 hour measurement. In contrast to the sample that contained bacteria, the sample that contained sterile medium gave a conventional value of R_p of 16,000 ohm·cm^2 after 32 hours of exposure. No active pitting was observed by SVET at the time of the polarization resistance analysis for the sterile control.

OCP in spent growth medium. The composition of the electrolyte can greatly affect the corrosion of carbon steel (Chapter 5). Bacteria can alter the composition of the

electrolyte, either by conversion of trace cations or anions into cellular material, or by the production of end products of metabolism, acids or alcohols. Corrosion of the carbon steel affected by changes in the medium due to bacteria, but with the bacteria removed from the medium was determined. Bacteria were grown in the medium described above to late exponential phase (for 24 hours). The bacteria were removed from the medium by centrifugation. The supernatant was then filter sterilized by passing the medium through a 0.2 μm membrane filter. The carbon steel was exposed to fifteen ml of this filter sterilized spent medium. The measurement of OCP versus time showed a similar trend to that observed for sterile fresh medium (Fig. 3). The initial potential was approximately -300mV/SCE, and the potential rose to approximately -200mV/SCE in the first hour of exposure. The OCP remained at this potential for the remainder of the experiment. The "noisy" behavior, indicative of pit initiation and pit repassivation was also observed, although the frequency of the transients decreased. These results indicated that the changes in the medium due to bacterial activity, in the absence of bacteria, did not induce perpetuated pitting.

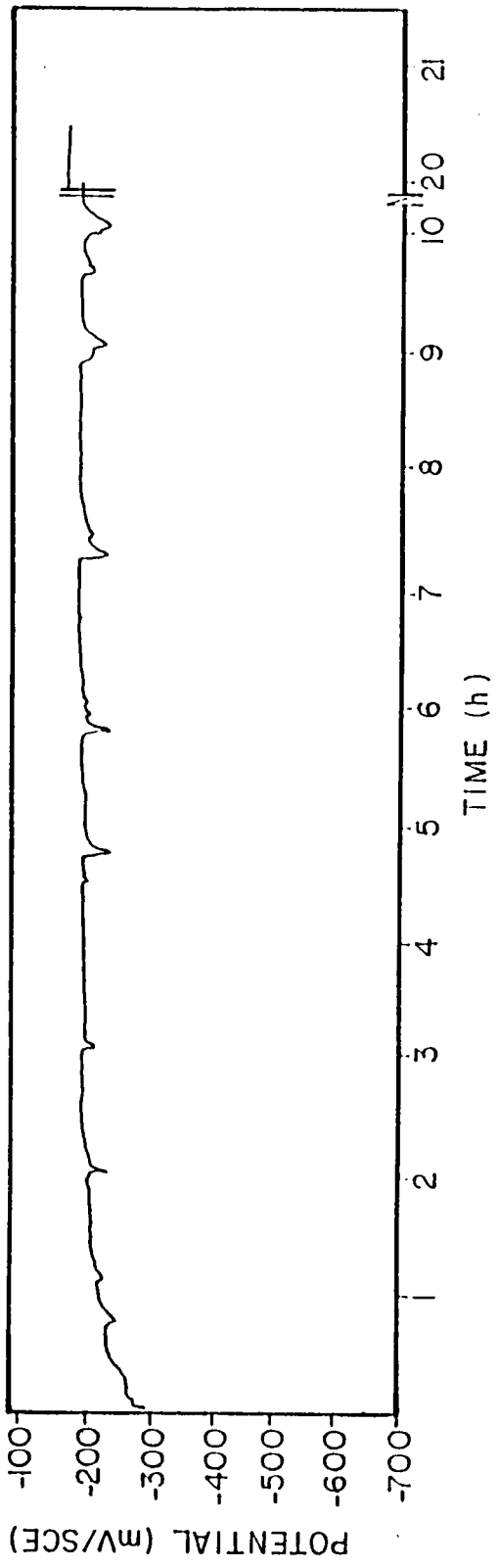

Figure 3. Open circuit potential vs time for carbon steel electrode in spent aerated medium.

DISCUSSION

Pitting of carbon steel in sterile medium. The potential transients in this study were characteristic of pitting corrosion previously discussed (5,7). For the short transients of a few minutes, the changes in potential were dominated by the capacitance of the passive surface. After pits initiated, the OCP dropped, and the capacitance of the passive surface was discharged producing the cathodic current equal to the anodic pitting current. If pits repassivated, then the OCP gradually rose. This rise is mainly associated with recharging of the passive surface. If pits continued to propagate, the OCP continued to drop. The cathodic current equivalent was then supplied by the slow oxygen reduction reaction. When the cathodic oxygen reduction reaction was sufficiently rapid, the rate of potential decrease slowed, and the contribution from capacitance discharge was negligible (7).

The conditions in the sterile medium used in this study favored repassivation following pit initiation. The pit which gave the greatest magnitude of anodic current density, 114$\mu A/cm^2$, formed after approximately 0.5 h., and corresponded to the lowest value of OCP, -300mV/SCE (Fig. 1). When the OCP rose to above -200mV/SCE, no anodic current was observed over the area containing this pit. Smaller pits, with anodic current densities over the pit of less than 20$\mu A/cm^2$ were observed at different sites on the

metal. These pits corresponded to drops in OCP of 20 to 70 mV.

The medium used in this study contained ionic species, as well as buffers, which are necessary for bacterial growth. The medium contained chloride, sulfate, and phosphate ions at concentrations of approximately 1mM, 0.2mM, and 0.2mM, respectively. Air was continuously bubbled through the media. An investigation has been carried out to determine the effect of medium components on the pitting of the steel under sterile conditions. It was shown that the presence of phosphate together with the aeration or stirring of the medium produced repassivation and inhibited propagating pits (Chapter 5).

Pitting of carbon steel in the presence of bacteria. In contrast, the presence or the metabolic activity of aerobic heterotrophic bacteria had a marked effect on the corrosion of the carbon steel in a system containing the same medium. The OCP, rather than rising above -200mV/SCE as in the sterile control, slowly dropped to a value of less than -600mV/SCE. The drop in OCP was not likely due to depletion of oxygen by bacterial respiration, since the medium was continually bubble with air. Bacterial growth was also limited by the supply of glucose, 0.28mM. These conditions should not lead an anaerobic environment. The SVET analysis revealed that the drop in OCP corresponded to continued propagation of an initiated pit. Thus, the

bacteria apparently altered conditions, that normally lead to repassivation of pits. As these bacteria are biofilm producers, these films may act as membranes over areas where pits initiate. The membranes prevent solute losses from the concentrated solution within the pit or diffusion of hydroxyl or inhibiting ions from the surrounding solution.

Effect of spent medium. Since phosphate in the medium has been shown to inhibit corrosion in the sterile medium (Chapter 5), the consumption of phosphate by bacteria may have decreased this inhibition. In order to test this hypothesis, bacteria were first grown then removed from the medium. Pit propagation was still inhibited in this sterile spent medium (Fig. 3). These results suggest that pit propagation observed when bacteria were present was not due to phosphate consumption from the bulk fluid, nor from other changes in the composition of the medium. This conclusion is reasonable with respect to the glucose and phosphate concentrations in the medium. The concentration of glucose and phosphate were approximately the same, 0.28mM glucose 0.2mM phosphate. The amount of glucose assimilated into cellular material is generally at least an order of magnitude greater than phosphate. Thus, with this limited supply of glucose, it is not likely that a high percentage of the phosphate would be utilized.

Polarization resistances. Polarization resistance is inversely related to the corrosion rate, as described by the

Stern-Geary equation, which incorporates the anodic and cathodic contributions to the polarization resistance. The values for R_p presented here are in good agreement with earlier measurements containing this same medium and bacterium (Chapter 1). In the presence of bacteria, R_p ranged from 6000 ohm·cm^2 at the onset of pitting to 1100 ohm·cm^2 after the pit had propagated and spread, while sterile steel had a value of 16,000 ohm·cm^2 when no pitting was apparent by the SVET.

Possible mechanisms of MIC. Organic acid production by anaerobic and facultately anaerobic bacteria has been proposed as a mechanism by which bacteria can increase the corrosion rate of metals (8). In these experiments, the bacteria slightly lowered the pH of the medium, from 7.3 to 6.6. However, by removing the bacteria and testing in the spent medium demonstrated that this lowering of the pH, or other changes, in the bulk medium did not appear to significantly affect pitting with respect to sterile medium. The culture used in this study was a strictly aerobic bacterium, and did not produce detectable levels of volatile organic acids (Chapter 1). In addition, the medium used in this study was continuously aerated, which would prevent anaerobic conditions in the bulk medium, or development of a fermentative metabolism. Although acid production by bacteria in close association with the metal surface could not be excluded, these results suggest that acid production

in the solution is not the major cause for the onset of corrosion facilitation.

Continued pit propagation requires the retention of aggressive ions and a low pH inside the pits (5). The dissolution current acts to increase the concentration of ions inside pits, and hydrolysis of ferrous ions maintains the low pH. In competition diffusion from the pit reduces the concentration. Pit propagation is then a function of the ability to maintain a critical level of aggressive ions inside a pit (5). Previous laboratory studies have demonstrated that the bacteria, used in this study, extensively colonized carbon steel coupons, and produced abundant extracellular polymer material (Chapter 1). Bacterial colonization of the metal may produce membranes that inhibit the diffusion of these aggressive ions from the pits. In addition, bacterial colonization of the surface may inhibit the diffusion of passivating ions, such as phosphate, from reaching the surface of the steel. These conditions could lead to the continued propagation of pits.

LITERATURE CITED

1. Dowling, N.J.E., J. Guzennec, M.L. Lemoine, A. Tunlid, and D.C. White. (1988) Analysis of carbon steels affected by bacteria using electrochemical impedance and direct current techniques. Corrosion **44**:869-874.

2. Dowling, N.J.E., E.E. Stansbury, D.C. White, S.W. Borenstein, and J.C. Danko. (1989) On-line electrochemical monitoring of microbially induced corrosion. in: Microbial Corrosion: 1988 Workshop Proceedings (G.J. Licina, ed.) EPRI R-6345, Research Project 8000-26, Electric Power Research Institute, Palo Alto, Ca. pp 5-1 5-17.

3. Hamilton, W.A. (1985) Sulphate-reducing bacteria and anaerobic corrosion. Ann. Rev. Microbiol. **39**:195-217.

4. Isaacs, H.S. (1988) The measurement of the galvanic corrosion of soldered copper using the scanning vibrating electrode technique. Corrosion Sci. **28**, 547-557.

5. Isaacs, H.S. (1990) Localized breakdown and repair of passive surfaces during pitting. Corrosion Science

6. Isaacs, H.S., and Y. Ishikawa, CORROSION/85, paper no. 55, National Association of Corrosion Engineers, Boston, Ma, (1985).

7. Isaacs, H.S., and Y. Ishikawa. (1985b) Current and potential transients during localized corrosion of stainless steel. J. Electrochem. Soc. **132**:1288-1293.

8. Little, B., P. Wagner, S.M. Gerchakov, M. Walch, and R. Mitchell. (1986) The involvement of a thermophilic bacterium in corrosion processes. Corrosion **42**:533-536.

9. Nivens, D.E., Nichols, P.D., Henson, J.M., Geesey, G.G., and White, D.C. (1986) Reversible acceleration of the corrosion of AISI 304 stainless steel exposed to seawater induced by growth and secretions of the marine bacterium Vibrio natriegens. Corrosion **42**:204-210.

10. Obuekwe, C.O., D.W.S. Westlake, J.A. Plambeck, and F.D. Cook. (1981b) Corrosion fo mild steel in cultures of ferric iron reducing bacterium isolated from crude oil II. Mechanism of anodic depolarization. Corrosion **37**:632-637.

11. Pankhania, I.P. (1988) Hydrogen metabolism in sulphate-reducing bacteria and its role in anaerobic corrosion. Biofouling **1**:27-47.

CHAPTER IX

EFFECT OF BACTERIAL BIOFILMS ON CARBON STEEL PIT PROPAGATION IN PHOSPHATE CONTAINING MEDIUM

ABSTACT

Chemical corrosion inhibitors are commonly added to aqueous systems to minimize the oxidation of steel. The efficiency of certain inhibitors may be reduced by bacteria. In the present study, the effect of microbial biofilms on carbon steel corrosion inhibition by phosphate was analyzed, using the scanning vibrating electrode technique (SVET) and monitoring of open circuit potential. Previous results have shown that carbon steel samples in sterile medium containing 0.2 mM phosphate, with 1.0 mM chloride and 0.2 mM sulfate, showed small anodic pitting sites that subsequently repassivated. Whereas, in the presence of bacteria some pits failed to become inactive and continued to propagate. In the present study, comparisons between viable bacteria and formaldehyde fixed bacteria on the pit propagation was analyzed. The results indicated that biofilms containing viable bacteria or containing fixed bacteria could cause pits to propagate. The time required for pit propagation was dependent on the concentration of bacteria as well as the viability of the bacteria. The results indicate that bacterial biofilms enabled pits, initiated by chemical corrosion, to continue to propagate either by reducing the efficacy of phosphate as a corrosion inhibitor or by maintaining the aggressive environment within pits.

INTRODUCTION

The scanning vibrating electrode technique (SVET), used for current density mapping over corroding metal surfaces, has been useful in understanding mechanisms of localized corrosion (2,3,4,5,6). This technique has recently been applied to the study of microbial influenced corrosion of carbon steel (Chapters 4,6). In a stirred sterile microbiological medium containing 1 mM chloride, 0.2 mM sulfate, and 0.2 mM phosphate, as well as a number of trace minerals, the carbon steel electrodes had high impedances and remained shiny for as many as nine days of exposure (Chapter 1), due to the corrosion inhibition by the phosphate (Chapter 5). However, analysis by the SVET revealed that carbon steel in this medium was not passive throughout the exposure. In fact, the samples showed small active anodic sites which subsequently became inactive (Chapter 5). In the presence of active bacteria, propagation of pits was favored over this pit repassivation (Chapter 6). The physical presence of bacteria was required for the pits to propagate, since spent microbial medium did not result in pit propagation. From those results we proposed that the microbial biofilm prevented active pits formed by chemical corrosion from repassivating (Chapter 6).

Pit propagation is dependent on the ability to maintain aggressive ions inside the pit (4). The dissolution current results in an increased concentration of ions, including

chloride ions, inside a pit, and the hydrolysis of ferrous ions results in localized lowering of the pH. Diffusion or convection decreases the concentration of aggressive ions in pits (4). Microbial biofilm formed on metal surfaces may act as a membrane which either reduces the flow of aggressive ions by diffusion or convection from the pits, or impedes the migration of inhibiting agent, in this case phosphate, from coming in contact with the metal. This mechanism is supported by the observation that in this same sterile medium, which was not stirred pits propagated rather than repassivated (Chapter 5).

Many bacteria produce extracellular polymer which acts to bind the bacteria to surface. Geesey et al. (1) have demonstrated copper dissolution in the presence of bacterial exopolymer. Nivens et al. (8) have shown a correlation between corrosion rate and bacterial exopolymer production on stainless steel. However, in unpublished work, we found, by FT-IR analysis, that most of the extracellular polymer remains associated with the killed bacteria. Therefore, in the present study, the "bacterial membrane" hypothesis was tested by exposing the carbon steel to formaldehyde fixed bacteria rather than isolated exopolymer. The scanning vibrating electrode technique (SVET) and open circuit potential (OCP) monitoring were used as indicators of pit propagation in the presence of viable and formaldehyde fixed bacteria.

MATERIALS AND METHODS

Bacteria and media. The same bacteria used in this study were used in a previous study of pit propagation (Chapter 1,4,6). The bacteria were grown in a medium containing basal salts (in mg/l, NH_4Cl, 50; $MgSO_4 \cdot 7H_2O$, 50; $CaCl_2 \cdot H_2O$, 5; KH_2PO_4, 27) 1 ml/l trace mineral solution (ref. 7), 1 g/L glucose, and 0.5 g/L MOPS buffer, to an optical density of 0.2 at 660 nm.

The bacteria to be used in the formaldehyde fixed experiments were fixed by the addition of formaldehyde at a final concentration of 4% for 0.5 hour. The formaldehyde and the spent bacterial growth medium were removed by centrifuging the bacteria and pouring off the supernatant. The cell pellet was then resuspended in the fresh medium, defined above, with the glucose and the MOPS concentrations reduced to 50 mg/l. The cells were centrifuged and resuspended three times in this fresh medium to remove the remaining formaldehyde. The viable bacteria were also washed three times and resuspended in the fresh medium. The final concentration of bacteria was adjusted in the fresh medium to yield an optical density of 0.03 or 0.2 at 660 nm, approximately 2×10^7 and 2×10^8 cells/ml as determined by acridine orange direct counting, respectively. The bacterial solution or sterile medium, 500 ml, was then added to flasks containing carbon steel electrodes and salt bridges connected to saturated calomel electrodes. Carbon

steel coupons with electrical leads soldered to the backs of the coupons were epoxy embedded. After abrasion down to a 600 grit finish, the edge between the metal and the epoxy was painted with a lacquer coating. The area of the exposed coupons was 1.5 cm^2. In some experiments, the carbon steel electrodes were exposed to sterile medium prior to exposure to bacteria. In those experiments, the bacteria were concentrated to an O.D. of 0.8 and enough of this suspension was added to flasks containing sterile medium to yield final optical densities of 0.03 or 0.2. Sterile medium was also added to the sterile controls to adjust the volumes.

Open circuit potential. The open circuit potential was monitored over time using a Solatron digital multimeter. The multimeter was connected to a Kiethly scanner and a computer data acquisition unit, so that measurements of several different electrodes could be made simultaneously. Readings were taken every 0.5 hour and stored in a Lotus 123 spreadsheet.

Current density mapping. Current density maps were obtained using a scanning vibrating electrode as described previously (4). The vibrating electrode is an insulated platinum wire which is positioned 100 μm over the surface of the metal. The electrode is attached to a piezoelectric reed which vibrates the electrode when an AC signal is applied to the reed. In these studies, the vibration frequency was 154 Hz. The vibration of the electrode

converts the potential fields in solution over the steel to an alternating signal. An E.G.and G. model 5210 lock-in amplifier was used to measure the alternating signal and to filter out signal not associated with the frequency of vibration. The scanning was performed with a fixed vibrating electrode position and moving the sample using stepper motors in 200 μm increments. Both the lock-in amplifier and the stepper motors were controlled by and data was acquired using a computer data acquisition unit programmed in ASYST language. The coupons were masked by pressure sensitive tape. The edge of the tap and the metal was coated with a lacquer coating to help prevent crevice corrosion. Thirty mm^2 ofthe carbon steel was exposed to solution.

Acridine orange direct counts. At the end of the OCP experiments, the metal samples were removed, and an O-ring extractor was clamped onto the sample (9). Basal salts, 500 μl, was added to the extractor, and the samples were sonicated for five seconds. The cells removed from the surface by sonication were added to 10 ml of basal salts. The sonication procedure was repeated twice. The cells were then serially diluted in basal salts, filtered using Nucleopore filters, stained with acridine orange, and counted using epiflourescence microscopy.

RESULTS

Current density mapping. Figure 1 shows the current density maps obtained by SVET analysis for a sample expose to sterile medium, followed by addition of formaldehyde fixed cells, O.D. 0.2 after 17 h. Figures 1 A,B,C show the current density maps for the carbon steel exposed to sterile medium over 16 hours. The positive Z-axis represents anodic current densities, whereas the negative Z-axis represents cathodic current densities. Note that the magnitude of the Z-axis scale is increased ten-fold in the last four frames. Figure 1A shows two small active sites adjacent to the lacquer coating after 3 hours of exposure to the sterile medium. After 4 hours of exposure (Fig. 1B), one of the active sites increased in magnitude and two additional anodic sites were observed. Figure 1C shows the same sample after 16 hours. The two active sites which were present after three hours became inactive, and three additional sites formed. The OCP of the sample was monitored during these experiments. The OCP showed potential fluctuation, due to the formation and repassivation of active anodic sites (6).

After 17 hours the medium was removed and replaced by medium containing formaldehyde fixed bacteria (0.2 O.D.). At 21 hours, it was observed that two of the active sites seen in Fig. 1C remained active and increased in magnitude. Those sites remained active until 30 hours (Fig. 1E,F), when

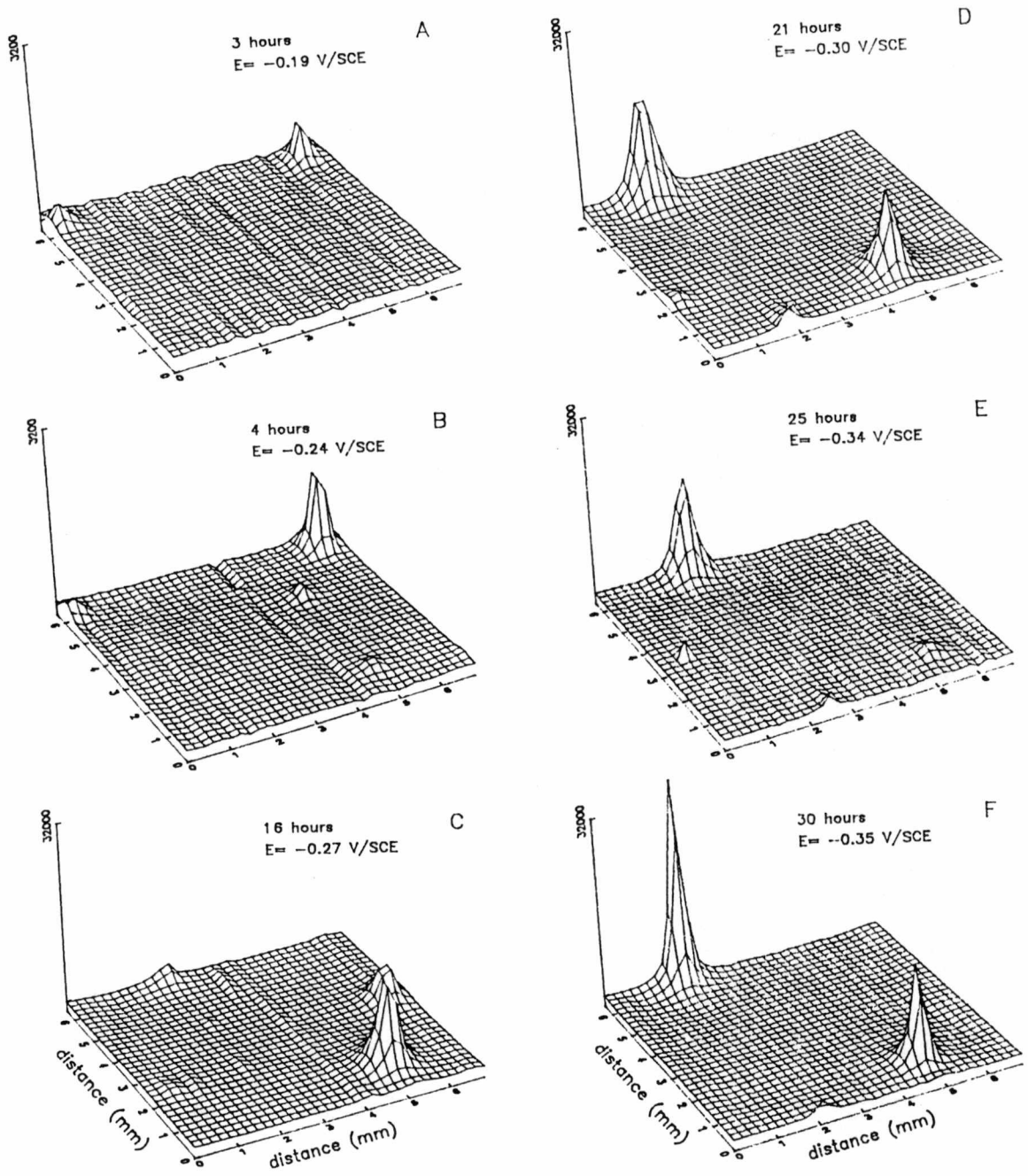

Figure 1. Current density maps over carbon steel sample exposed to sterile medium (Fig. 2A,B,C), then exposed to approximately 10^8 formaldehyde fixed bacteria/ml (0.2 O.D.) (Fig. 2D,E,F).

the experiment was terminated. The OCP showed a steady drop during the remainder of the experiment, as the magnitude of the local anodic sites increased.

Effect of bacteria on carbon steel. In this study (Fig. 1) as well as with other studies using the SVET, correlation between pit propagation and a steady drop in OCP has been observed (4,6, Chapter 5,6). The drop in OCP was used to indicate irreversible pit propagation in the presence of bacteria, under several different conditions. Figure 2A compares the effect of bacteria under growing conditions at different concentrations with sterile control. The potential of the steel in the sterile flask remained high compared to the steel exposed to bacteria. Fluctuations in potential, characteristic of pitting and repassivation (6), were also observed. The potential of the steel exposed to bacteria initially was lower than that of the sterile control, and the potential gradually rose to -200 mV/SCE. After 12 hours in the solution containing the higher concentration of bacteria and 22 hours in the solution containing the lower concentration of bacteria, the potential gradually dropped to -600 mV/SCE. Loosely adhered orange corrosion products were observed on the steel samples exposed to bacteria. Virtually identical results were obtained upon replication of this experiment.

Figure 2B shows the effect of formaldehyde fixed bacteria on the OCP of the steel. The potential of the

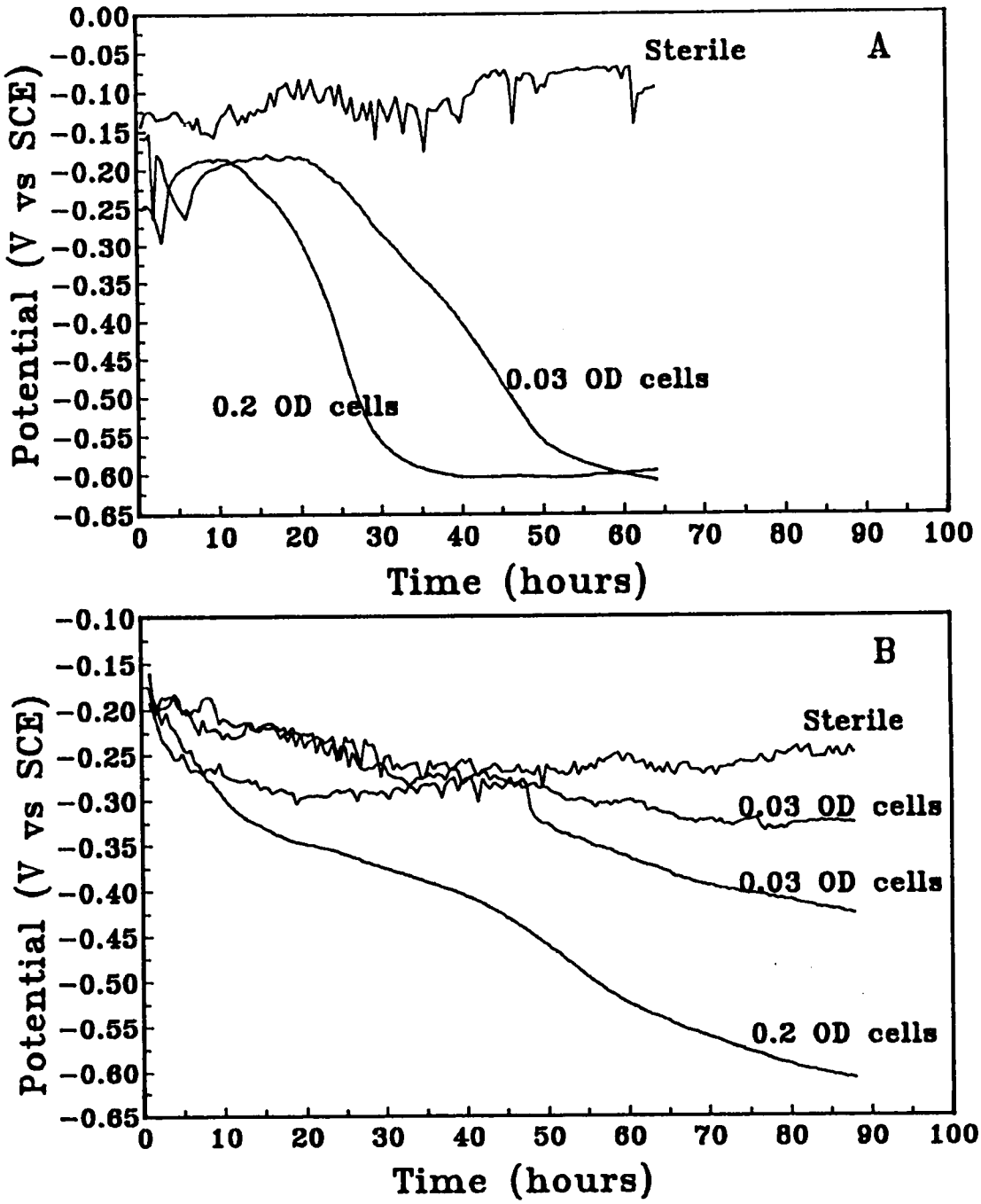

Figure 2. Carbon steel open circuit potential exposed to bacteria without prior exposure to sterile medium. A) OCP of steel exposed to viable bacteria at the optical density indicated. B) OCP of steel exposed to formaldehyde fixed bacteria, at the optical density indicated.

sterile control remains high and fluctuations in potential were observed. The potential for one of the samples exposed to 0.03 O.D. cells is similar to the sterile control for the first 50 hours. Following this time the potential gradually dropped. The other sample exposed to 0.03 O.D. cells also showed a gradual decrease in OCP after 50 hours. The samples exposed to higher concentrations of fixed bacteria showed a more rapid drop in OCP to a final value of -600 mV/SCE at 90 hours. After 90 hours of exposure, 0.1 ml of solution was removed from the flask and plated on agar medium containing glucose, yeast extract, and peptone, 100 mg each per liter of basal salts, to check for viable bacteria and contamination. No growth was observed on the agar medium after one week of incubation.

After termination of the experiments shown in Fig. 2, the number of bacteria associated with the electrode surfaces and with the corrosion products was determined (Table 1, for Fig. 2). The numbers of cells associated with the surface in the flasks containing viable bacteria at 0.03 O.D. was greater than 10^8 cells/cm^2 and was three to 16 times greater than the number of surface associated bacteria in the formaldehyde fixed flasks. The numbers of surface associated bacteria in the 0.2 O.D. flasks were similar for the viable and formaldehyde fixed bacteria, at approximately 10^9 cells/cm^2.

Table 1
Numbers of surface associated cells

Samples from Figure 3

Treatment	cell concentration[a]	AODC range[b]
viable	0.03	1.7(±0.8) - 6.7(±3.2)
formaldehyde fixed	0.03	0.4(±0.1) - 0.5(±0.3)
viable	0.2	15 (±6.2) - 27 (±6.4)
formaldehyde fixed	0.2	12 (±3.7) - 12 (±6.6)

Samples from Figure 4

Treatment	cell concentration	AODC range
viable	0.03	9.2(±3.2) - 16 (±8.3)
formaldehyde fixed	0.03	1.0(±0.4) - 1.6(±0.5)
viable	0.2	26 (±6.5) - 29 (±6.7)
formaldehyde fixed	0.2	8.5(±3.0) - 19 (±7.3)

[a] cell density at 660 nm at the begining of the experiment.
[b] Acridine orange direct counts (AODC) times 10^8 cells/cm^2. The range is for two samples.
The values represent the means and standard deviations for 10 fields counted.

Effect of bacteria on pretreated carbon steel. Figure 3 shows the effect of viable and formaldehyde fixed bacteria on carbon steel samples preexposed to sterile medium. Figure 3A shows the effect of viable bacteria at different concentrations on the carbon steel OCP. Prior to the addition of bacteria, the OCP is high and shows fluctuations, due to pitting and repassivation. Following the addition of bacteria the potential drops percipitously to -650 mV/SCE in the 0.2 O.D. flask and to -250 mV/SCE in the 0.03 O.D. flask. These drops may be due to the consumption of oxygen by the bacteria, since these drops were not observed in the steel exposed to formaldehyde fixed bacteria (Fig. 3B). After this initial rapid drop in potential, the potential rose to and remained at about -200 mV/SCE for several hours, then showed a more gradual decline, apparently due to the propagation of anodic sites. The steel exposed to formaldehyde fixed bacteria also shows a high potential prior to addition of bacteria, and a slower drop in potential. These experiments were also duplicated, and similar results were obtained for each sample. At the end of this experiment the number of surface associated bacteria were enumerated by AODC (Table 1). The steel surfaces exposed to 0.03 viable bacteria was approximately 10^9 cells/cm^2, this value was an order of magnitude greater than the steel exposed to fixed bacteria. The steel exposed

to 0.2 O.D. viable bacteria was $2x10^9$ cells/cm^2, and was slightly greater than the 0.2 O.D. fixed bacteria.

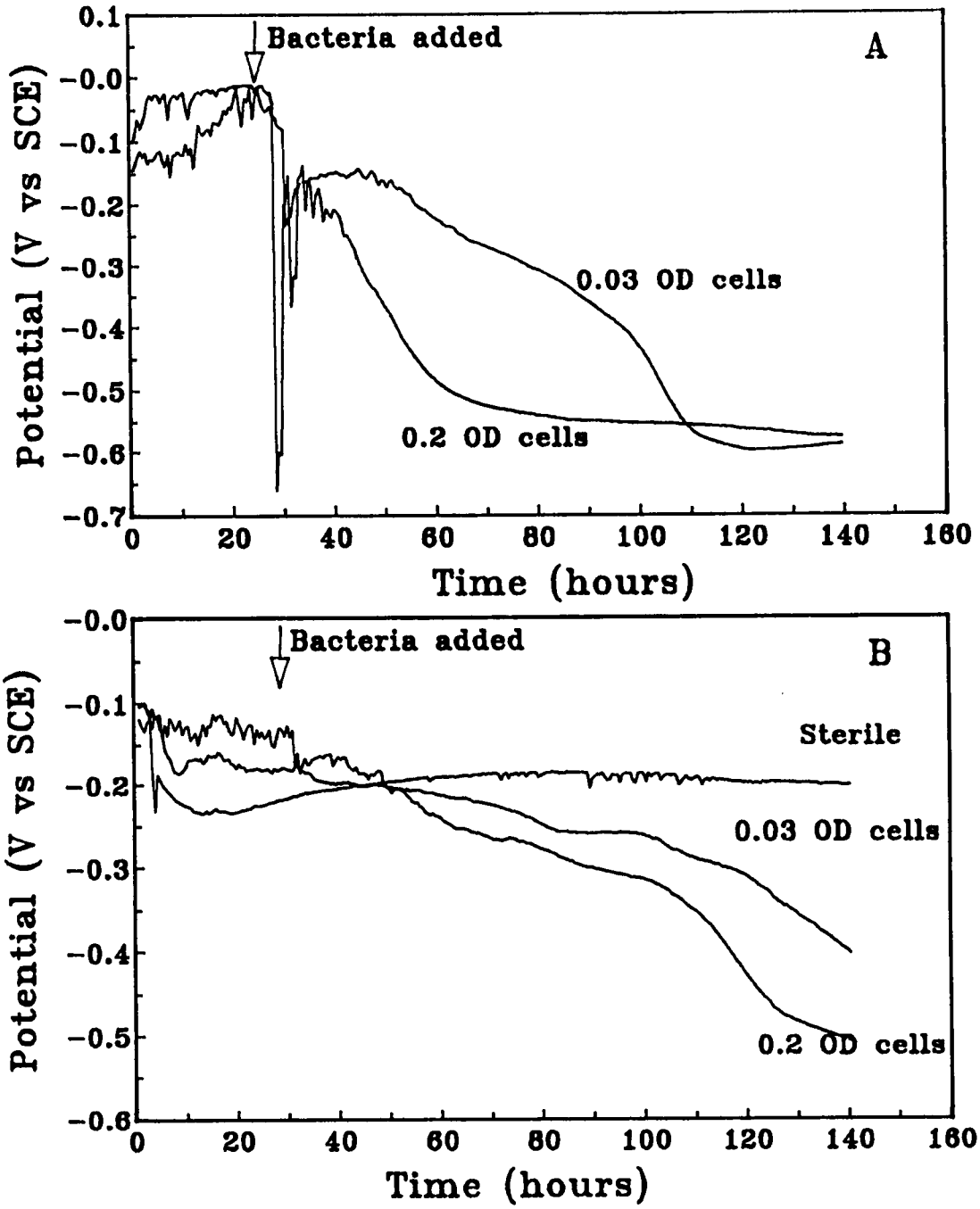

Figure 3. Open circuit potential of carbon steel exposed to sterile medium, followed by exposure to bacteria. A) OCP of steel exposed to viable bacteria. B) OCP of steel exposed to formaldehyde fixed bacteria.

DISCUSSION

The "bacterial membrane" hypothesis proposed here, assumes that the fixed bacteria can adhere to the surface of the metal to form a film. The bacteria used in this study were originally isolated from a biofilm associated with a steel pipe tubercle. AODC values showed that high numbers of fixed bacteria (although not as high as experiments with viable bacteria) were found in association with the metal surface and the corrosion products (Table 1). In addition to the bacteria, the bacterial extracellular polymer likely adds to the formation of the film (Chapter 1).

SVET analyses in Fig. 1A-C show that when the steel was exposed to sterile medium small pits initiated and subsequently became inactive. However, following the addition of a high concentration of fixed bacteria the pits did not passivate and corrosion was established. After the fixed bacteria were added, two of the initiated pits failed to repassivate, and continued to propagate, as shown in Fig. 1D-F. These SVET results are in agreement with previously reported data on the effect of bacteria on carbon steel (Chapter 6). The establishment of stable corrosion shown by SVET has been correlated with a steady drop in the OCP in a number of studies (4,6, Chapter 5,6). Therefore, in the remaining experiments, large and continuous drops in OCP were taken to represent the establishment of stable pit propagation.

The effect of viable and fixed bacteria on carbon steel corrosion, without prior exposure to any solution, was investigated. Cell concentration giving an 0.03 O.D. was chosen because that was the final optical density bacteria used in the previous SVET study of carbon steel corrosion exposed to bacteria (7). As in Fig. 2, exposure to the formaldehyde fixed bacteria, produced continuous propagation of local anodic sites, and the potential dropped. Fixed cells at 0.03 O.D. showed pit propagation after 50 hours of exposure. Experiments were also performed with cells at 0.003 O.D. to see if lower concentrations of bacteria also gave corrosion. The results of those experiments were similar to the sterile control (data not shown). Few bacteria were attached to the surface in the 0.003 O.D. solution. These results suggest that a minimum number of cells are required to form a film and cause pit propagation. In addition, the time required for pit propagation is dependent on the concentration of cells.

The results with viable bacteria (Fig. 2B) showed the same characteristics as previously reported results (Chapter 6). The bacteria produced pit propagation with the time required for propagation being dependent on the concentration of bacteria. It is interesting to note that the viable bacteria caused pits to propagate more rapidly than the fixed bacteria (Fig. 2). This indicates that 1) the viable bacteria produced a film more rapidly than the

fixed bacteria or 2) bacterial metabolic activity, either synthesis of addition cellular or extracellular material or some other metabolic activity contribute to pit propagation. In order to test these hypotheses, the effect of localized metabolic activity on the localized corrosion of steel is being tested (Chapter 8).

The effect of prior exposure to the sterile inhibiting medium, showed similar results to the steel exposed immediately to bacteria. Prior to exposure to bacteria, the potential fluctuations indicated pitting and repassivation (6). Following exposure to bacteria the potential dropped as pits propagated. Again the time required for pit propagation was dependent on the cell concentration, and also on the viability of the bacteria, as viable bacteria resulted in more rapid pit propagation than fixed bacteria. At the end of the experiment, high concentrations of bacteria were found associated with the surface and/or the corrosion products of the steel, indicating that films of bacteria did form on the metal in both the viable bacteria and the fixed bacteria experiments.

The results of this study indicate that bacteria, whether viable or fixed and bacterial exopolymer can form films on the surface of carbon steel and prevent initiated pits from repassivating. The propagation of pits is presumably due to the formation of a biofilm, which helps maintain an aggressive environment within the pits or

inhibits the flow of inhibiting ions coming into contact with the surface. The results also demonstrate that viable bacteria result in a faster rate of pit propagation, suggesting that additional mechanisms involving microbial metabolic activity may be participating in pit propagation.

LITERATURE CITED

1. Geesey, G.G., M.W. Mittelman, T. Iwaoka, P.R. Griffiths. (1986) Role of bacterial exopolymers in the deterioration of metallic copper surfaces. Materials Performance **25**:37-40.

2. Isaacs, H.S., (1987) The use of the scanning vibrating electrode technique for detecting defects in ion vapor-deposited aluminum on steel. Corrosion **43**:594-598.

3. Isaacs, H.S., (1988) The measurement of the galvanic corrosion of soldered copper using the scanning vibrating electrode technique. Corrosion Sci. **28**:547-557.

4. Isaacs, H.S., (1990) The pitting of iron in dilute chloride and sulfate solutions. Advances in Localized Corrosion, eds. H.S. Isaacs, V. Bertocci, J. Kruger, and Z. Szklarska-Smialowska. NACE.

5. Isaacs, H.S., and Y. Ishikawa. (1985) CORROSION/85, paper no. 55, National Association of Corrosion Engineers, Boston, Ma.

6. Isaacs, H.S., and Y. Ishikawa. (1985) Current and potential transients during localized corrosion of stainless steel. J. Electrochem. Soc. **132**:1288-1293.

7. Nichols, P.D., J.M. Henson, J.B. Guckert, D.E. Nivens, and D.C.White. (1985) Fourier transform-infrared spectroscopic methods for microbial ecology: analysis of bacteria, and bacteria-polymer mixtures adn biofilms. J. Microbiol. Methods **4**:79-94.

8. Nivens, D.E., P.D. Nichols, J.M. Henson, G.G. Geesey, and D.C. White. (1986) Reversible acceleration of the corrosion of AISI 304 stainless steel exposed to seawater induced by growth and secretions of the marine bacterium Vibrio natriegens. Corrosion **42**:204-210.

9. Nivens, D.E., J.B. Guckert, K. Kroeger, J.Q. Chambers, and D.C. White. Microbial biofilm isolation device for off-line analysis. J. Microbiol. Methods, submitted.

CHAPTER X

SPATIAL AND TEMPORAL RELATIONSHIPS BETWEEN LOCALIZED MICROBIAL METABOLIC ACTIVITY AND ELECTROCHEMICAL ACTIVITY OF STEEL

ABSTRACT

The relationship between the localized microbial and electrochemical activities on corroding steel surfaces was investigated. The scanning vibrating electrode technique provided a sensitive means for defining local anodic and cathodic currents associated with corrosion. Localized bacterial metabolic activity was determined using autoradiography of bacterial incorporated ^{14}C-acetate into insoluble cell material. Microautoradiography of individual bacteria, with the incorporated acetate, was used to determine percentages and morphological types of active bacteria. The results showed a correlation between the location of anodic activity of the steel and the location of incorporated label. Although the results do not necessarily indicate a role for bacterial activity in the initiation of pitting, the results suggest that the actively metabolizing bacteria may exacerbate the propagation of pits by colonizing active anodic sites.

INTRODUCTION

Much of the microbial influenced corrosion (MIC), both from field observations and from laboratory investigations is localized. Bacteria tend to colonize surfaces in a nonuniform manner as microcolonies (13). The metabolic activities of heterogeneously colonized bacterial biofilms on steel surfaces can result in differences in aeration or catalytic activity of the steel surface, leading to localized attack. In order to gain a better understanding of microbial influenced corrosion, and to develop rational countermeasures, studies contrasting localized microbial activity and localized corrosion of steels must be performed. One difficulty in the study has been the difficulty in resolving and in correlating events in time and space. Most electrochemical polarization techniques provide average information for the whole electrode. Also, techniques for studying microbial activities in complex environments often only provide a mean value for relatively large samples.

Scanning microelectrode techniques have been used to map potential fields over corroding or polarized metal surfaces (8). These techniques have provided useful information of localized electrochemical activities. A scanning vibrating electrode technique (SVET) was used to map potential fields over metal samples (3,4,5,6,7). The vibrating electrode technique converts the potential fields

to AC signals. Using a lock-in amplifier all frequencies not associated with the frequency of vibration can be filtered, greatly reducing the noise inherent in the microelectrode techniques. The SVET has recently been applied to the study of MIC (Chapters 4,6,7), and has shown that bacteria can assist in the propagation of pitting corrosion.

Techniques for studying microbial activity at localized sites are also being developed. Mittelman and White (12) have used autoradiography after bacterial incorporation of radiolabelled metabolic precursors to study activity of bacteria in differential fluid shear environments. In addition microautoradiographic techniques have been used to examine the activity of individual bacteria within complex communities (10,15).

In this work, the techniques for studying localized microbial metabolic activity were combined with the SVET to determine the relationship between microbial metabolic activity and electrochemical activity. The objectives of this work were 1) to determine if nonuniform microbial metabolic activity on steel samples during colonization could be resolved, 2) to determine the percentages and morphological types of the metabolically active bacteria, and 3) to determine the relationship between the microbial metabolic activity to the anodic or cathodic activity of corroding steel samples.

MATERIALS AND METHODS

Bacteria and media. The bacteria used in this study were the same as those used in previous studies of MIC (14, Chapters 1,2). They have been identified as a strictly aerobic Pseudomonas sp., a facultative aerobe Hafnia sp., and the sulfate reducing bacterium Desulfovibrio gigas. The Desulfovibrio gigas was cultivated on API sulfate reducer medium. The medium used for cultivation of the Pseudomonas sp. the Hafnia sp. and for the experiments contained basal salts (in mg/l NH_4Cl, 50; $MgSO_4 \cdot 7H_2O$, 50; $CaCl_2 \cdot 2H_2O$, 5; KH_2PO_4, 27; pH=7.2), 1ml/l mineral solution (10), and 50 mg/l each of glucose, yeast extract, peptone, and sodium lactate.

During experiments, the medium continuously flowed into a 500 ml flask at a rate of 0.1 h^{-1}. The flasks for the study of microbial activity of sessile bacteria in a continuous flow system were described previously 2). Epoxy embedded coupons, of 304 stainless steel and of C1020 carbon steel, abraded with 600 grit emery paper, were suspended in different flasks. The samples were removed aseptically over time.

Bacterial activity. After removal of the coupons from the flowing system, tubes with O-ring seals were clamped onto the coupons (14). Basal salts solution, 400 μl, containing 2.5 μCi ^{14}C-acetate was added to the tubes. The sessile bacteria on the coupons were incubated with this

^{14}C-acetate solution for 30 min. After the 30 min incubation, the bacteria were killed with 2% glutaraldehyde in a 0.1 M cacodylate buffer. The killed control samples were treated in the same way, with the exception that the biofilms were killed with the 500 μl glutaraldehyde solution for 15 min prior to exposure to the ^{14}C-acetate. Any unincorporated ^{14}C-acetate was removed by exchanging the solution five times with the glutaraldehyde solution. The samples were then dehydrated by increasing concentrations of acetone (50%, 75%, 100%, 100%). A 100 μl aliquot of the final acetone wash was placed in scintillation cocktail and counted using a scintillation counter to determine if unincorporated ^{14}C-acetate or labelled nonadhered bacterial cells remained in the solution. The samples were then air dried. A similar procedure was used in electron microscopy to maintain the spatial integrity of the samples (2). The samples were then exposed to X-ray film for seven days.

The sample preparation procedure for determining the activity of individual sessile bacteria was similar to the procedure described above. Steel samples were removed from the flasks and O-ring tubes were clamped onto the samples. Basal salts solution, 500 μl, containing 2.5 μCi of ^{14}C-acetate was added to the tubes. The bacteria were incubated with this solution for 30 min., then killed with the glutaraldehyde solution, described above. The glutaraldehyde solution was removed from the tubes and

replaced with 500 μl of basal salts. The sessile bacteria on the steel surface were removed from the surface by sonication for 5 sec. The bacteria removed from the surface were placed in 9.5 ml of basal salts solution. This sonication procedure was repeated twice. The basal salts solution containing the labelled bacteria was serially diluted in basal salts to obtain an appropriate concentration of cells for microscopic enumeration.

The bacteria were filtered with 0.2 μm average pore size membrane filters. The technique for microautoradiography has been extensively described (15). Briefly, microscope slides were dipped into photographic emulsion (Kodak NBT-2) diluted 2 to 1 with distilled water. The filters were placed on the emulsion, and allowed to incubate for seven days in the dark at a temperature of 4°C. The slides were then developed using Dectol developer. The bacteria were stained with acridine orange in a citrate buffer (pH 6.6). Destaining of the slides was done in citrate buffers of decreasing pH (6.6, 5.0, 5.0, 4.0,4.0, ten min each). The filters were removed from the slides and the bacteria remained immobilized in the photographic emulsion (15). Developed silver grains around the fluorescing bacterial cells were indicative of incorporation of the ^{14}C acetate.

Scanning vibrating electrode technique. The scanning vibrating electrode technique was used to obtain potential field maps as described previously (Chapter 7).

The samples for the SVET analysis were carbon steel coupons. A small area of the coupon, approximately 135 mm^2, was exposed to solution, by masking most of the coupon with thin pressure sensitive tape. The edge of the tap and the metal was coated with a lacquer coating, to help prevent crevice corrosion.

RESULTS

Bacterial activity on stainless steel. The autoradiograms in Figure 1 show the localization of bacterial activity associated with the 304 stainless steel sample. After six hours of exposure, little activity of bacteria was seen associated with the stainless steel samples (not shown). Little activity is seen associated with the killed controls, showing that the radiation from the sample is not due to unincorporated acetate. This can be see from Figure 1A and 1B where there is little activity of the glutaraldehyde fixed controls after three and four days. Figures 1C and 1D show the activity of the bacteria on the stainless steel after two and three days of exposure, respectively. Figure 1C shows that the activity of the bacteria was greater on parts of the sample than on other areas after two days of exposure. This nonuniform microbial activity could result in differential aeration of the sample. After three days of exposure the activity of the bacteria on the surface is relatively uniform over the surface of the sample.

Activity of individual bacteria. Figure 2A shows the activity of individual bacteria removed from the surface after two days of exposure, and Figure 2B shows the killed control. Developed silver grains can be seen in association with the bacteria, indicating uptake of the ^{14}C-acetate. No silver grains can be seen associated with the glutaraldehyde

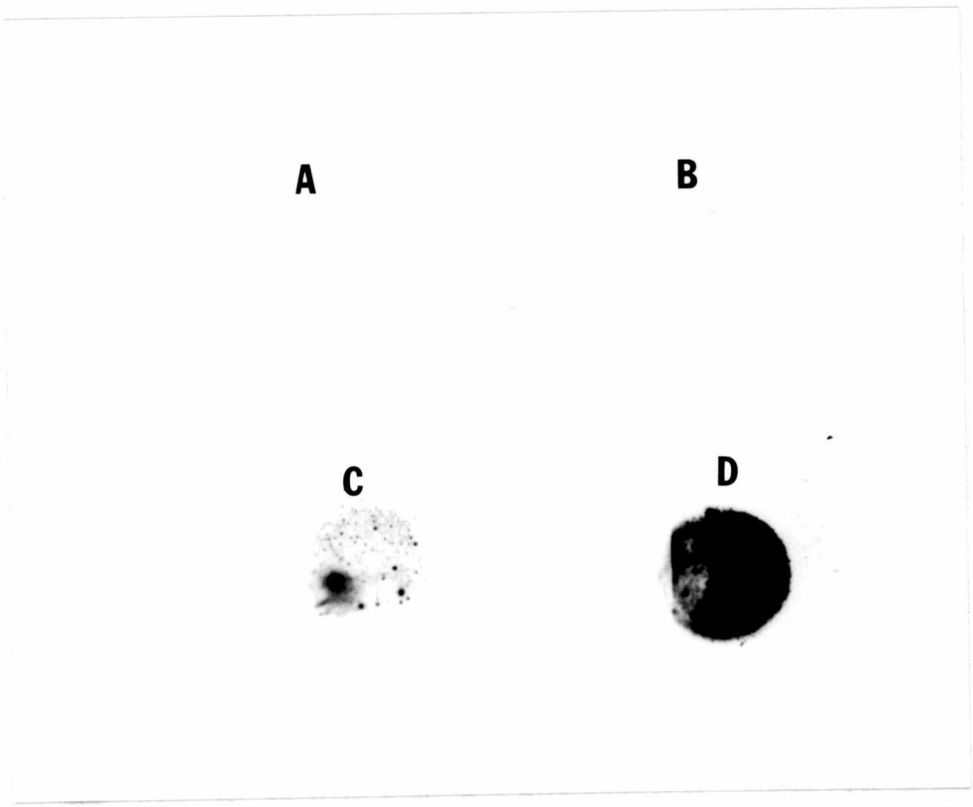

Figure 1. Autoradiograms of 304 stainless steel samples exposed to bacteria in a flowing system then incubated for 30 min with 2.5 μCi ^{14}C-acetate. A) Sample exposed to bacteria for 2 days then killed prior to exposure to acetate. B) Same as 2A but exposed to bacteria for 3 days. C and D) ^{14}C-acetate incorporation activity of bacteria exposed to flowing system for two and three days, respectively.

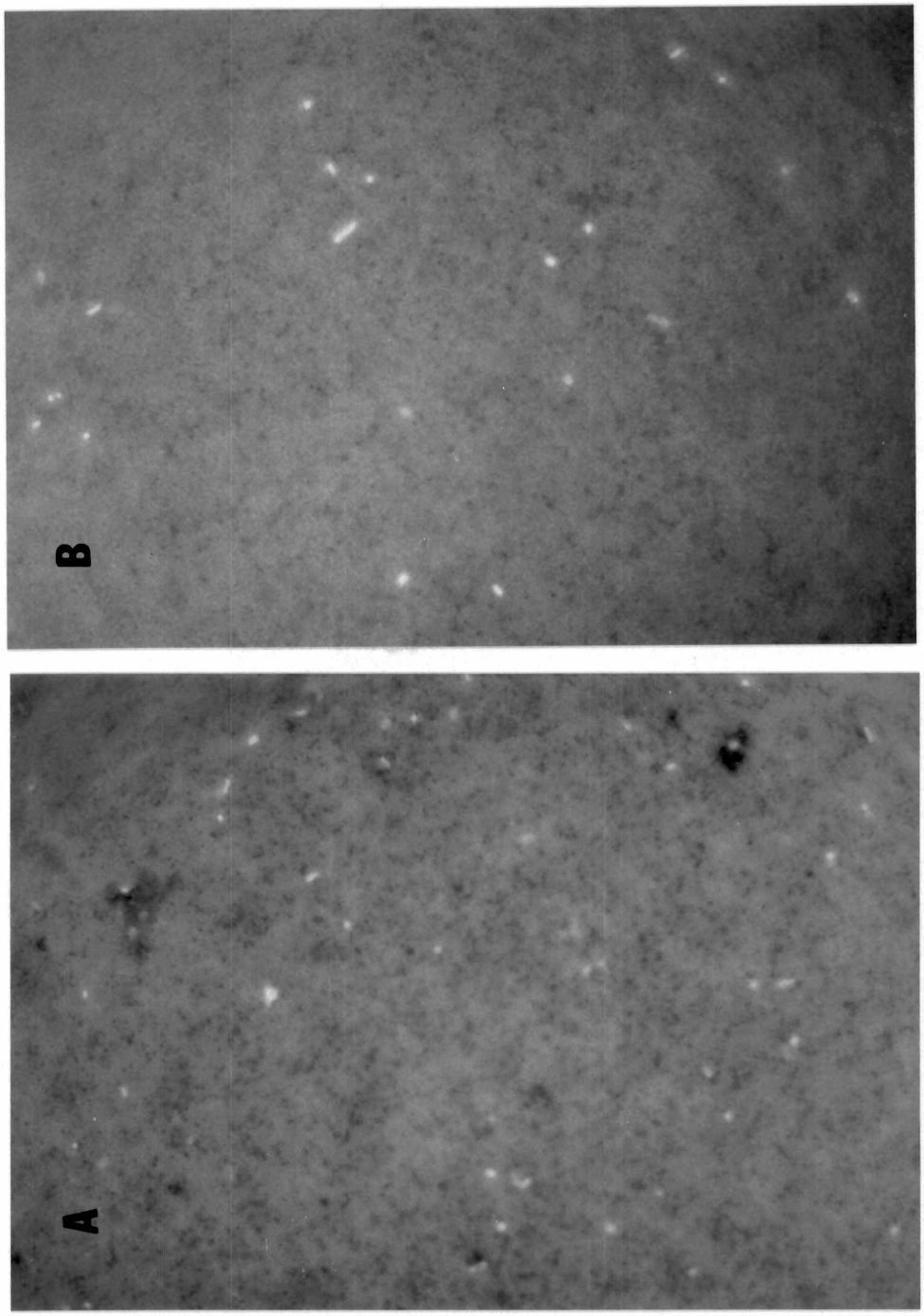

Figure 2. Autoradiograms of sessile bacteria after exposure to flowing system for two days. A) Bacteria exposed to 2.5 μCi ^{14}C-acetate for 30 min. B) Bacteria killed with glutaraldehyde prior to exposure to ^{14}C-acetate.

fixed bacteria, suggesting that the ^{14}C-acetate is incorporated into cellular material and not adsorbed onto the bacteria. The incorporation of ^{14}C-acetate is not uniform for all the bacteria in the biofilm, and not all bacteria show incorporation. This indicates that the 30 min incubation time may be insufficient for the diffusion of the acetate to all levels of the biofilm, or that bacteria within the biofilm have varying growth rates. In addition, the smaller aerobic bacteria were labelled preferentially over the larger Desulfovibrio. This preferential labeling does not indicate that the aerobic bacteria are more active in the biofilm, but only that they are more capable of incorporating the acetate under the experimental conditions used. The number of surface bound bacteria and the number of bacteria with associated silver grains are shown in Table 1.

Bacterial activity on carbon steel samples. The distribution of bacteria with incorporated ^{14}C-acetate on the carbon steel surfaces is shown in Figure 3. Little silver development was observed for the glutaraldehyde fixed controls (Figure 3A,B,C,D). In some experiments using longer times of exposure to the X-ray film, some development of silver grains was observed for the killed controls, suggesting that some unincorporated label was associated with either the metal or adsorbed to the bacteria. In future experiments, unlabelled acetate will be added to the

Table 1
Numbers of bacteria and active bacteria on metal surfaces

Steel	Time	Total cells[a]	Active cells	Total cells (killed control)
304	6 hours	0.4 ± 0.2	0.2 ± 0.1	0.6 ± 0.3
C1020	6 hours	1.4 ± 0.4	0.4 ± 0.1	1.0 ± 0.4
304	2 days	5.7 ± 1.9	1.9 ± 0.8	4.8 ± 2.2
C1020	2 days	10 ± 3.0	3.6 ± 1.0	7.3 ± 3.1
304	3 days	25 ± 5.0	10 ± 2.0	ND[b]
C1020	3 days	22 ± 4.0	10 ± 3.0	5.0 ± 3.2

[a] All cell numbers are times 10^6 cells/cm^2.
[b] Not done.

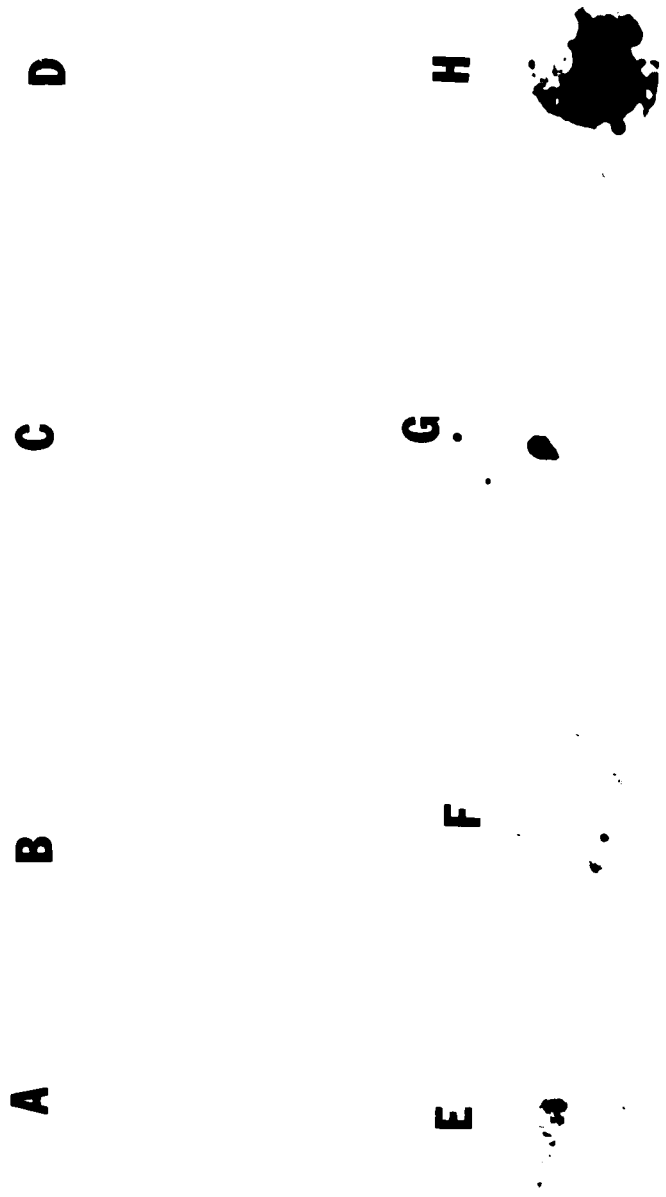

Figure 3. Autoradiograms of C1020 carbon steel samples exposed to bacteria in a flowing system, then incubated for 30 min with 2.5 μCi ^{14}C-acetate for 30 min. A,B,C,D) Killed controls after exposure to the flowing system for six hours, one day, two days, and three days, respectively. E,F,G,H) Samples exposed to ^{14}C-acetate after exposure to the flowing system for six hours, one day, two days, three days, respectively.

glutaraldehyde solution to help remove the unincorporated label.

Nonuniform activity was seen on the samples after six hours and after one day of exposure (Figure 3A and 3B). After two days of incubation in the flowing system, most of the uptake activity is seen in one spot near the middle of the sample (Figure 3C). This activity corresponded to a small tubercle on the surface of the steel. After three days of exposure, several localized areas of activity could be seen (Figure 3D). These sites of activity were also associated with small tubercles on the surface of the metal.

The number of bacteria metabolizing the acetate and the total number of bacteria associated with the surface of the carbon steel are shown in Table 1. As was seen in the autoradiogram, the cell counts reveal that the carbon steel was colonized more rapidly than the stainless steel. Also, not all the cells showed uptake of the acetate.

Relationship between local electrochemical activity and microbial activity. The localized electrochemical activity obtained by the SVET of carbon steel exposed to bacteria is shown in Figure 4. Figure 4A shows several areas of anodic activity after two days of exposure to bacteria. Figure 4B shows a contour map of the same data. Figure 4C is an autoradiogram of the sample after one hour of exposure to ^{14}C-glucose and development as described in the materials and methods.

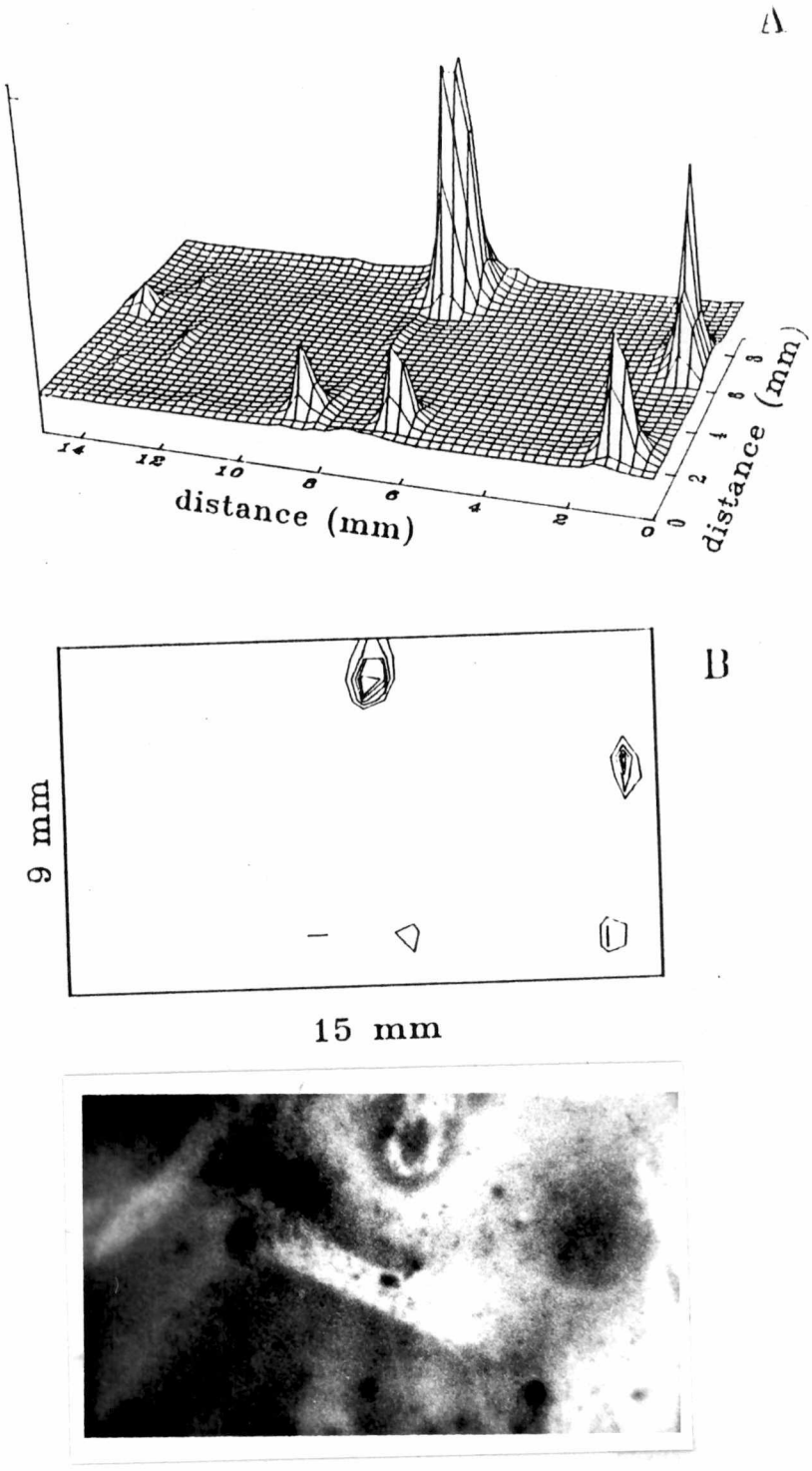

Figure 4. Current density map obtained by the SVET of carbon steel sample after two days of exposure to bacteria. B) Contour map of the data of 4A. C) Autoradiogram of sessile bacteria on sample seen in 4A, incubated with ^{14}C-glucose for 1 h.

DISCUSSION

Jack (9) has demonstrated that changes in bacterial consortia within biofilms, changed the corrosion rates of carbon steel. In particular, the presence of sulfate reducers caused an increased corrosion rate, even though the total biomass of the biofilm was less than consortia without sulfate reducers. This indicates that in addition to microbial biomass, the metabolic activities of particular bacteria within biofilms were important to microbial influenced corrosion. Understanding the activities of individual bacteria within complex biofilm consortia is important in understanding mechanisms of corrosion facilitation by key organisms such as sulfate reducers, and in establishing countermeasures against corrosion.

In this study, we demonstrated that the biosynthetic activities of individual bacteria within a biofilm consortia could be analyzed, using ^{14}C-acetate as a bacterial metabolic precursor. Because acetate is used as a precursor in bacterial lipid synthesis, acetate should be incorporated into the cellular material of all bacteria. However, acetate was not equally incorporated into all of the bacteria on the steel surfaces. This suggests that the bacteria within the biofilm either had different growth rates or were exposed to nutrient limiting conditions within the biofilm. The large sulfate reducers showed little incorporation of the acetate. This is likely due to the

incubation conditions rather than the lack of metabolic activity of the sulfate reducers. The samples were removed from the flask and exposed to air prior to incubation with the acetate. This removal may have inhibited the activity of the strictly anaerobic sulfate reducers. In future studies, the labelled precursors will be added directly to the flask to gain a better understanding of sulfate reducer activity under in situ conditions.

With the biofilm consortium used here, it was possible to distinguish between the large sulfate reducers and the small aerobic bacteria. However in more complex systems, these morphological distinctions cannot be made. Nucleic acid probes have been used to identify bacteria in complex communities (1). The nucleic acid probes in combination with autoradiographic techniques should provide further information regarding the activity of specific bacteria in complex communities such as biofilms.

The autoradiographic techniques in conjunction with scanning microelectrode methods allowed better understand of the relationship between localized microbial metabolic activity and localized electrochemical activity. The biosynthetic activity indicated by the developed silver grains of the autoradiograms corresponded most strongly with tubercles formed on the carbon steel, and with anodic activity observed by the SVET. Several explanations can account for this increased ^{14}C at these anodic sites.

First, the unincorporated acetate may have formed an insoluble abiotic precipitate with the oxidized iron. As mentioned, in some cases under long exposure times, exposure of the film was seen in the killed controls. Therefore some of the acetate may have formed precipitates with the oxidized iron. However, the amounts of acetate bound to the corrosion products was small compared to that incorporated into the cellular material (Figure 1 and 3). Second, the nonuniformly metabolizing bacteria may have caused differential polarization of the sample and resulted in active anodic sites. Third, the actively metabolizing bacteria may have preferentially colonized the corrosion products of the corroding steel. Using these techniques it was not possible to distinguish between the second and third possibilities. In order to address this difficulty, reporter technology is being developed, where location of actively metabolizing luminescent bacteria can be established prior to the onset of corrosion (11).

Whether the differential metabolic activity of the bacteria resulted in initiation of localized anodic sites or was caused by bacterial colonization of the corrosion products is an area for future investigation. However, either case could result in the acceleration of corrosion. In a previous study, the physical presence of microbial biofilms, whether viable or nonviable, caused initiated pits to propagate rather than repassivate (Chapter 7). We

proposed that the microbial biofilm, containing bacteria and extracellular polymer, impeded the flow of inhibiting ions to the surface, or impeded the flow of aggressive ions away from the pits. Propagation of pits was more rapid when viable bacteria were present than in the presence of killed bacteria. Therefore, in addition to the microbial biofilm, some metabolic activity of the bacteria contributed to the propagation of the pits. Here we demonstrated that most of the biosynthetic activity of bacteria occurred over the anodic sites. Therefore, the rapid pit propagation in the presence of the viable bacteria may be due to the synthesis of additional biological membrane over the active anodic sites.

The results of this study demonstrated that autoradiography in conjunction with the scanning vibrating electrode technique can be used to determine relationships between localized microbial metabolic activity and localized electrochemical activity. In addition, microautoradiography was used to determine the percentage and morphology of the individual actively metabolizing bacterial cells. Reporter technology should further help to establish relationships between localized microbial metabolic activity and localized corrosion.

LITERATURE CITED

1. Amann, R.I., L. Krumholz, and D.A. Stahl. Fluorescent-Oligonucleotide probing of whole cells for determinative, phylogenetic, and environmental studies in microbiology. J. Bacteriol. **172**, 762-770.

2. Franklin, M.J., D.E. Nivens, M.W. Mittelman, A.A. Vass, R.F. Jack, N.J.E. Dowling, R.P. Mackowski, S.L. Duncan, D.B. Ringelberg, and D.C. White. (1989) An analog MIC system with specific bacterial consortia, to test effectiveness of materials selection and countermeasures. CORROSION/89 paper no. 513. New Orleans, La.

3. Isaacs, H.S., (1987) The use of the scanning vibrating electrode technique for detecting defects in ion vapor-deposited aluminum on steel. Corrosion **43**, 594-598.

4. Isaacs, H.S., (1988) The measurement of the galvanic corrosion of soldered copper using the scanning vibrating electrode technique. Corrosion Sci. **28**, 547-557.

5. Isaacs, H.S., (1990) The pitting of iron in dilute chloride and sulfate solutions. Advances in Localized Corrosion, eds. H.S. Isaacs, V. Bertocci, J. Kruger, and Z. Szklarska-Smialowska. NACE.

6. Isaacs, H.S., and Y. Ishikawa. (1985) CORROSION/85, paper no. 55, National Association of Corrosion Engineers, Boston, Ma.

7. Isaacs, H.S., and Y. Ishikawa. (1985) Current and potential transients during localized corrosion of stainless steel. J. Electrochem. Soc. **132**:1288-1293.

8. Isaacs, H.S., and B. Vyas. (1981) "Scanning Reference Electrode Techniques in Localized Corrosion" Electrochemical Corrosion Testing, ASTM STP 727, (F. Mansfeld and U. Bertocci eds.) ASTM, p. 3-33.

9. Jack. R.F., (1990) The effects of increased bacterial metabolic diversity on the corrosion of carbon steel. Masters Thesis, University of Tennessee.

10. Meyer-Reil, L., (1978) Autoradiographic and epifluorescence microscopy combined for the determination of number and spectrum of actively metabolizing bacteria in natural waters. Appl. Environ. Microbiol. **36**:506-512.

11. Mittelman, M.W., J.M.H. King, G.S. Sayler, and D.C. White. Light production by a Pseudomonas fluorescens (lux) reporter strain as an endpoint for bacterial adhesion. Appl. Environ. Microbiol., submitted.

12. Mittelman, M.W., and D.C. White. (1989) Effects of shear stress on the adhesion, activity, and biofilm constituents of Pseudomonas atlantica on stainless steel. Abst. Annual Meeting of the American Society for Microbiology, p. 356, New Orleans, La.

13. Nivens, D.E., P.D. Nichols, J.M. Henson, G.G. Geesey, and D.C. White, (1986) Reversible acceleration of the corrosion of AISI 304 stainless steel exposed to seawater induced by growth and secretions of the marine bacterium Vibrio natriegens. Corrosion **42**:204-210.

14. Nivens, D.E., J.B. Guckert, K. Kroeger, J.Q. Chambers, and D.C. White. Microbial biofilm isolation device for off-line analysis. J. Microbiol. Methods, submitted.

15. Tabor, P.S., and R.A. Neihof. (1982) Improved microqutoradiographic method to determine individual microorganisms active in substrate uptake in natural waters. Appl. Environ. Microbiol. **44**, 945-953.

VITA

Michael John Franklin was born in Atlanta, Georgia on August 31, 1962. He attended elementary school and middle school in Athens, Georgia, and he graduated from Clarke Central High School in 1980. He entered the University of Georgia in September, 1980 and graduated in May, 1984, with a Bachelor of Science degree in Microbiology. He reentered the University of Georgia in September, 1984 to study the ecology of methanogenic bacteria in marine sediments, under the direction of Dr. William Wiebe. Much of his research was performed at the University of Georgia Marine Institute at Sapelo Island, Georgia. He received a Master of Science degree in Microbiology in August, 1986. In September, 1986 he entered the University of Tennessee, Knoxville to study microbial ecology under the direction of Dr. David White. His research involved studying the mechanisms by which sessile bacteria facilitated the corrosion of steel. He received the Doctor of Philosophy degree in May, 1991.

During his graduate studies, Michael has worked as a graduate teaching assistant and as a graduate research assistant. He has authored or coauthored ten peer reviewed publications, and has presented four abstracts to national meetings of the American Society for Microbiology. He is a member of the American Society for Microbiology, and the National Association of Corrosion Engineers.